

*Electron Spin Resonance Studies  
of  
Biologically Significant Cobalt  
Complexes, Bio-organic Radicals  
and Radical-Cations.*

*by*

*Ramakrishna D. N. Rao*

A Thesis submitted for the Degree of  
Doctor of Philosophy  
in the  
Faculty of Science  
at the  
University of Leicester

UMI Number: U346599

All rights reserved

INFORMATION TO ALL USERS

The quality of this reproduction is dependent upon the quality of the copy submitted.

In the unlikely event that the author did not send a complete manuscript and there are missing pages, these will be noted. Also, if material had to be removed, a note will indicate the deletion.



UMI U346599

Published by ProQuest LLC 2015. Copyright in the Dissertation held by the Author.  
Microform Edition © ProQuest LLC.

All rights reserved. This work is protected against  
unauthorized copying under Title 17, United States Code.



ProQuest LLC  
789 East Eisenhower Parkway  
P.O. Box 1346  
Ann Arbor, MI 48106-1346

#### ABSTRACT

Electron spin resonance studies of biologically relevant cobalt complexes, bio-organic radicals and radical-cations.

D.N. Ramakrishna Rao

This work is described in three major sections.

(1) A Range of cobalamins and cobaloximes have been studied by electron-addition and photolysis methods with special reference to alkyl derivatives because of its role in several coenzyme B<sub>12</sub>-dependent enzyme reactions.

Photolysis of a range of alkylcobalamins and alkylcobaloximes at 77K resulted in the homolysis of Co-C bond to give Co(II) derivatives and the respective alkyl radicals. Methylcobalamin gave a radical-pair where the alkyl(solvent) radical was trapped at distance of 8.3 Å from Co(II), however radicals were not so precisely trapped in the case of methylcobaloxime. Electron-addition at 77K gave different results for cobalamins and cobaloximes. All alkylcobaloximes gave Co(I) derivatives upon annealing above ca. 150K while cobalamins gave Co(II) derivatives. Several derivatives of cobalamins and cobaloximes have been studied by electron addition and photolysis and the nature of intermediates and products have been identified by e.s.r. The relevance of our work with respect to the role of cobalamins in enzymatic reactions and cobalt chemistry is discussed.

Some studies on cobalt complexes of porphyrins, peptides and phthalocyanins have been done to compare with cobalamins and cobaloximes.

(2) Studies on electron-addition to a range of disulphide containing proteins at 77K showed that electrons are efficiently trapped by disulphides to form RS-SR<sup>-</sup> type of radicals.

(3) Radical-cations of some aromatic, heterocyclic, aliphatic and inorganic derivatives have been prepared using a recently developed technique of radiolysis of frozen freon solutions, and, they were studied by e.s.r. spectroscopy. This method offers an interesting comparison to PES and theoretical results and thus it has helped to understand their electronic structure better.



Thesis

19. 4. 1984



Dedicated in the Loving Memory  
of my Parents who made unselfish  
sacrifices to make me a  
Scientist.

Jñānā shikashatti jeevana thā  
kewda nashth padaṁ bhā dēva.

STATEMENT

The work described in this thesis was carried out by the author in the Department of Chemistry, University of Leicester during the period of May 1980 to May 1983. All work recorded in this thesis is original unless otherwise acknowledged in the text or by references.

No part of this thesis is concurrently being submitted for another degree in any other university.

Dated: SEP 1, 83

R Rao  
R. Rao

#### ACKNOWLEDGEMENTS

I would like to thank Professor Martyn Symons, who initiated me into the area of e.s.r. spectroscopy. It is a memorable experience for me to associate with Professor Symons who has shown an amazing tolerance, patience, encouragement, kindness and moreover comradeship during those days when results were not forthcoming and to the days when results were overflowing. His method of approach in the pursuit of knowledge has helped me to widen my scientific outlook.

I would like to thank Mrs Ann Crane for drawing the diagrams. The technical assistance obtained from the staff of the workshop and glass blower, Mr Dennis Hopkins, is gratefully acknowledged.

Financial assistance obtained through an SERC grant and cancer research fund is gratefully acknowledged.

R. Rao.

#### PREFACE

This thesis is broadly classified into two major parts namely, cobalt complexes and radical cations. A major part of this thesis is dedicated to cobalamins, cobaloximes and biologically relevant cobalt complexes. A small part includes some studies on manganese complexes which were done essentially to compare with the cobalt complexes. Work on bio-organic radicals (chapter 5) was initiated accidentally, when  $RS\cdot SR^-$  type of radicals were observed in our work with proteins. Studies on cation radicals were undertaken during the final phase of this work when a simple method was developed to produce radical cations. A large number of such radicals have been studied to evaluate e.s.r. parameters and to understand their electronic structures. The first chapter deals with a review of reaction mechanism of enzymes dependent upon  $CoB_{12}$  and methylcobalamin.

#### ABBREVIATIONS

dACH <sub>2</sub>	; Deoxyadenosyl
DMB:Bzm	; 5,6 Dimethylbenzimidazole
CoB <sub>12</sub> or dACbl	; CoenzymeB <sub>12</sub>
Cbl or B <sub>12</sub>	; Cobalamin
B <sub>12r</sub>	; Cobalamin(II)
B <sub>12s</sub>	; Cobalamin(I)
MW	; Molecular Weight
py	; Pyridine
L	; Ligand
B	; Base(axial ligand);Where appropriate it is used for DMB
MTHF	; 2-methyltetrahydrofuran
mM	; Millimolar
CM-cellulose	; Carboxymethyl cellulose
ml	; Milliliter
NTP	; Nucleotide triphosphate
ATP	; Adenosine triphosphate
CTP	; Cytidine triphosphate
DPPH	; Diphenylpicryl hydrazyl
TPNH or NADP	; Nicotinamide adenine dinucleotide
DmgH	; Dimethylglyoxime
EHPG	; Ethylene bis (o-hydroxy phenyl)glycine
PTH	; Phthalocyanins
TPP	; Tetraphenyl porphyrin
BSA	; Bovine serum albumin

SOMO	; Semi-occupied molecular orbital
P	; Phosphate group
CoA	; CoenzymeA
E	; Enzyme
EBH <sup>+</sup>	; Acidic group on the enzyme
TSPP	; Tetra sulphophenyl porphyrin
en	; Ethylene diamine
DCPIP	; Dichlorophenol indophenol
FeCN	; Ferricyanide
i.p.	; Ionization potential
Ph	; Phenyl
Me	; Methyl
DMSO	; Dimethyl sulphoxide
n.b.	; Non-bonding
PES	; Photoelectron spectroscopy
MeFH <sub>4</sub> ; MeTHF	; Methyl tetrahydrofolate
HOMO	; Highest occupied molecular orbital
AdO	; Adenosyl
ts	; Temperature-sensitive

## CONTENTS

<u>Chapter 1</u>		<u>page</u>
Mechanism of action of enzymes dependent upon coenzymeB <sub>12</sub> and methylcobalamin: A literature survey.	1	
<u>Chapter 2</u>	<u>Cobalamins</u>	
Introduction	...	24
Experimental	...	30
Results & Discussion	...	32
Radiolysis results	...	32
Photolysis results	...	39
<u>Chapter 3</u>	<u>Cobaloximes</u>	
Introduction	...	45
Experimental	...	49
Results & Discussion	...	52
Radiolysis results	...	52
Photolysis results	...	58
<u>Chapter 4</u>	<u>Some cobalt and manganese complexes</u>	
Introduction	...	62
Experimental	...	63
Results & Discussion	...	65
Cobalt porphyrins	...	66
Cobalt phthalocyanins	...	68



Cobalt peptide complexes	...	...	...	69
Cobalt carnosine complexes	...	...	...	70
Manganese porphyrins	...	...	...	72

#### Chapter 5      Bio-organic radicals

Introduction	...	...	...	75
Experimental	...	...	...	76
Results & Discussion	...	...	...	77

#### Chapter 6      Radical cations

Introduction	...	...	...	82
Experimental	...	...	...	84
Results & Discussion	...	...	...	84
(a) Radical cations of some aromatic derivatives				84
(b) Radical cations of some heterocyclic derivatives				89
(c) Radical cations of some amides, thioamides and dimethylsulphoxide	...	...	...	92
(d) Radical cations of some nitroalkanes			...	95
(e) Radical cations of dinitrogen tetroxide			...	98

CHAPTER 1MECHANISM OF ACTION OF ENZYMES DEPENDENT UPON COENZYME B<sub>12</sub>  
AND METHYLCOBALAMIN: A LITERATURE SURVEY.

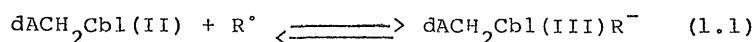
The use of cobalt in living systems is confined almost exclusively to the reactions of cobalamins. The very fact that a special ligand has evolved in order to capture this rare element and to separate it from all other elements is an indication of its value. The ligand corrin, is special in that

(1) it forces the chemistry of cobalt to be low spin.

(2) It provides such a strong field that the redox potentials of Co(I)/Co(II) and Co(II)/Co(III) are close to those of  $H_2/H^+$ , i.e. the cobalt(III) form is stable in all mildly oxidizing conditions, which allows transport of the metal in oxidizing media outside cells in a very stable form.

(3) Roughly it has a planar geometry with a strong field in the plane making the 5 and 6 co-ordination positions reactive.

(4) It makes Co(I) species a "super" nucleophile. Now the availability of cobalt in a low spin  $d^7$  configuration with an unpaired electron in  $d_{z^2}$  orbital results in a species which is a weak radical scavenger. Thus it permits the reaction shown in eq 1.1 to be reversible. The reaction in the reverse



direction generates a radical  $R^\bullet$  which becomes the source of catalysis of radical rearrangements and ribonucleotide reduction in  $B_{12}$ -dependent enzyme reactions.  $CoB_{12}$  and methylcobalamin are the major source of free radical reactions and act as very useful biological "Grignard reagents" (1-6). Cobalamins are found virtually in all animal tissues but they are absent in plants (7). They are mainly found in three forms in the human body. Blood plasma contains about 70% methylcobalamin and 30% of hydroxocobalamin and coenzyme  $B_{12}$ . Human liver contains mainly coenzyme  $B_{12}$  and hydroxocobalamin (8,9).

In the following sections a brief review is given on the theoretical and model studies to the understanding of pathways and mechanisms of enzyme catalysed reactions that are dependent upon  $CoB_{12}$  and methylcobalamin (Fig 1,1).

$CoB_{12}$  is known to participate as a coenzyme in the enzymatic rearrangements and a reduction reaction (Table 1,1). A unifying feature of the seemingly quite different chemical reactions catalysed by these enzymes is that the coenzyme serves as an intermediate carrier of a hydrogen atom. The rearrangement reactions of  $CoB_{12}$  can be classified into two types shown by equations 1.2 and 1.3. The overall reaction of eq 1.3 is irreversible unlike reaction 1.2.

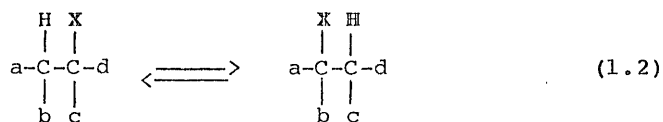


Figure 1.1  
Structure of alkylcobalamin.

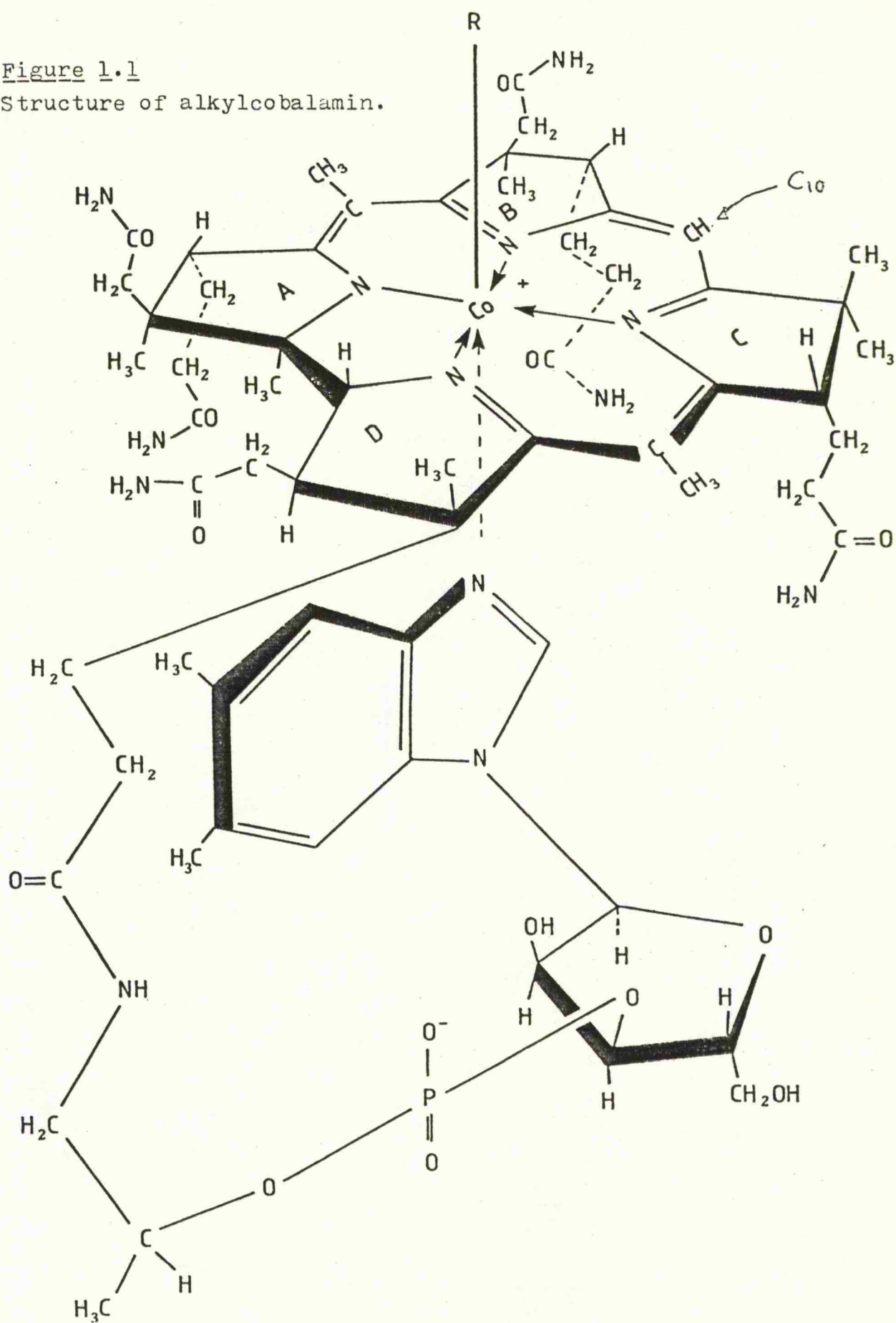
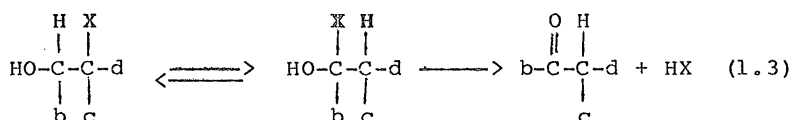


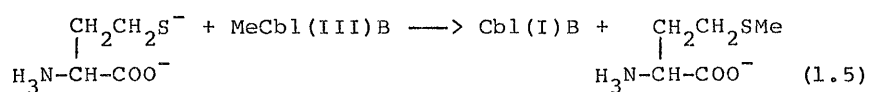
TABLE 1.1 Enzymatic reactions catalysed by coenzyme B<sub>12</sub>

Reaction type	Enzymes	a	b	c	d	x
eq 1.3	Diol dehydrase	OH	H	H	H or CH <sub>3</sub>	OH
eq 1.3	Glycerol dehydrase	OH	H	H	CH <sub>2</sub> OH	OH
eq 1.3	Ethanolamine ammonia-lyase	OH	H	H	H or CH <sub>3</sub>	NH <sub>2</sub>
eq 1.2	(R)-methylmalonyl CoA mutase	H or CH <sub>3</sub>	H	CO <sub>2</sub> H	H	COSoA
eq 1.2	(S)-Glutamate mutase	H	H	H	CO <sub>2</sub> H	CHNH <sub>3</sub> CO <sub>2</sub> <sup>-</sup>
eq 1.2	alpha-methylene glutarate mutase	H	H	H	CO <sub>2</sub> H	C(=CH <sub>2</sub> )CO <sub>2</sub> H
<u>Amino mutases using either</u>						
eq 1.2	(S)-3,6 diamino hexanoate (beta-lysine mutase)	CH <sub>2</sub> CHNH <sub>3</sub> CH <sub>2</sub> CO <sub>2</sub> <sup>-</sup>	H	H	H	NH <sub>2</sub>
eq 1.2	(R)-2,6-diamino hexanoate (alpha-lysine mutase)	(CH <sub>2</sub> ) <sub>2</sub> CHNH <sub>3</sub> CO <sub>2</sub> <sup>-</sup>	H	H	H	NH <sub>2</sub>
eq 1.2	(R)-2,5-diamino pentanoate (ornithine mutase)	CH <sub>2</sub> CHNH <sub>3</sub> CO <sub>2</sub> <sup>-</sup>	H	H	H	NH <sub>2</sub>
eq 1.2	alpha- or beta leucine (Leucine 2,3 amino mutase)	(CH <sub>3</sub> ) <sub>2</sub> CH	H	H	CO <sub>2</sub> H	NH <sub>2</sub>



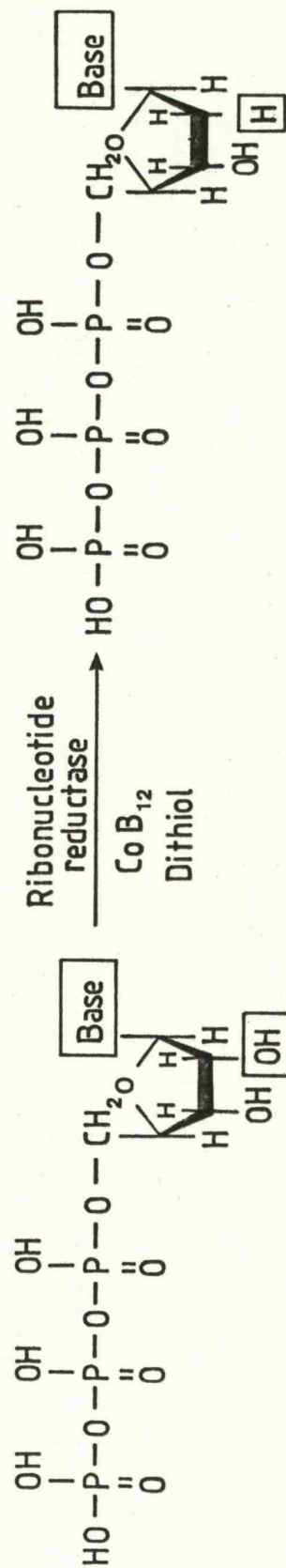
In both these reactions a hydrogen atom and a group change places. Ribonucleotide reductase (present in certain microorganisms) catalyses reaction 1.4. This reaction is also catalysed by enzymes which are not dependent on  $\text{CoB}_{12}$  as in E.coli and human systems.

Methionine synthetase dependent upon methylcobalamin catalyses the reaction 1.5. Reactions 1.4 and 1.5 will be considered at the end of this chapter and rearrangement



reactions 1.2 and 1.3 will be discussed in the following sections. This discussion is initiated by considering some important generalities. The mechanism of an enzyme reaction is related to the following factors:

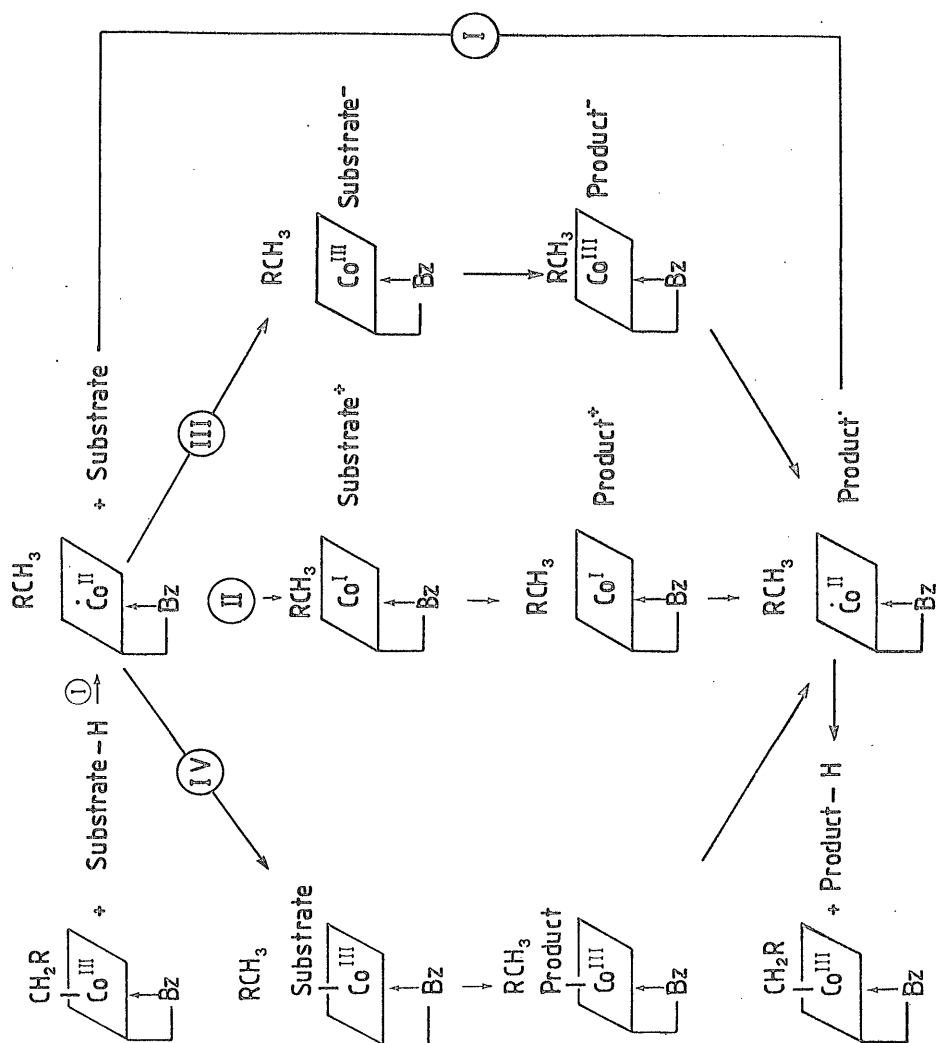
- (1) Nature of enzymes and coenzyme
  - (2) Enzyme-coenzyme interaction
  - (3) Enzyme-coenzyme-substrate (or substrate analog) interaction
  - (4) Stereochemical course of enzyme reaction and influence of each of the three components of the complex on the reaction.
- Figure 1.2 depicts the possible pathways for  $\text{CoB}_{12}$  reactions



Reaction of ribonucleotide reductase

(eq 1.4)

Figure 1.2. Possible mechanisms for Co-C bond cleavage in presence of substrate.





and the generalities considered above will be discussed under each sub-heading to determine the possible enzymatic pathway.

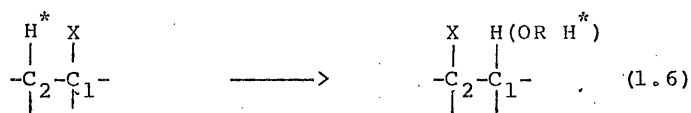
#### 1.NATURE OF ENZYMES AND COENZYME

##### The role of enzyme

(a) Understanding the structural requirements of an enzyme to perform the desired rearrangement reaction depends on solving the following aspects of the reaction. (a) Whether to devise a pathway for the isomerisation of the substrates based on the use of very reactive free radicals produced by Co-C bond fission or Co-H species produced by the beta-elimination reaction. (b) How to achieve the magnitude and direction of steric distortion necessary to labilise the Co-C bond according to the chosen mechanism. (c) How to suppress unwanted side reactions of free radicals or Co(I) species.

Diol dehydrase is one of the most thoroughly studied enzymes and hence a brief description of this will be given here. Diol dehydrase isolated from Klebsiella pneumoniae consists of two dissimilar subunits with a total MW of 250,000. Both the components (referred to as f and s components) are necessary for catalytic activity (10,11). It also requires <sup>the</sup>SH groups and monovalent cations for its activity (12). A main feature in the reactions 1.2 and 1.3 is to abstract a hydrogen from the substrate molecule and eventually transfer it back to the substrate on the adjacent carbon atom. Experiments with coenzymes and substrates specifically labelled with deuterium or tritium have shown (eq. 1.6) that this does happen (13-16). This reaction is

initiated by  $\text{CoB}_{12}$  which by homolysis of the Co-C bond

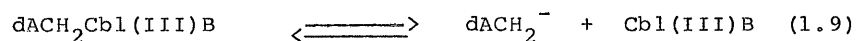
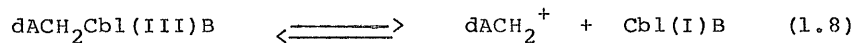


generates a reactive  $\text{dACH}_2$  free radical which can abstract a hydrogen atom from the substrate to form deoxyadenosine. The rearranged substrate free radical can now abstract a hydrogen from deoxyadenosine molecule to give the products shown in eq, 1.6.

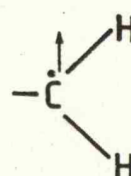
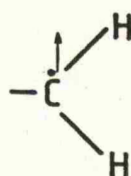
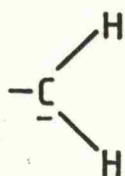
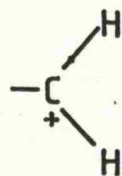
#### NATURE OF THE COENZYME

##### Role of Co-C bond

According to Cram(17) the possible species from homolytic (eq, 1.7) or heterolytic cleavage (eq 1.8 and 1.9) of  $\text{CoB}_{12}$  are a face to face species (insert 1.1) with a certain blend



of diradical or zwitterionic character, face to edge zwitterions (insert 1,2 and 1,3), face to edge singlet diradical (insert 1,4) and face to edge triplet diradical (insert 1,5). A diradical can remove a hydrogen atom from a substrate molecule whereas zwitterions can remove either a hydride or



2e



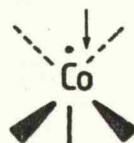
1.1



1.2



1.3



1.4



1.5

Inserts 1.1 - 1.5

proton. The mechanism of Co-C bond cleavage will be discussed in detail in chapter 2 but a brief account of its role in relation to enzyme reaction is given here.

Halpern and co-workers (18) have shown that the Co-C dissociation energies for alkyl(py)cobaloximes consistently appear to lie in the range 20-30 K cal's per mole and they conclude that the dissociation energies for alkyl cobalamins and  $\text{CoB}_{12}$  will also be in the same range. This is compatible with the proposed role of  $\text{CoB}_{12}$  as a  $\text{dACH}_2$ -radical precursor. Very little additional activation would be required for homolysis of such a weak bond to occur at rates consistent with those of the enzymatic process. Lenhert (19) has proposed a similar idea namely that interaction between  $\text{CoB}_{12}$  and the enzyme or enzyme-substrate complex could lead to destabilisation of Co-C bond by increasing steric interactions between the adenine and or ribose ring and corrin nucleus. The energetic cost of breaking the Co-C bond would then be recouped from improved binding between  $\text{dACH}_2$ , cobalamin and enzyme.

#### Role of the corrin ring and its amide chains

The hydrogen atom at C-10 position of the corrin ring has been shown to be photolabile and reactive (20). 10-chloro and 10-bromo analogs of the coenzyme retain partial activity with diol dehydrase (21). Since the affinity for the enzyme did not decrease by these substitutions, it was concluded that the halogen substituents, by their effects on the electronic structure of the corrin ring, decrease the reactivity of Co-C

bond via their effects on Co-N equatorial bonds. Binding of coenzyme analogs (containing modified propionamide side chains) with diol dehydrase has shown that amide nitrogens are involved in hydrogen bonding with enzyme in the enzyme-coenzyme complex (22).

#### Cobalt alpha-site (lower ligand)

CoB<sub>12</sub> devoid of nucleotide (DMB) loop is found to be partially active as a coenzyme (23). This suggests that the nucleotide ligand in the cobalt axial position does not participate directly in the catalysis. This idea is further exemplified by the fact that the DMB ligand can be replaced by several heterocyclic bases without altering the enzyme activity (24). It has been suggested that it is important in the enzyme recognition of coenzyme and also the steric requirement it exerts on cobalamin prior to hydrogen abstraction. This arrangement generated by both cobalt and DMB has been referred to as an "entatic" state (25) or "rack" mechanism (26). This type of metal-ligand arrangement is deemed to be a unifying feature operative in metalloenzyme catalysis.

#### Cobalt beta-site (upper ligand)

The role of cobalt-beta-site in the activation of Co-C bond and binding to the enzyme: Several coenzyme analogs containing different ligands in the cobalt-beta site have shown that the adenine and sugar portion of the dACH<sub>2</sub> ligand is essential for coenzyme activity (27).

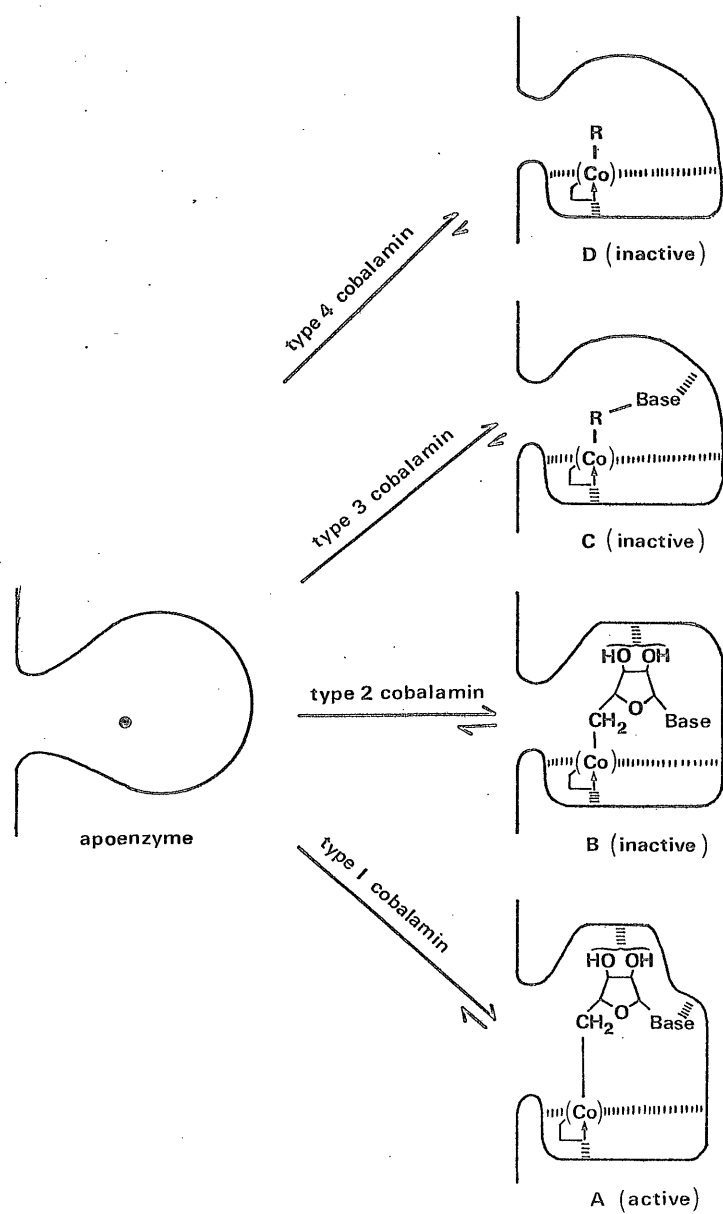
### 2. ENZYME-COENZYME INTERACTIONS

Studies using coenzyme analogs to find its effect on the

reactivity and affinity for the enzyme have given a clear picture of the nature of enzyme-coenzyme interactions. Coenzyme analogs can be classified into four categories. Type 1 cobalamins have coenzyme activity and show high affinity for the enzyme ( $K_m \approx 1$  micro mole). These analogs contain an adenine or purine and slightly modified D-ribose moiety. Type 2 cobalamins are the analogs that contain bases other than adenine. They do not serve as coenzymes and are weak competitive inhibitors with respect to deoxyadenosylcobalamin. The bound analogs of this type can be at least partially displaced by the normal coenzyme, suggesting reversibility of binding of these analogs to the enzyme. Type 3 cobalamins are the analogs whose D-ribose is replaced by L-ribose or other groups. They are inactive as coenzymes but function as very strong competitive inhibitors ( $K_i < 1$  micro mole) with respect to  $\text{CoB}_{12}$ . Type 4 cobalamins are modified on both adenine and ribose moieties. Both Type 3 and Type 4 cobalamins form an irreversible complex with the enzyme.

From the structure-function relationship of these analogs, and to account for activation of the Co-C bond in the resulting complex, a possible mechanism was proposed for interaction of the coenzyme with the enzyme (Fig 1.3). This mechanism is based on the assumption that the apoprotein has sites at which it interacts with the cobalamin moiety (corrin ring, its side chains and nucleotide loop) and the adenosyl moiety (adenine and ribose) of the coenzyme (28). Type 1 cobalamins bind tightly to the enzyme by interaction at both

Figure 1.3. Proposed mechanism for the binding of  $\text{CoB}_{12}$  and its analogs to dioldehydrase.



the D-ribose and base moieties in addition to cobalamin moiety. These interactions lead to activation and cleavage of the Co-C bond. In the absence of substrate the activated Co-C bond is cleaved by reaction with oxygen resulting in irreversible inactivation of the holoenzyme. With Type 2 analogs the affinity for the enzyme is relatively weak owing to inadequate interaction at the base moiety. As a result, the Co-C bond is not sufficiently activated. Type 3 analogs are able to interact with the enzyme only via the adenine and cobalamin moieties. Activation of the Co-C bond of these analogs is not possible because they lack the ribofuranosyl moiety or a structure closely resembling it. A possible explanation for the very tight interaction between this type of analogs and the enzyme is that the coenzyme binding site needs to undergo conformational change to accommodate the more flexible alkyl chain. Type 4 cobalamins can interact with apoenzyme only at the cobalamin moiety. The affinity of this analog for the enzyme is still high. This indicates that the contribution of interactions at the adenosyl moiety to the binding of the enzyme is rather small. Hence activation of the Co-C bond is impossible in this case. Figure 1.3 shows a diagrammatic picture of coenzyme-enzyme interactions.

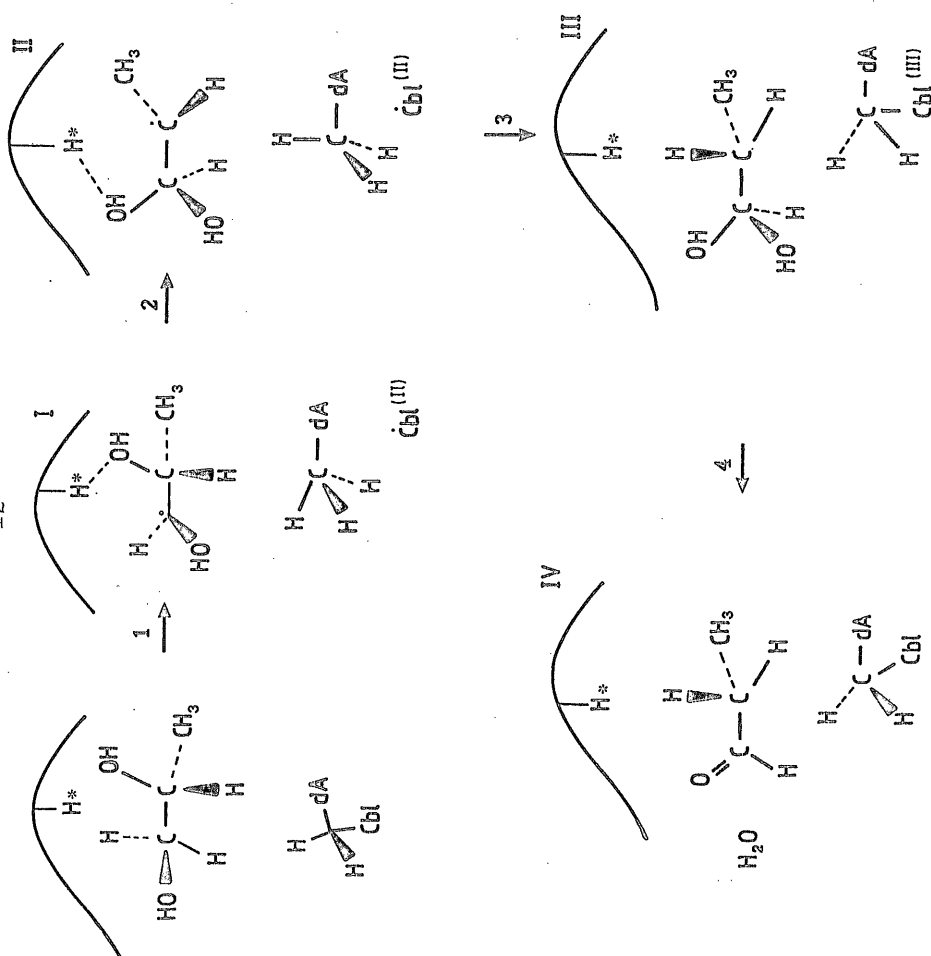
Toraya and Fukui (28) have reported that they have obtained a direct evidence for the binding site of diol dehydrase and for adenosyl portion of the coenzyme.

### 3. Enzyme-Coenzyme-Substrate interactions

Figure 1.4 shows a possible mechanism for the rearrangement



Figure 1.4. Proposed mechanism for  $\text{CoB}_{12}$ -dependent enzyme reactions.



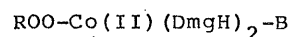
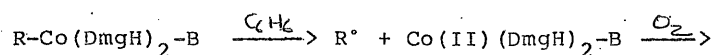
reaction of  $\text{CoB}_{12}$  dependent enzymes. Mechanism is discussed under each step.

#### STEP 1

(a) Formation of a ternary complex of enzyme, coenzyme and substrate.

(b) Homolysis of Co-C bond and hydrogen abstraction from the substrate. Both the events are aided by mutual interaction within the ternary complex. The most likely mechanism for the generation of radical intermediate is a concerted molecule induced homolysis of Co-C bond with cobalt catalytically activating the substrate C-H bond. A reasonable transition state for this is represented in <sup>the</sup> intermediate 1 (Figure 1.4). B represents the polarisable base on the enzyme. Pre-coordination of C-1 (of substrate) is not necessary for C-H activation (29,30). Formation of this intermediate is supported by spectroscopic, kinetic and several model reactions. The most essential feature of this step is the homogeneous catalytic activation of the C-H bond by cobalt. The formation of a three-centered transition state is well known and it has been proposed to occur during the unimolecular thermolysis of cobaloxime Co-C  $\text{sp}^3$  bonds (31,32). Polarisable Lewis bases are most effective reagents for inducing homolysis as they can stabilise the nascent radicals by electron donation and hence make their formation energetically favourable (33). Kinetic evidence for this type of catalysis is provided by thermal insertion of oxygen to cobalt after Co-C bond fission in cobaloximes. The reaction

becomes independent of oxygen concentration in polarisable solvents such as benzene (eq 1.10) (34). Additional evidence can be produced in the favour of molecule-induced homolysis in



(1.10)

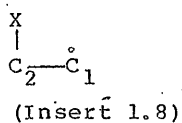
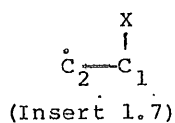
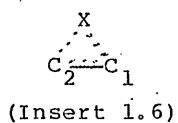
studies using the coenzyme analog with the ribose ether oxygen being replaced by a  $-CH_2-$  group (35). This analog exhibits significantly less coenzyme activity although the modification had no appreciable effect on  $K_m$  (36) since the C-5 atom is wedged between the ether oxygen and the substrate hydrogen. Its close proximity to the oxygen lone pair of electrons would be expected to have a favourable effect on step 1. Photochemical and flash photolysis studies reveal that  $Co(II)$  and organic radicals have an extremely rapid recombination rate (37-39). The generation of an "entatic" or "strained" state is in agreement with the observed accumulation of  $Co(II)$  and substrate radicals at high levels during the enzymatic reactions. Since steric effects that prevent diffusion controlled radical termination reactions in solutions are known to be primarily responsible for any unusual longevity of organic radicals. Finlay *et al.* (40) have reported that substrate radicals accumulate to approximately 40% of the total Enzyme-substrate complex. Positive evidence for the formation of  $Co(II)$ ...radical pair comes from e.s.r.

spectroscopy. It has been shown in the case of diol dehydrase (41-44), ethanolamine ammonia-lyase (45) and ribonucleotide reductase reactions a characteristic e.s.r. spectrum consisting of a doublet is formed during the reaction. This is attributed to a Co(II) radical pair and the distance between the two species is calculated to be about 10-12 Å (47). This radical pair disappears when all the substrate has reacted to form products. These results imply that after cleavage of the Co-C bond the formation of substrate derived radical and subsequent reaction takes place in the protein active site. Thus the three species are in a triangular relationship with substrate being aided by a weak hydrogen bond forming group on the protein. This explains the need of a -SH group of the protein for catalytic activity (12).

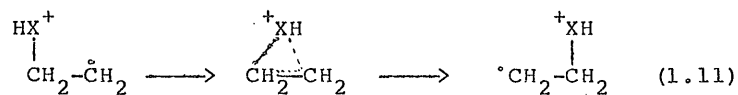
#### STEP 2

Migration of group X (cf, Table 1.1) is the essential event of this step. Several possibilities exist for the rearrangement of group X. Both experimental and theoretical considerations are given below to support the proposed intermediate 2.

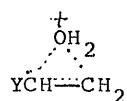
Evidence presented so far supports the formation of free radicals by homolysis of the Co-C bond (cf. eq 1.7). Obviously the substrate-derived species should be a radical (rather than an anion or cation) to promote the reaction. Also in the case of propane 1,2 diol it is necessary to show which of the two hydroxy groups migrates. This leads to three possible radicals (inserts 1.6-1.8). MO calculations (48-51) and studies on model compounds (52,53) suggest that un-aided rearrangement



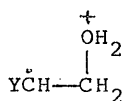
of a substrate-derived radical or carbanion to a product related radical or carbanion can be discounted for dioldehydrase, ethanolamine ammonia-lyase, amino mutase and glutamate mutase. ab initio calculations were made (49) to explore the possibility that protonation of X in e.g. insert 1.7 could facilitate its migration via a bridged Transition state rather than a dissociation-recombination step (eq 1.11). Calculated parameters for open and bridged species



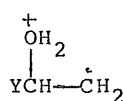
(insert 1.9, 1.10 and 1.11, X=OH, Y=Me or OH) are energetically



Y = OH or CH<sub>3</sub>



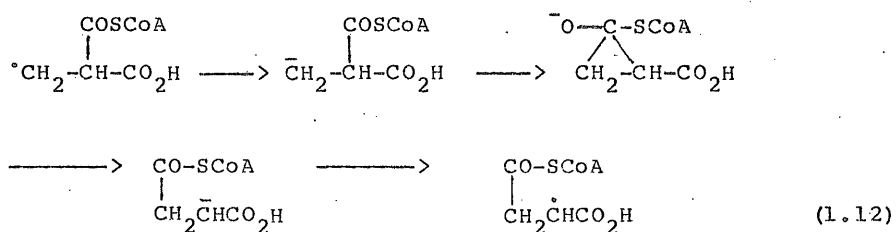
(Insert 1.10)



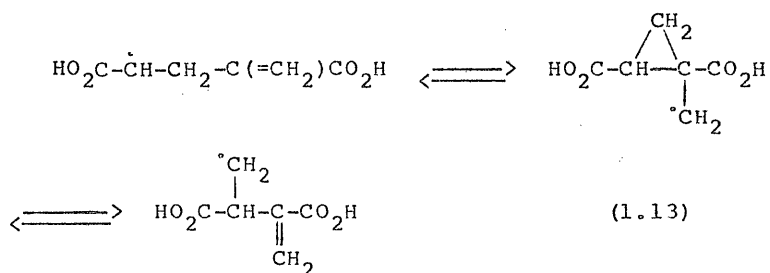
(Insert 1.11)

indistinguishable suggesting that protonation or hydrogen bonding with group X can lead to migration as depicted in eq

1.11 and step 2. This mechanism has been invoked for enzymatic systems such as diol dehydrase, ethanolamine ammonia-lyase, amino mutase and methylmalonyl-CoA mutase. In methylmalonylCoA mutase reaction carbanions have also been invoked (54) as intermediates because a substrate-derived carbanion can reasonably be converted to a product-related carbanion via the oxyanion of a cyclopropanol (eq, 1.12). For alpha-methylene glutarate mutase it may be sufficient to consider rearrange-



ment via radical intermediates alone (eq, 1.13) because but-3-enyl and cyclopropyl carbinyl radicals are known to interconvert rapidly.



STEP 3

The product-related radical abstracts a hydrogen from deoxyadenosine resulting in the  $\text{dACH}_2$  radical which immediately recombines with  $\text{Co(II)}$ . This pathway is consistent with the results of all experiments with isotopically labelled substrates (13-15).

STEP 4

This is the dehydration step and it is applicable only to those enzymes which follow the reaction of eq 1.3. This step is apparently non-enzymatic as it results in the loss of a molecule of water or ammonia once it is released from the active site.

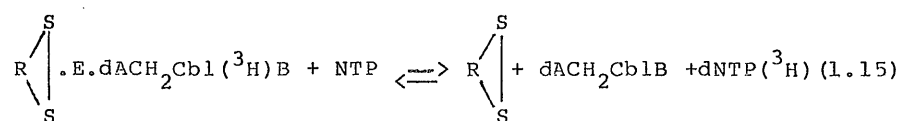
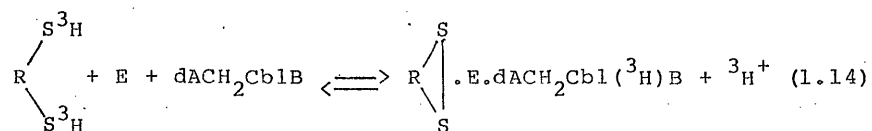
MECHANISM OF RIBONUCLEOTIDE REDUCTASE REACTION

This enzyme catalyses a reduction reaction (cf, eq 1.4) and hence it differs from rearrangement reactions discussed above.

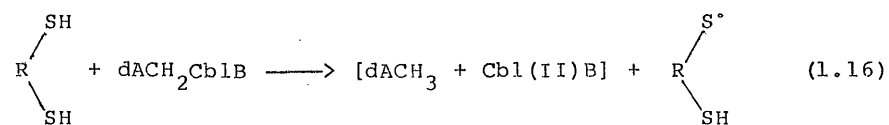
Nature of the enzyme

This is an allosteric enzyme and nucleotide triphosphates bind both catalytic and allosteric sites. This enzyme also needs a dithiol cofactor such as dihydrolipoate or glutathione. A characteristic of this enzyme is that it catalyses an exchange of a hydrogen between water in the medium and the 5'methylene group of the coenzyme that is covalently bonded to cobalt (55, 59-64). For this exchange to occur it requires a dithiol substrate  $\text{CoB}_{12}$ , a suitable nucleotide and the enzyme. It has been found that both nucleotide and ribonucleotides are equally good in promoting exchange. It is suggested that

nucleotide substrates promote exchange by binding at the catalytic site whereas deoxyribonucleotide promote exchange by binding at the allosteric sites (61). When the reaction is done in a medium of deuterium oxide or tritium oxide the label is incorporated at the 2' position of the deoxyribonucleotide product (55,56-58). This is attributed to a rapid exchange between dithiol cofactor and water in the medium. Abeles and Beck(55) have proposed a mechanism for the exchange process and this is shown in eqs. 1.14 and 1.15. Another reaction catalysed by ribonucleotide reductase is



the degradation of  $\text{CoB}_{12}$ . Dithiol and nucleotide substrates must be present for the catalysis of this reaction (65-68). The products of the degradation are  $\text{B}_{12r}$  and deoxyadenosine both being tightly bound to the coenzyme-binding site (eq 1.16). This mechanism is not directly related to the reduction





reaction of the enzyme.

In the catalysis of the reduction reaction e.s.r evidence shows the formation of radical-pairs (69-71). Two types of radical-pairs were detected. One of the radical pairs is formed in a rapid reaction (6-100 ms) at 37°C followed by freeze quenching at 130K. This has been attributed to homolysis of the Co-C bond and the radical-pair is  $\text{Co(II)} \cdot \text{dACH}_2$  (72-74). This is often referred to as "tight" radical-pair. The second type of radical-pair is obtained in a slow reaction after 10 mins of incubation at 37°C. This is called the "relaxed" radical pair and the e.s.r. spectrum of this is similar to the e.s.r. spectra of radical-pairs formed in other  $\text{CoB}_{12}$ -dependent reactions. It is thus evident that this enzyme catalyses more than one reaction and the mechanism of the reduction reaction is still not firmly established. Two mechanisms are proposed and one of them is shown in figure 1,5.

#### COBALAMIN-DEPENDENT METHYL TRANSFER REACTIONS

In the preceding sections the role of  $\text{CoB}_{12}$  as a coenzyme was discussed. In the following section the role of methylcobalamin as a coenzyme is discussed. Methylcobalamin act as a coenzyme in two types of reactions. (1) Reactions leading to the synthesis of methionine, methane and acetate.

(2) Bio-methylation of metals.

##### (1) Reactions leading to the synthesis of methionine

Methylcobalamin is one of the three coenzymes that transfer methyl groups in biological reactions. The other two being

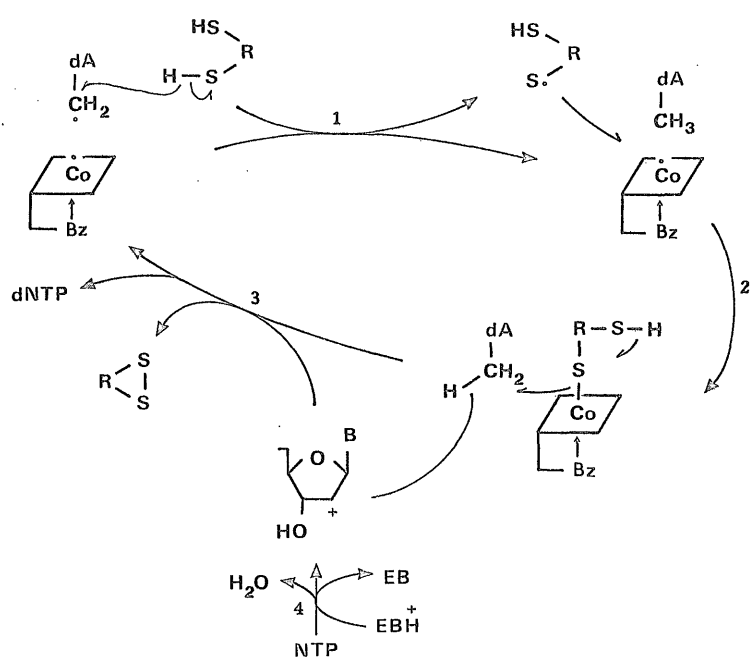
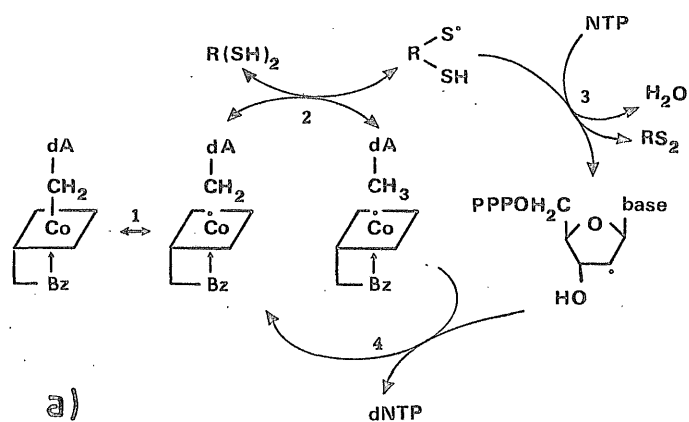
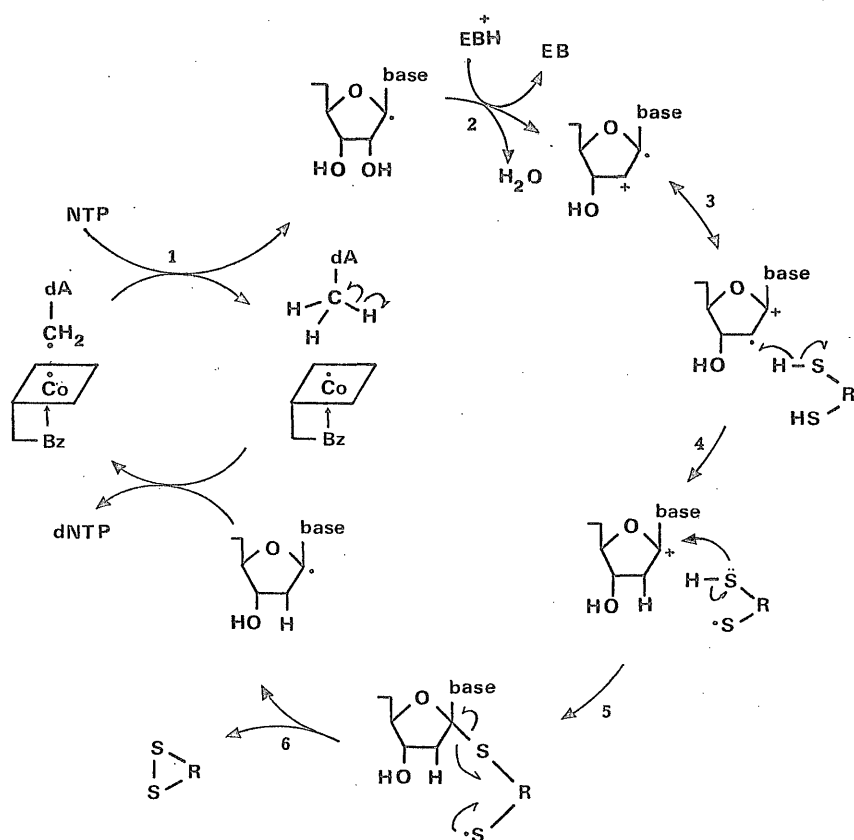


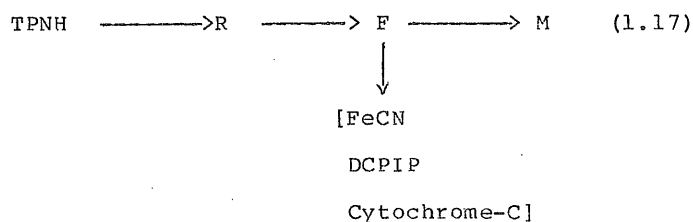
Figure 1.5. Radical mechanisms proposed for cobalamin-dependent ribonucleotide reductase.



(c)

Figure 1.5. Radical mechanisms proposed for cobalamin-dependent ribonucleotide reductase.

S-adenosyl-methionine and N-methyltetrahydrofolate. Of these only methylcobalmin can transfer the methyl group as an ion or a free radical. The other two species are thought to transfer methyl as a carbonium ion. Three major metabolites of biological importance are synthesised by methylcobalmin they are methionine, methane and acetate. Methionine is one of the products of methionine synthetase, the other product is tetrahydrofolate which is also an important coenzyme involved in the synthesis of purines and pyrimidines. Methionine synthetase is the first mammalian cobalamin-dependent enzyme studied, the other two mammalian enzymes, leucine, 2,3 amino-mutase and methylmalonylCoA-mutase were studied later. The mechanism for activation and catalysis of methionine synthetase is shown in figure 1,6 (75). When the enzyme is isolated, it contains the  $B_{12}$  moiety in  $B_{12r}$  form. Activation of this form (step a) is facilitated most efficiently by adenosylmethionine and a reducing system consisting of TPNH and two small flavoproteins (designated as R and F). This system provides an electron apparently through the reaction 1.17. The reaction of reduced M protein with adenosylmethionine releases methyl radical which methylates  $B_{12r}$ .



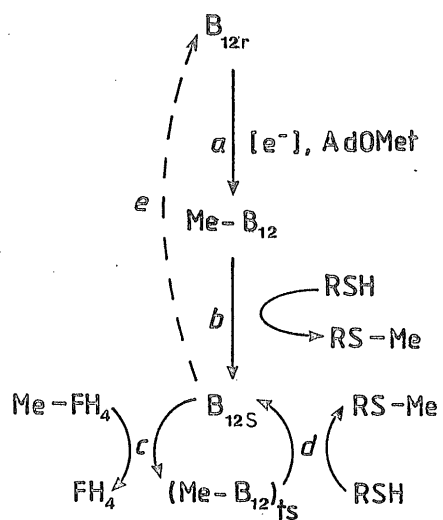


Figure 1.6. Proposed mechanism for the synthesis of methionine by methionine synthetase

This reaction apparently proceeds by a single concerted reaction. The activated enzyme containing methylated cobalamin enters into the catalytic cycle at the completion of step b. In this reaction one molecule of homocysteine is methylated and the cobalamin(I)-enzyme complex is formed. In step c this complex reacts with methyltetrahydrofolate to give a temperature sensitive methylated cobalamin which is similar to but not identical to methylcobalamin produced in step a. Its low temperature spectrum is similar to that of the "base-on",

form of methylcobalamin produced in step a. Its high temperature form resembles the "base-off" form of methylcobalamin (of step, a) or that of isomeric methylcobalamin in which the methyl group occupies the lower coordination sphere (alpha-site) (76). The temperature dependent conversion of the bound chromophore might be facilitated by a concomitant change in apoprotein conformation, this is consistent with a large value of  $\Delta S$  (75). In step d, the temperature-sensitive species is demethylated by homocysteine to give methionine and cobalamin (I) form. In step e, this complex is degraded to the inactive  $B_{12r}$  form. Kinetic studies (75) indicate that at steady state the rate constant for step d, is at least eight times larger than that for step c and 89% of total  $B_{12}$  is present in the reaction exists as  $B_{12s}$  form [cobalamin(I)]. This suggests that the activation of enzyme (step a and b) are the main reactions and the degradation reaction (step e) is secondary.

Methylcobalamin is also involved in the synthesis of methane and acetate in several acetogenic bacteria via "methane cycle". Acetate is the key intermediate in this cycle and it is formed by the reduction of carbon dioxide with hydrogen. The reduction step is some way coupled to phosphorylation but the mechanism is not known. The mechanism for the synthesis of acetate is known, and it is shown in figure 1.7 (77,78).

#### BIO-METHYLATION OF METALS

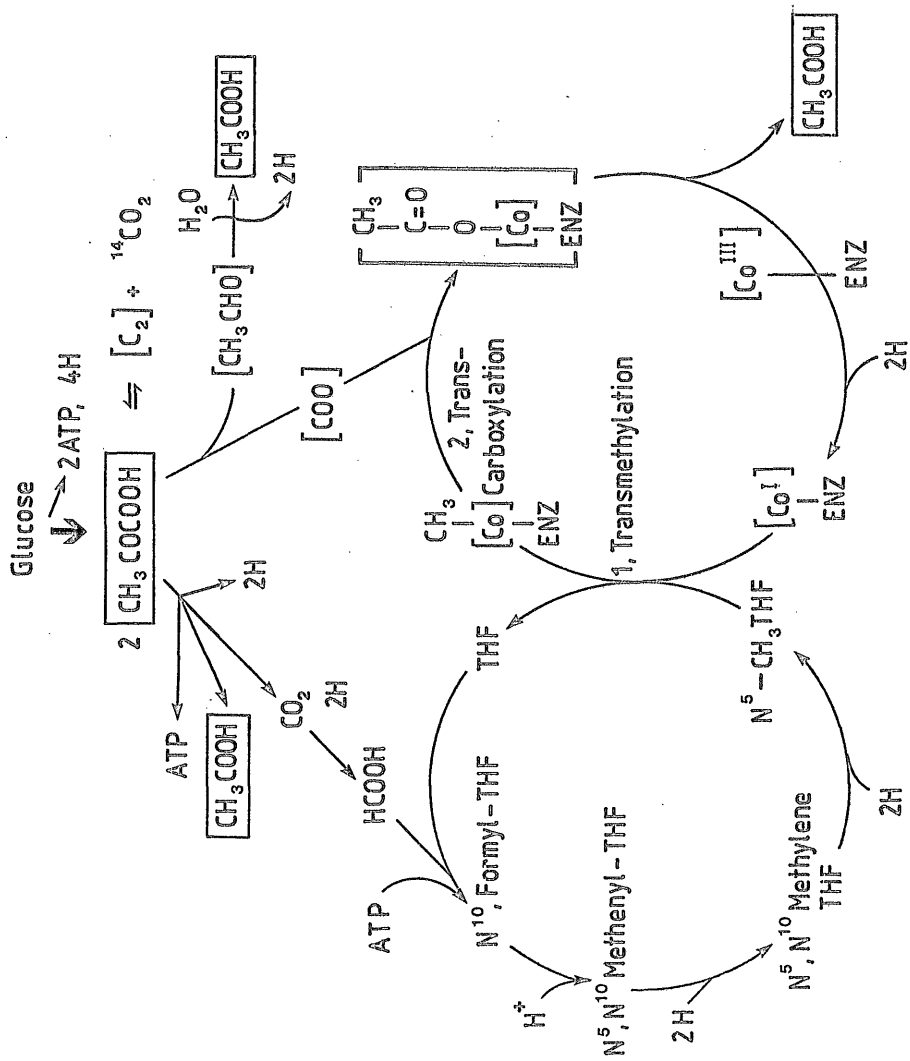
Methylated metals have high environmental significance because of bioaccumulation and bio-hazard. Methylcobalamin is shown to be a methylating coenzyme in biomethylation reactions of metals. Methylated metals are thermodynamically unstable in water but kinetically stable. Metals that are lower in their periodic groups form metal alkyls which are kinetically more stable, for example Hg, Pt and Pb form potentially more stable systems whereas Pd, Cr and Cd do not form stable systems. Methylation of metals takes place predominantly by the transfer of methyl radical or methyl anion.

#### Examples of methyl carbanion transfer

Co-ordination of DMB to the cobalt atom is very important in determining the kinetics of methyl transfer to metals via methyl anion. This is illustrated by the fact that methylation of mercuric ions by "base-on" methylcobalamin is 1000 times faster than in "base-off" species (79).

The coordinating nitrogen atom of DMB is a "hard" Lewis base and therefore this may be expected to co-ordinate to a

Figure 1.2. Outline of the mechanism of synthesis of acetate by C. thermoaceticum.

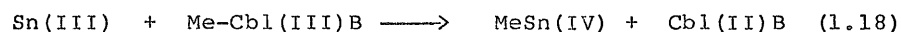




"hard" Lewis acid. Hence a balance exists between the capacity of a metal ion for methylation and its ability to inhibit methylation by co-ordinating to DMB. "Soft" acids such as Hg(II), Pd(II) and Tl(III) react rapidly with methylcobalamin in displacing methyl anion. Figure 1.8 shows the methylation of Hg(II) ions.

#### Examples of methyl radical transfer

For this reaction to occur the attacking species must be a free radical. Sn(III) can be methylated by radical transfer to give  $B_{12r}$  and methylated Sn(IV) (eq. 1.18) (81). A similar mechanism has been proposed for Cr(II) (82). RS radicals such



as homocysteine radicals can be methylated by this mechanism (83). Methionine synthetase is the only example wherein homocysteine anions attack the Co-C bond of methylcobalamin leading to methyl carbonium ion transfer.

#### Labilisation of Co-C bond by outersphere interaction

The last two sections describes the electrophilic and free radical attack on Co-C bond. In this section reactions involving interactions with the corrin ring leading to labilisation of the Co-C bond is discussed. Methylation reactions with Pt and Ir salts have been extensively studied and hence they are discussed below.

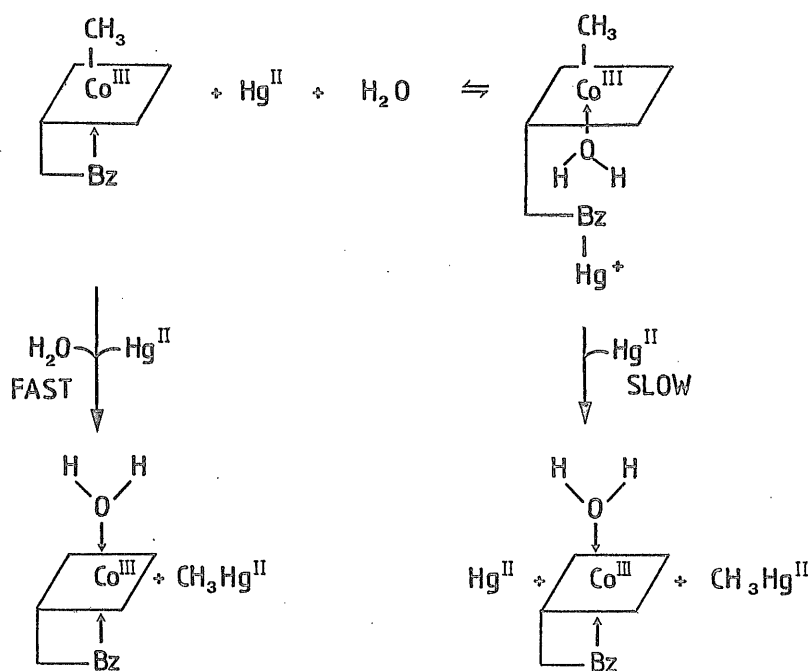


Figure 1.8. Methylcobalamin-dependent methylation of Hg (II) salts.

### Methylation of Pt

This reaction needs Pt salts in both the oxidation states. Initially Pt(II) salt forms an outer sphere complex with the corrin ring through amide side chains. Then Pt(IV) salt interacts with this complex catalysing the transfer of two electrons between the two Pt centers. This is called the "redox-switch" mechanism (83) (Fig 1.9).

### Interaction with hexachloroiridate

In this reaction iridium(IV) interacts with methylcobalamin to give a Co(IV) species by electron loss. This leads to the loss of methyl radical which reacts with hexachloroiridate to give chloromethane (84) (Fig, 1.10). Au(III) salts also give chloromethane by a similar mechanism (85).

### Biological significance of interaction of methylcobalamin with Pt.

cis-dichloro diamino platinum(II) and some of the related Pt(II) complexes are shown to be potentially anti-carcinogenic. Some of these complexes form stable complexes with CoB<sub>12</sub> and methylcobalamin and they are potent inhibitors of B<sub>12</sub>-dependent methionine synthetase and ribonucleotide reductase. Methylcobalamin has been implicated as an important constituent in rapidly dividing cells in spleen, the human foetus and several neoplasms (86). Demethylation of methylcobalamin through activation of Co-C bond by complexation with Pt(II) is supposed to inhibit the growth of B<sub>12</sub>-dependent mutants of E. coli B (84-87). Some of the symptoms of Pt(II)-anti cancer drugs like neuropathy are similar to that

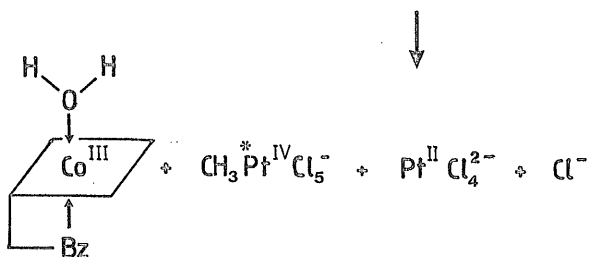
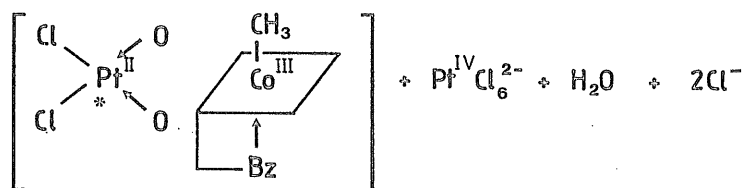
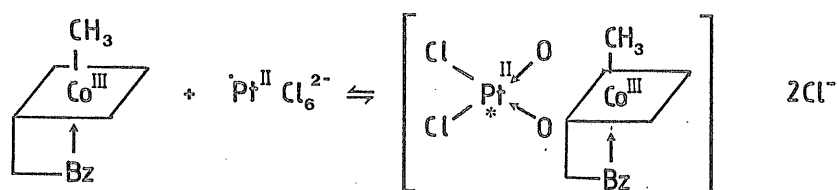


Figure 1.2. Methylcobalamin-dependent methylation of platinum salts.

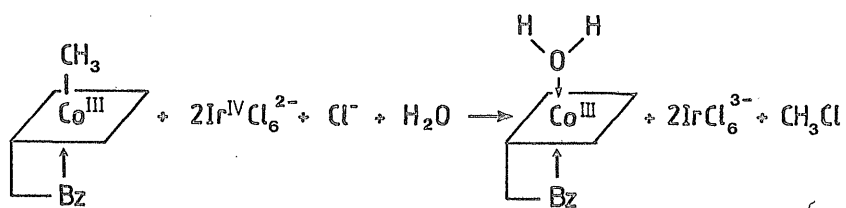
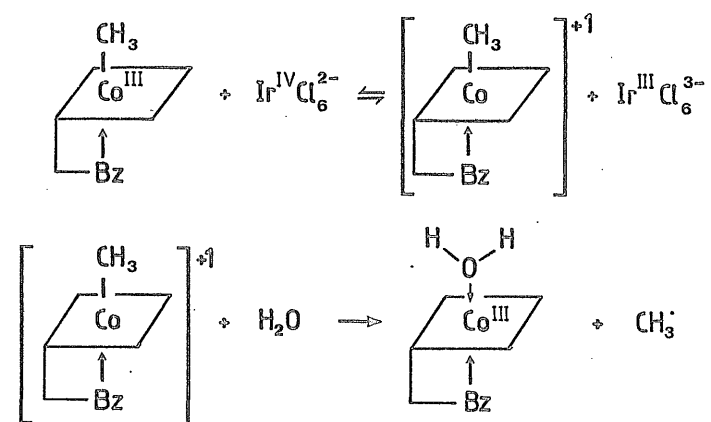


Figure 1.10. Oxidative cleavage of methylcobalamin by Ir (IV).

associated with vitamin B<sub>12</sub> deficiency(84-87).It is suggested that one of the sites of action of anti-cancer Pt(II) drugs is cobalamin which may retard or prevent the growth of cancer cells.

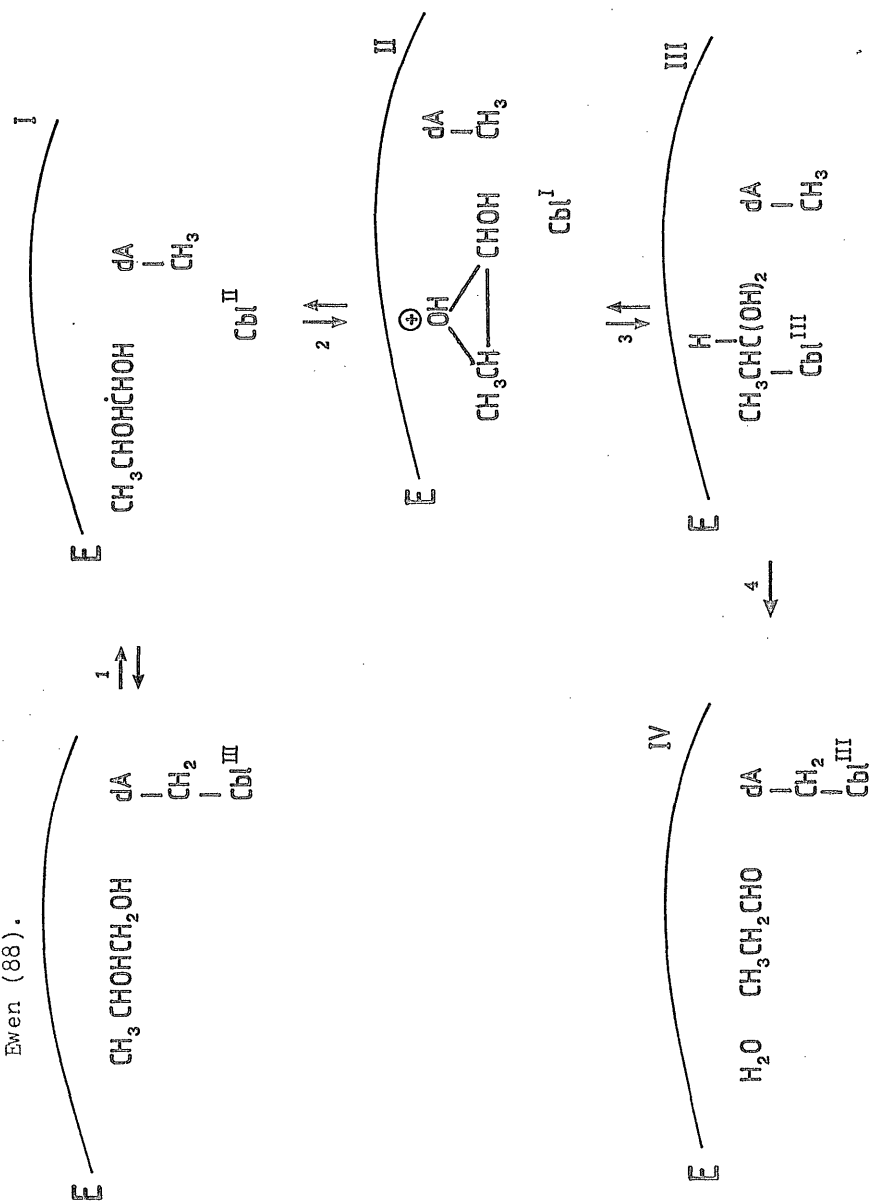
CHAPTER 2COBALAMINSINTRODUCTION

Figure 1.4 depicts one of the mechanisms proposed for  $\text{CoB}_{12}$  dependent rearrangement reaction. An alternative mechanism proposed by Ewen(88) is shown in Fig 2.1. One of the major differences between the two mechanisms is the intermediate formation of Co(I) and Co(III) forms of cobalamin in the mechanism proposed by Ewen. The formation of  $\overset{\text{H}_2}{\text{Co}}(\text{I})$  form is strongly supported by the nitrous oxide inhibition of  $\text{CoB}_{12}$  dependent enzyme reaction(89,90). The formation of Co(III) form of the coenzyme is also supported by some of the observations in the model experiments of enzymatic rearrangements(91,92) and by mechanisms involved in the synthesis of some alkylcobaloximes(34).

In methionine synthetase the  $\text{B}_{12r}$  form of the enzyme is inactive, but it is activated when it is reduced to the  $\text{B}_{12s}$  form. It is the latter form that catalyses the transfer of methyl group from methyltetrahydrofolate to homocysteine (cf, Fig 1.6).

Ribonucleotide reductase also differs in some of its mechanistic aspects such as the formation of different Co(II)...radical pairs. It is thus evident that  $\text{CoB}_{12}$  and methylcobalamin under different enzymatic conditions, play different roles i.e., facilitate rearrangement, effect

Figure 2.1. Proposed mechanism for the CoB<sub>12</sub>-dependent enzyme reactions by Ewen (88).



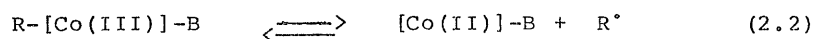
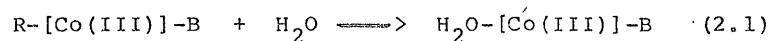


reduction or transfer a methyl group. In order to perform these functions it has to exist in different oxidation states which is determined by the mechanism of Co-C bond cleavage. Dissociation of the Co-C bond is also necessary to generate alkyl radicals to initiate radical reaction and a cobalt(II) center for the formation of a complex with the substrate-related or product-related radicals. Hence the chemistry of Co-C bond has been extensively studied in several laboratories. Halpern and co-workers have done a great deal of work on the thermochemistry of Co-C bonds (18). Saveant and co-workers have studied the electrochemistry of Co-C bond (93,94). A large number of other workers have used pulse-radiolysis and photolysis to study the reactions of Co-C bonds in cobalamins and model cobaloximes under various experimental conditions (93-112). The relevance of Co-C bond cleavage in enzymatic reactions has been discussed in chapter 1 but a brief discussion pertinent to the results presented in this chapter will be made. The Co-C bond of alkylcobalamins can be dissociated by homolysis or heterolysis according to equations 1.7-1.9.

#### Homolysis of Co-C bond

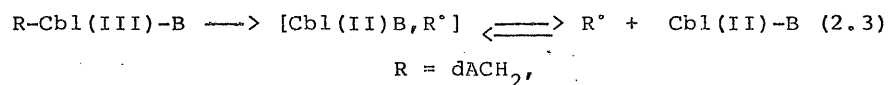
(a) Photolysis. Two types of chemical reactions can be distinguished;

(i) Photoaquation (eq 2.1). (ii) Photoreduction (eq 2.2).

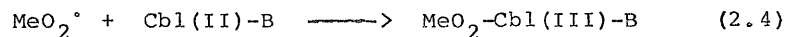
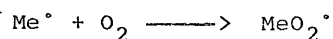
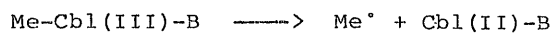


In this chapter only photoreduction will be considered.

Photolysis of  $\text{CoB}_{12}$  at 200K leads to Co-C bond cleavage; the bond remains in a state of incipient homolysis stabilised within the matrix. On annealing it leads to the  $\text{B}_{12r}$  form (107) (eq, 2.3). Endicott and Netzel (100) have disputed this. They have argued that neither methylcobalamin



nor  $\text{CoB}_{12}$  gave any long lived homolysis precursors, but they proposed a mechanism shown in eq, 2.4. Ghanekar *et al.* (105)



have, however, observed the formation of exchange coupled  $\text{Co(II)} \dots$  radical pairs in their studies of  $\text{CoB}_{12}$ . Johnson and co-workers have shown that the photolysis of  $\text{CoB}_{12}$  in the presence of a spin-trap t-butyl nitroxide produced  $\text{B}_{12r}$  and the trapped  $\text{dACH}_2$  radical (106). Similar results were obtained for ethylcobalamin.

Hogenkamp and co-workers studied the effect of oxygen on the homolysis of Co-C bond. They have shown that methylcobalamin in the presence of oxygen gave aquocobalamin and

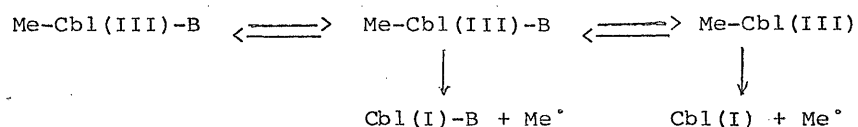
formaldehyde but in the absence of oxygen,  $B_{12r}$  and formaldehyde were produced. Dolphin *et al.* (113) have shown that higher alkylcobalamins such as ethylcobalamin produced ethylene from the initially formed ethyl radical by beta-elimination of a hydrogen atom.

Several laboratories have studied the photolysis of  $CoB_{12}$  and alkylcobalamins in the presence of amino alcohols or diols in order to provide a non-enzymatic model for diol dehydrase and ethanolamine ammonia-lyase systems (114-116). A number of substrates such as hydroxyalkyl- or amino hydroxyalkyl cobalamins have also been studied as model systems for cobalt substrate interaction. These systems have not been discussed here due to lack of space.

Photolysis of "base-on" and "base-off" cobalamins have shown that "base-on" form is more photolabile than the corresponding "base-off" forms (37, 102, 117).

Examples of nucleophilic and electrophilic attack on Co-C bond were discussed in the previous chapter. A brief discussion of reductive cleavage of Co-C bond will be presented in this section.

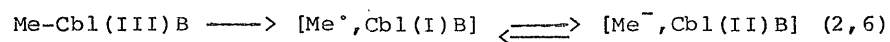
Hydrogenation of methylcobalamin in the presence of platinum yields methane and  $B_{12r}$ . A similar hydrogenation of  $CoB_{12}$  could not be demonstrated apparently due to the steric effects of the larger nucleoside moiety (118). However, electrochemical reduction of  $CoB_{12}$  and methylcobalmin has been demonstrated and it was shown to follow the scheme in eq. 2.5 (94, 101).



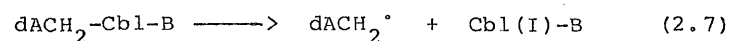
(eq 2.5)

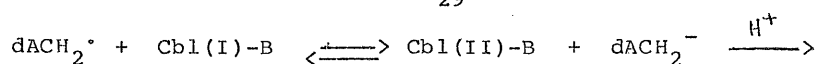
("Base-off" forms)

Electron addition at 77 K gave different results. Seki et al. have shown that  $\text{CoB}_{12}$  gave  $\text{Co(I)}$  and  $\text{dACH}_2^\bullet$  radicals. Upon warming above 77K,  $\text{Co(I)}$  gave  $\text{B}_{12\text{r}}$  (98). Bachman et al. carried out similar work on methylcobalamin, and they proposed that methylcobalamin at 77K produced an electron adduct which dissociated at 150K to give a methyl radical and a  $\text{Co(I)}$  fragment which were in equilibrium (in a cage) with a methyl anion and  $\text{Co(II)}$  (eq 2.6). The equilibrium of this reaction



is assumed to be towards the left and hence no e.s.r. paramagnetic species were observed. Blackburn and co-workers (108) using <sup>a</sup>pulse-radiolysis method, proposed that  $\text{CoB}_{12}$  results in an electron adduct which decays to give  $\text{B}_{12\text{r}}$  and a  $\text{dACH}_2^-$  anion. Two mechanisms have been proposed for this (eq, 2.7 and 2.8) and in both the cases  $\text{B}_{12\text{r}}$  is the end product.





The present work on cobalamins was initiated with the following aims;

(1) One of the main purposes was to add an electron to Co-C  $\sigma^*$ -orbital and to study the spin distribution.

(2) It was also of interest to study the structure of the electron-adduct formed by electron addition to cobalamins at 77 K.

(3) The Co(II)....radical pair has been observed in several  $B_{12}$  dependent enzymatic reactions but not in non-enzymatic systems, except in the case of  $\text{CoB}_{12}$  (105). Hence it was of interest to observe it in the case of methylcobalamin.

(4) To study the effect of substituted alkyl ligands on electron addition and photolysis.

Two methods have been used to generate paramagnetic centres. They are; (1) photolysis and (2) radiolysis.

The primary event in the radiolysis of dilute solutions of a solute (frozen at 77K) in a glassy medium such as methanol/water system is the loss of an electron from the solvent. This electron, being mobile, moves in the matrix until it is trapped by the solute. Thus, anion-radicals formed in a low temperature matrix can be studied by e.s.r. spectroscopy.

The first part of this chapter describes the radiolysis and the second part describes the photolysis work of cobalamins.

EXPERIMENTAL

CoenzymeB<sub>12</sub> and cyanocobalamin were obtained from Sigma chemicals. CD<sub>3</sub>I (99 atom%) was supplied by Aldrich chemicals and <sup>13</sup>CH<sub>3</sub>I (90 atom%) was supplied by Prochem Ltd. Aquocobalamin was prepared by the method of Kaczka *et al.* (119). Methylcobalamin, CD<sub>3</sub>cobalamin and <sup>13</sup>CH<sub>3</sub> cobalamin were prepared as described in methods in enzymology (120). A typical preparation is described as follows;

80 mg of cyanocobalamin or hydroxocobalamin and 8 mg of cobaltous nitrate were dissolved in 8 ml of water. Argon was bubbled through the solution for 40 mins. 20 mg/ml of sodium borohydride was then bubbled with argon for 10 mins and 0.8 ml of this was added to the cobalamin solution and argon was continued to stream for a further 10 mins. 0.07 ml of methyl iodide was added to the solution and it was stored in the dark. The optical spectrum of a sample of this solution was checked for methycobalamin. For the preparation of other alkylcobalamins, <sup>The</sup> corresponding alkyl iodides were used.

Acetylcobalamin was prepared by the method of Smith *et al.* (121) as described by Dolphin (120).

Extraction of cobalamins

Cobalamins were extracted from the reaction mixture with a 50% phenol solution in methylene dichloride (1;1) until the aqueous layer was colourless. Water (40% by volume) was added to the phenol extract to remove salts. The water layer was separated after repeated washings and finally the phenol extract was diluted (by ten times the volume of extract) by

methylene dichloride. To this, water (5% of the volume of organic layer) was added and repeatedly extracted until the organic layer was colourless. The aqueous solution containing cobalamin was washed with methylene dichloride to remove traces of phenol and was freeze-dried. All operations were done in the dark. The products of all preparations were extracted as above and purified. Methylcobalamin was purified by CM-cellulose chromatography and the purity of the preparations was checked by paper chromatography and optical spectroscopy (120).

$^{13}\text{CN}$ -cyanocobalamin was prepared by mixing  $\text{K}^{13}\text{CN}$  and one equivalent of aquocobalamin in a nitrogen atmosphere. Dicyanocobalamin was prepared using more than two equivalents of cyanide. In all these cases the final concentration of aquocobalamin was not more than 5 mM. Samples for radiolysis were prepared by dissolving cobalamins in  $\text{D}_2\text{O}/\text{CD}_3\text{OD}$  or water/ethyleneglycol so that the final concentration of cobalamins was 10-20 mM. Glassy beads were made by pipetting out drops of the solution directly into liquid nitrogen. Beads were transferred to sample bottles and were irradiated in a Vickrad cell with doses upto 6 Mrad. E.s.r. spectra were measured at 77K on a Varian E-109 spectrometer calibrated with a Hewlett-Packard 5246L frequency counter and a Bruker B-H12E field probe which were standardised with DPPH.

Samples for photolysis were prepared as described above except samples were placed in 1mm (diameter) capillary tubes (made from supracil glass) and they were irradiated

at 77K for upto six hours using a 100 Watt high pressure mercury lamp equipped with a uv light filter.

E.s.r.spectra were recorded and annealing experiments were carried out by decanting liquid nitrogen and monitoring the spectrum. Liquid nitrogen was added whenever significant changes were observed. In all these studies great care was taken to avoid any fortuitous photolysis of methylcobalamin as it is highly photolabile.

## RESULTS AND DISCUSSION

### RADIOLYSIS WORK

#### Spectral interpretation

In many cases, parallel (z) features for Co(II) complexes were relatively well defined, but the "perpendicular" ( $x, y$ ) features were poorly defined, and only approximate data have been derived there from. Pilbrow and co-workers have made a detailed study of such spectra and have concluded that the principal directions for  $A_{xx}, A_{yy}$  and  $g_{xx}$  and  $g_{yy}$  are probably far apart for corrin ring systems (122). Hence it is extremely difficult to extract principal values accurately, and this task has not been attempted. Nevertheless, in some cases it was possible to extract good "perpendicular" values for the  $^{14}\text{N}$  and  $^{13}\text{C}$  components, the latter being facilitated by comparing well defined features for the  $^{12}\text{C}$  and  $^{13}\text{C}$  Spectra. For all substrates in dilute solution in  $\text{CD}_3\text{OD} + \text{D}_2\text{O}$  solvents, electron capture was efficient since the normal intense violet colour due to trapped electrons was largely suppressed.

#### Cyanocobalamin



A typical e.s.r. spectrum obtained from dilute solutions of cyanocobalamin after exposure to  $^{60}\text{Co}$  gamma-rays at 77 K is shown in figure 2.2. This spectrum is better defined than that of Seki *et al.* (98), enabling  $\bigcirc$  to extract some of the e.s.r. parameters (table 2.1). The parallel features are flat-topped, almost certainly as a result of coupling to  $^{14}\text{N}$ . Indeed in one region at least, this was just resolved. The resulting coupling constant is given in table 2.1. Replacing  $^{12}\text{CN}$  by  $^{13}\text{CN}$  gave an extra doublet splitting as indicated in fig 2.2b. On slight annealing, these features were replaced by features characteristic of  $\text{B}_{12\text{r}}$  (figure 2.3). The retention of  $^{14}\text{N}$  hyperfine features and loss of  $^{13}\text{C}$  features confirm that  $^{13}\text{CN}^-$  ligands are lost in preference to DMB ligands.

#### The dicyano derivative

The e.s.r. spectrum obtained at 77 K differed slightly from that obtained on annealing, but the changes seem to indicate minor lattice or solvation modifications rather than chemical changes. For the  $(^{13}\text{CN})_2$  derivative, only one  $^{13}\text{C}$  splitting was observed, as can be seen by comparing the spectra in figures 2.4a and 2.4b. These results show that, in contrast with the mono cyano derivative, <sup>the</sup> dicyano derivative lost one cyanide at 77 K. However, the  $\text{CN-B}_{12}$  anion lost  $\text{CN}^-$  at temperatures in the region of 150 K, it can not be deduced from this result that the parent anion for the dicyano derivative is not a significant intermediate. All one can say is that it is far less stable than that of cyanocobalamin.

#### Aspects of structure-cyanocobalamin<sup>a</sup> anion

Figure 2.2. First-derivative X-band e.s.r. spectra obtained from cyanocobalamin :  
 (a)  $^{12}\text{CN}$  and (b)  $^{13}\text{CN}$ . Features are assigned to parent anions.

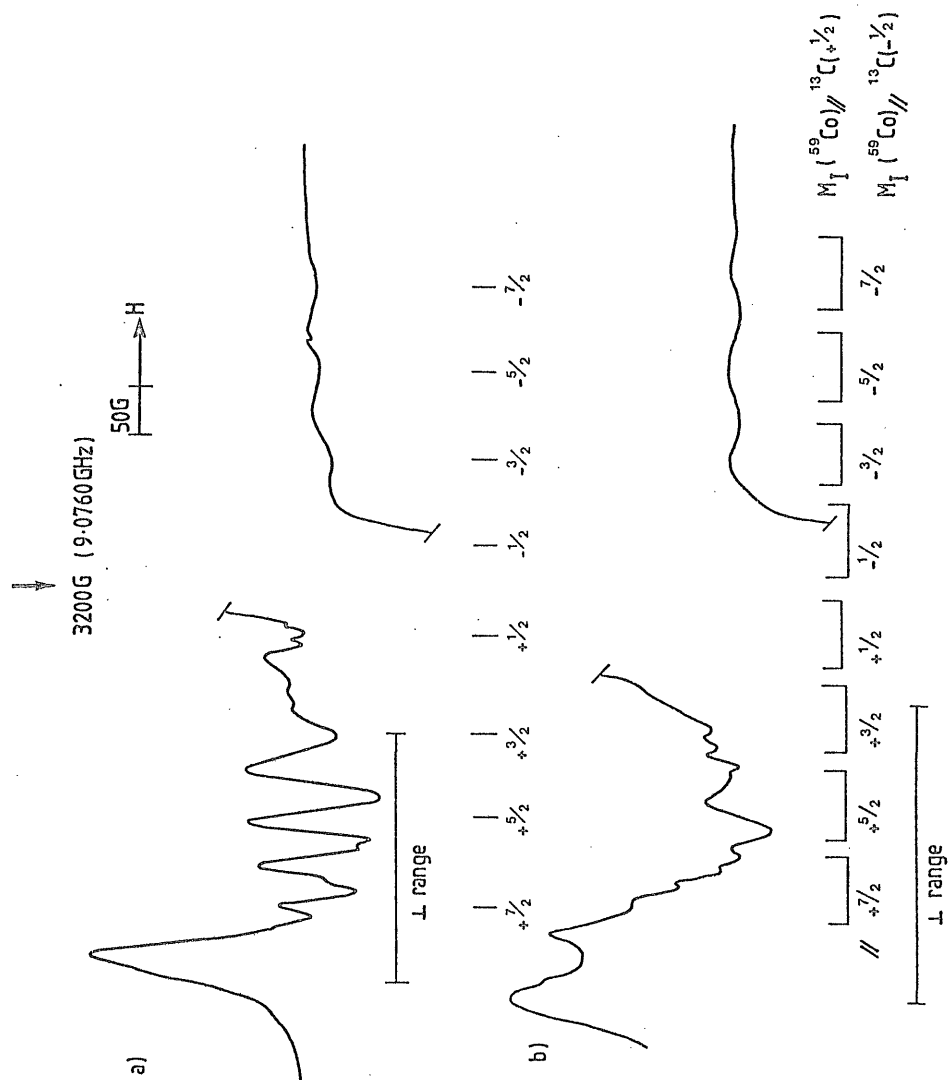
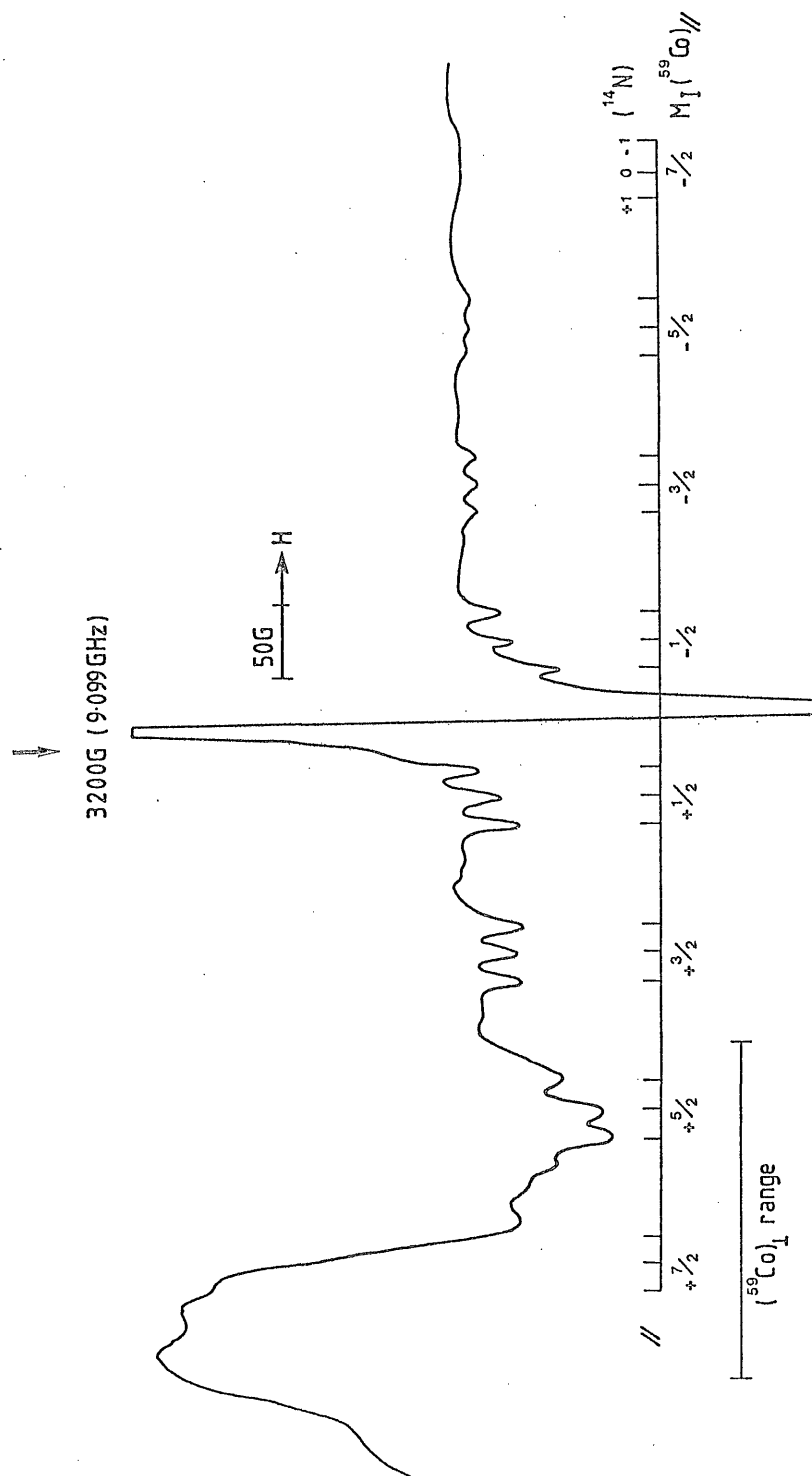


Figure 2.2. First-derivative e.s.r. spectrum of B<sub>12</sub>r.



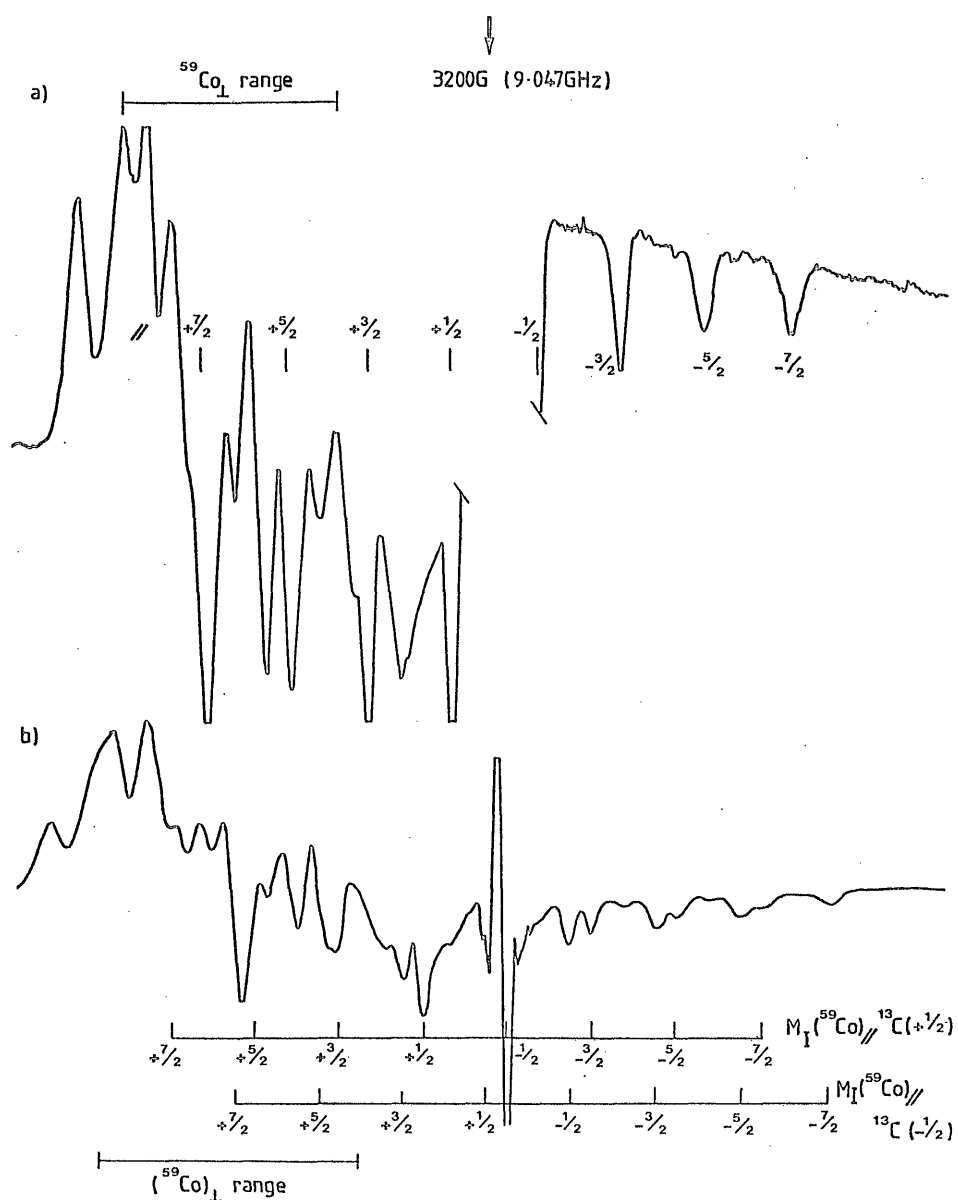


Figure 2.4. First-derivative e.s.r. spectra obtained from dicyanocobalamin (a)  $^{12}\text{CN}$  and (b)  $^{13}\text{CN}$ .

Table 2.1 E.s.r. parameters for CN-cobalamin derivative and related compounds

Radical	Nucleus	Hyperfine coupling constants/G <sup>a</sup>		g-Values		
		A <sub>z</sub>	A <sub>x</sub>	A <sub>y</sub>	g <sub>z</sub>	g <sub>x</sub> g <sub>y</sub>
(CN-B <sub>12</sub> ) <sup>-b</sup>	<sup>59</sup> Co	87	ca.40	ca.40	2.009	ca.2.22 ca.2.22
	<sup>14</sup> N	ca.13	-	-		
	<sup>13</sup> C	70	ca.60	ca.60		
(B <sub>12</sub> CN) <sup>-c</sup>	<sup>59</sup> Co	85	ca.12	ca.12	2.004	ca.2.17 ca.2.17
	<sup>13</sup> C	65	ca.55	ca.55		
Co(CN) <sub>5</sub> <sup>2-d</sup>	<sup>59</sup> Co	81	(-)26	(-)26	2.004	2.17 2.17
	<sup>13</sup> C <sub>ax</sub>	37	31	31		

(a) = 0.1 mTelsa. The <sup>59</sup>Co perpendicular data are rough approximations.

(b) The anion of B<sub>12</sub>

(c) The monocyanoide derived from the dicyanide by electron addition.

(d) ref 123.

The form of  $g$  and  $A$  tensor components show that, to a first approximation, the semi-occupied metal molecular orbital is  $3d_{z^2}$ . This is confirmed by the  $^{14}\text{N}$  and  $^{13}\text{C}$  tensor components, which are characteristic of sigma-bonding rather than pi-bonding. It is interesting to compare the new  $^{13}\text{C}$  data with those of others (table 2.1). In particular, there is a large increase on going from the axial CN for  $\text{Co}(\text{CN})_5^{2-}$  complexes to the present structure (123). This does not reflect the presence or absence of a sixth ligand, since both six co-ordinated cyanocobalamin anion and the five-coordinated derivative gave comparable coupling constants to  $^{13}\text{C}$ . Thus it seems to be connected to strong binding to the corrin ring relative to the four equatorial cyanide ligands in  $\text{Co}(\text{CN})_5^{3-}$ . Thus it in turn, suggests  $3d_{z^2} 4s$  admixture rather than  $3d_{z^2} 4p$  admixture. The former removes electron density from the  $x-y$  plane in the anti-bonding orbital, whilst the latter for 5-coordination, shifts spin-density into the empty site, away from the axial ligand. It is interesting that the latter mechanism seems to be relatively unimportant despite the fact that it would reduce the antibonding effect of the unpaired electron.

#### Methylcobalamin

For this derivative, and also the ethyl and deoxyadenosyl derivative ( $\text{CoB}_{12}$ ) no characteristic Co(II) features were seen at 77 K, but a broad and unresolved feature ( $H_{ms} = 17 \pm 3$  G) was obtained in addition to signals from solvent radicals ( $\text{CD}_3\text{OD} + \text{CD}_3$ ). This is assigned to the electron adducts with the

electron in a  $\pi^*$  corrin orbital with a low spin density on cobalt. Since the width of this feature did not change on going from  $-\text{CH}_3$  to  $-\text{CD}_3$ ,  $^{-13}\text{CH}_3$ ,  $\text{C}_2\text{H}_5$  or adenosyl, the unpaired electron cannot be closely involved with these groups. On annealing to 150 K there was no change in the spectrum. However on annealing to ca. 183 K the central features were lost and clear features for a Co(II) derivative grew in (species A in figure 2.5). These features were lost on warming to room temperature and re-cooling, but were not replaced by other e.s.r. signals.

The e.s.r. parameters for species A (table 2.2) are not those expected for a normal Co(II) complex with the excess electron in the  $d_{x^2-y^2}$  orbital. However, with  $g_{\parallel} > g_{\perp} > 2.0023$  and  $|A_{\parallel}|(^{59}\text{Co}) > |A_{\perp}|(^{59}\text{Co})$  they are normal for a complex with a  $d(x^2-y^2)$  configuration. These parameters were unchanged on going to  $\text{CD}_3$  or  $^{-13}\text{CH}_3$  derivatives.

#### The ethyl derivative

The methyl derivative was unique in giving this  $d_{x^2-y^2}$  complex (A). The ethyl derivative also gave no yield of any species exhibiting  $^{59}\text{Co}$  hyperfine coupling at 77 K, but on annealing to ca. 183 K or on exposure to visible light, a good spectrum of  $\text{B}_{12r}$  derivative grew in, with loss of the  $\pi^*$  corrin anion species.

#### The acetyl derivative

This gave a normal electron adduct at 77 K similar to, but not identical with the  $\text{B}_{12r}$  derivative. On annealing to ca. 160 K these features were replaced by those for normal  $\text{B}_{12r}$ .

Figure 2.5. First-derivative X-band e.s.r. spectrum obtained from methylcobalamin. Features are assigned to Co ( $d_{x^2-y^2}$ ) complex.

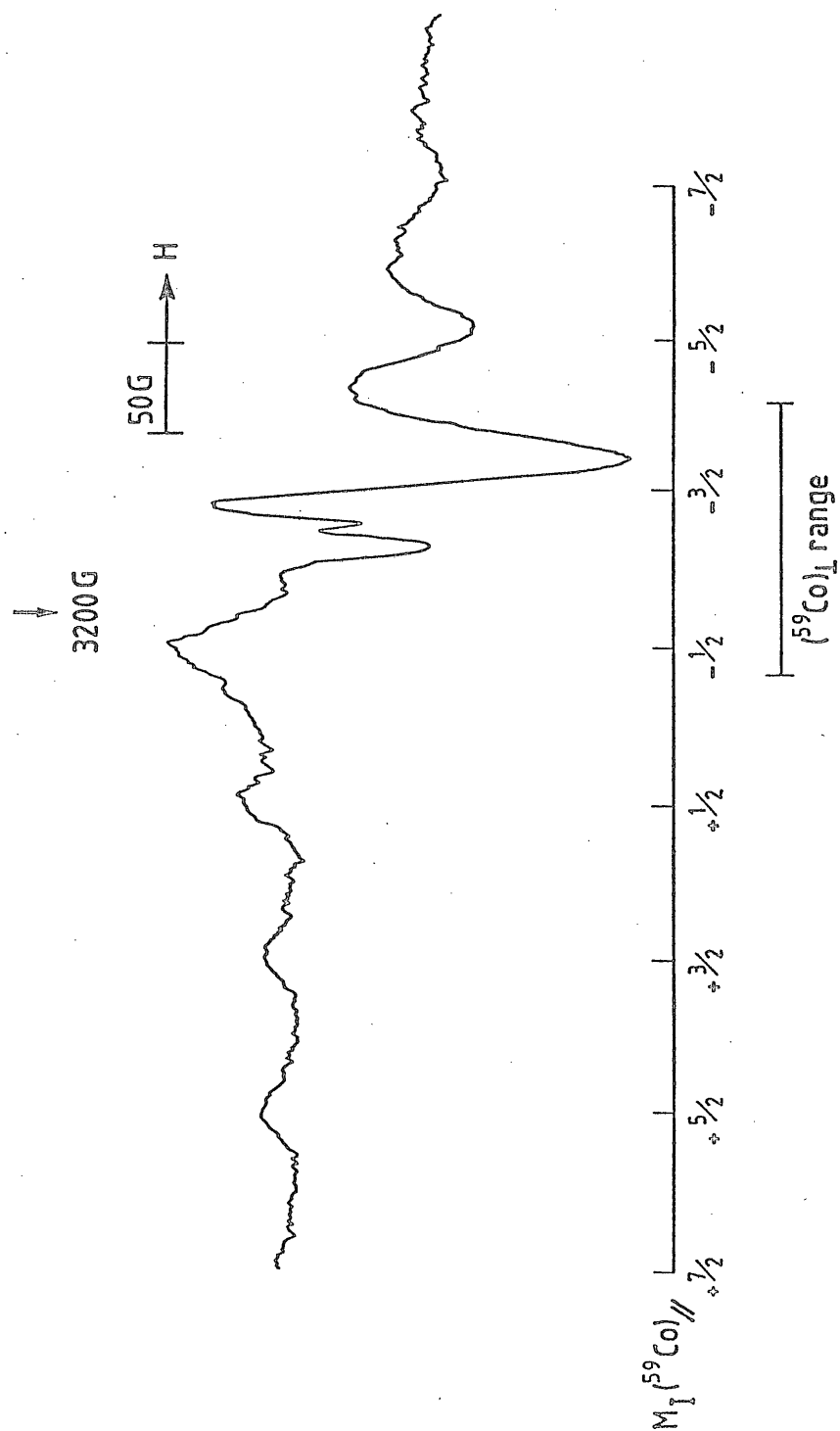




Table 2.2 Some experimental parameters for methylcobalamin and related

compounds

Radical	nucleus	Hyperfine coupling g-values constants/G <sup>a</sup>			
		$A_{\parallel}$	$A_{\perp}$	$g_{\parallel}$	$g_{\perp}$
B <sub>12</sub> r	<sup>59</sup> Co	108	NR	2.003	2.32
	<sup>14</sup> N	18	NR		
B <sub>12</sub> (d <sub>x<sup>2</sup>-y<sup>2</sup></sub> )	<sup>59</sup> Co	87	30	2.077	2.016
	<sup>14</sup> N	10	NR		
(CH <sub>3</sub> CoB <sub>12</sub> ) <sup>-</sup>	<sup>59</sup> Co	106	NR	2.006	2.28
	<sup>14</sup> N	17	NR		

(a) = 0.1 mTelsa

NR Not resolved.

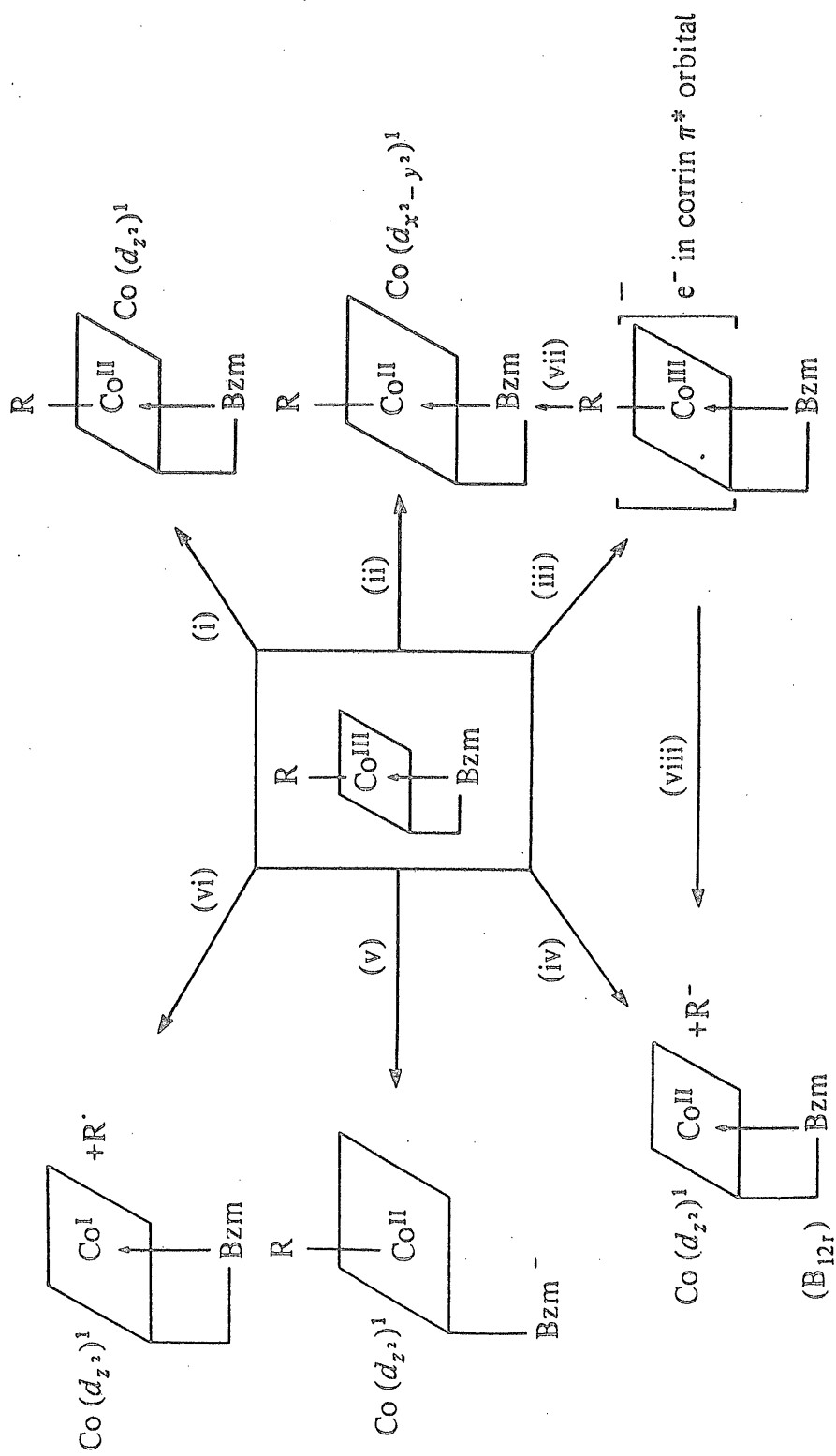
Coenzyme B<sub>12</sub>

This work confirms the results of Seki *et al.* (98) in that, as with the methyl and ethyl derivatives, there was no evidence for any species with a high spin-density on cobalt after exposure at 77 K. A 17 G line was obtained however, on annealing to 160 K this was lost and signals from B<sub>12r</sub> grew in.

Mechanism of electron addition to alkylcobalamins

These results are not easy to interpret. It seems that the following pathways are available on electron addition (Figure 2.6). Reactions (i) and (v) are unlikely since the electrons in the products are in  $\sigma^*$  Co-C orbitals, and one expects to see strong  $^{13}\text{C}$  hyperfine coupling as is found, for example, from  $^1\text{H}$  in  $\text{M-H } \sigma^*$  systems (125, 126). This was never seen. Also, although the  $^{59}\text{Co}$  hyperfine coupling should be reduced because of delocalisation onto the alkyl carbon, the general form of the spectrum should not differ greatly from that for cyanocobalamin. Hence (i) and (v) are ruled out for all but for the acetyl and cyano derivatives. In these cases (v) can be ruled out because  $^{14}\text{N}$  coupling was observed. Clearly (iv) does not occur at 77 K. Also (ii) does not occur at 77 K since this should give distinctive  $g$ -shifts and large  $^{59}\text{Co}$  hfs. This leaves (iii) and (vi) as the remaining possibilities. Both should give  $g = 2$  signals, which are observed, but these were not due to  $^{\bullet}\text{CH}_3$  or  $^{\bullet}\text{C}_2\text{H}_5$  radicals, neither of which could be detected. One of the purposes in using  $\text{CD}_3\text{OD}$  and  $\text{D}_2\text{O}$  solvent systems was that it has been previously shown that  $^{\bullet}\text{CH}_3$  radicals formed from photolysis at 77 K can be seen by

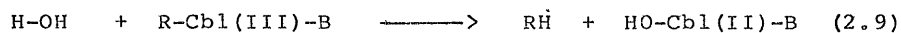
Figure 2.6. Pathways for electron addition to various alkylcobalamins.



e.s.r.spectroscopy(127).Furthermore  $^{\bullet}\text{CH}_3$  radicals are stable in such media at 77 K (see photolysis section below).The less reactive ethyl radicals would also be expected to be stable in this medium.Since they were not detected even in trace yields after long irradiation times,their formation is most improbable.Thus process (vi) seems to be unlikely.Although Seki *et al.*(98) and Bachman *et al.*(99) presented optical evidence for  $\text{B}_{12\text{s}}$  formation at 77 K with the coenzyme. There is clear evidence for spectral modification,but the spectra were not identical with the normal spectrum for  $\text{B}_{12\text{s}}$ ,and could possibly have been due,for example,to the (corrin) $^-$  derivative whose spectrum is not known.

It can be concluded that,at least for the methyl and ethyl derivatives,reaction (iv) is unlikely,and hence (iii) is favoured.Absence of strong coupling to  $^{59}\text{Co}$  is expected since the  $(\text{d}_{\text{xz}})$  and  $(\text{d}_{\text{yz}})$  orbitals are occupied,so the  $\pi^*$  level will be localised mainly in the corrin ring.Weak coupling to  $^{59}\text{Co}$ ,if present,must be lost in the line widths,the coupling can not be greater than ca.5-10 G.For the ethyl derivative,a thermal pathway involving electron transfer from the corrin ring into the  $\text{d}_{\text{z}^2}$  orbital must be ultimately favoured, accompanied by Co-C bond cleavage.Since  $\text{B}_{12\text{r}}$  was then formed,this must formally be process (viii).It seems most likely that ethyl anions would leave in preference to DMB,so it may be that protonation is an intimate factor contributing to this reaction,giving ethane as a product.It is not clear

just how such a protonation can occur prior to or during the bond-breaking process, but it can be suggested that it comprises a concerted process involving water, such as shown in eq. 2.9. These results suggest that until such solvation can occur, the excess electron is unwilling to move into the  $d_z^2$  orbital.



The results for the alkyl derivatives make an interesting contrast with those for the cyano complex. In this case because of the more ionic Co-C bond, the electron is able to occupy the  $d_z^2$  sigma\* orbital, with facile loss of  $\text{CN}^-$ . It was surprising that the acetyl derivative behave like the cyano derivative rather than the alkyl derivatives with an initial electron capture into the  $d_z^2$  orbital without ligand loss, followed on annealing by loss of acetyl anion. Probably simultaneous protonation is also required, to give  $\text{CH}_3\text{CHO}$ . This multiplicity of mechanism is quite remarkable. In the particular case of the methyl derivative, analysis of the reaction products for the formation of  $\text{CH}_4$  or  $\text{CH}_3\text{D}$ . In fact, the former was just detectable, but  $\text{CH}_3\text{D}$  was formed in readily detectable yields. Thus Co-C bond breakage must ultimately occur. If so, the expected  $\text{B}_{12\text{r}}$  must have reacted at room temperature with other products, since recooling the solutions gave no detectable features for this species. Further work is needed to unravel these complicated mechanisms,

but it is hoped that these results shed some light on a difficult problem.

#### Conclusions from radiolysis work

Finally, to what extent these new results for the alkyl derivatives impinge on the conclusions of others, especially the divergent conclusions of Blackburn et al. (198) (favouring reaction (iv) in the figure 2.6), of Savéant et al. (93) favouring (vi), of Seki et al. (98) and Bachamn et al. (99) both favouring (vi) in some form or another. It can be concluded that (vi) does not occur at low temperatures, and favour (iii) to give the  $\pi^*$  anion as a better explanation of the results. This may or may not be important at room temperature, but it has the advantage that the electron is retained and is ready to move into the  $d_{z^2}$  orbital. This can be very rapid and avoids all the difficulties associated with reactions (iv) and (vi).

#### PHOTOLYSIS WORK

##### Spectral interpretation

##### Methylcobalamin

At low microwave powers, well defined signals from methyl and  $^*CD_2OD$  radicals were detected (Figure 2.7a). At high powers, very weak features in the low field region indicated a minor yield of normal  $B_{12r}$  but intense features from a novel Co(II) species dominated (Figure 2.7b) (species A). After annealing above 77 K to remove the signals from  $^*CH_3$  and  $^*CD_2OD$  radicals, broad features in the  $g = 2$  region became better

Figure 2.7. (a) First-derivative X-band e.s.r. spectrum of methylcobalamin at low microwave powers. Features are assigned to  $\dot{\text{C}}\text{H}_3$  and  $\dot{\text{C}}\text{D}_2\text{OD}$  radicals.

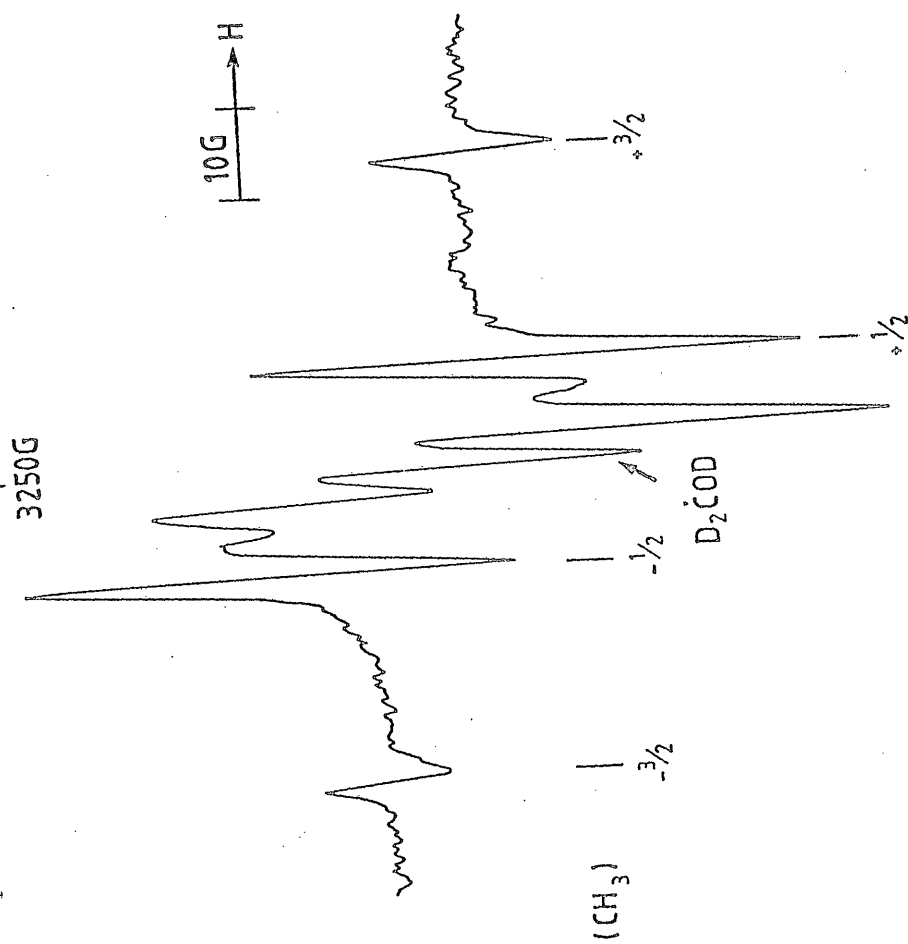


Figure 2.2 (b) First-derivative X-band e.s.r. spectrum of methylcobalamin at high microwave powers. Features are assigned to  $B_{12}$  ( $\alpha$ ) and species A.

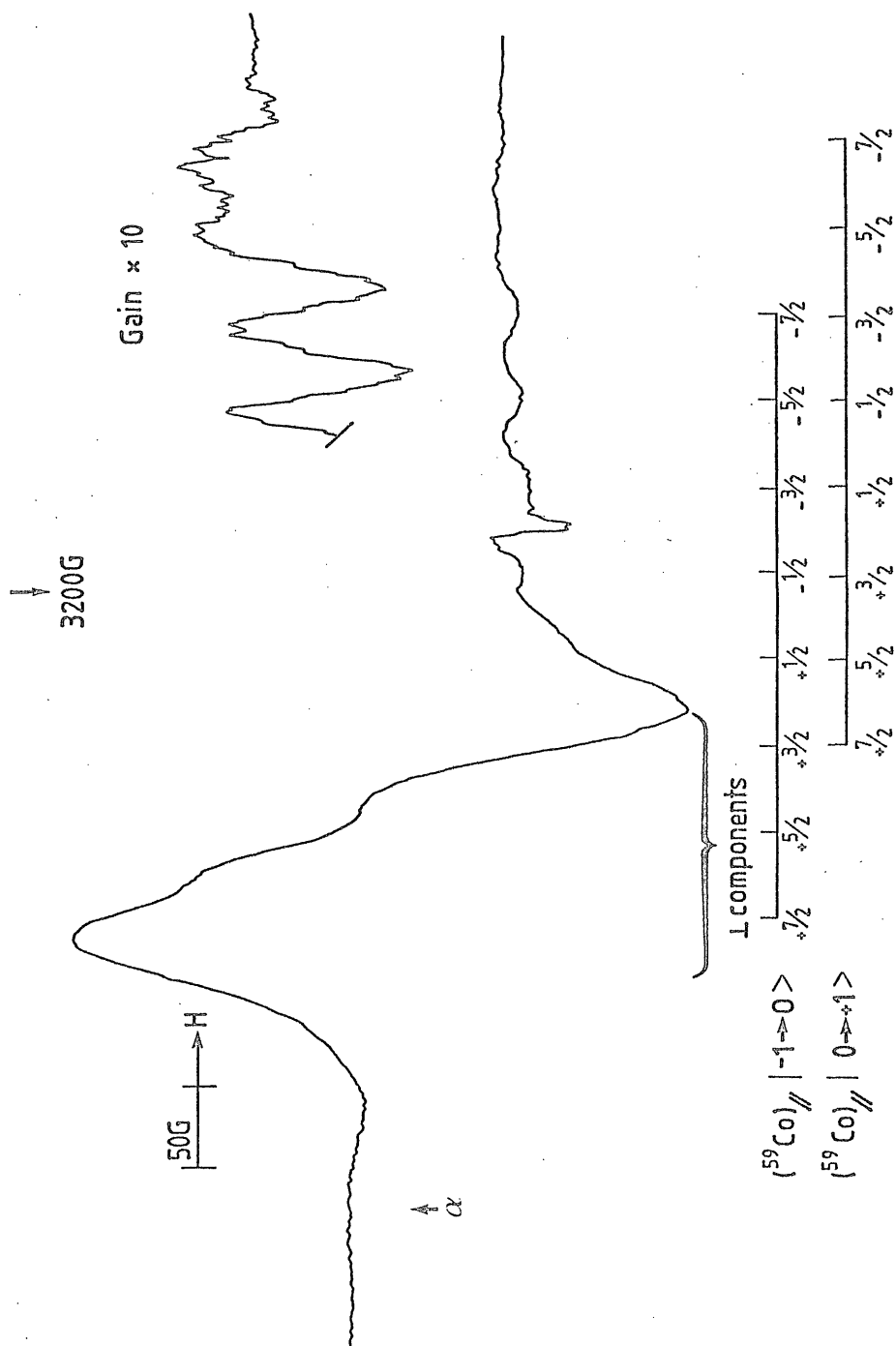
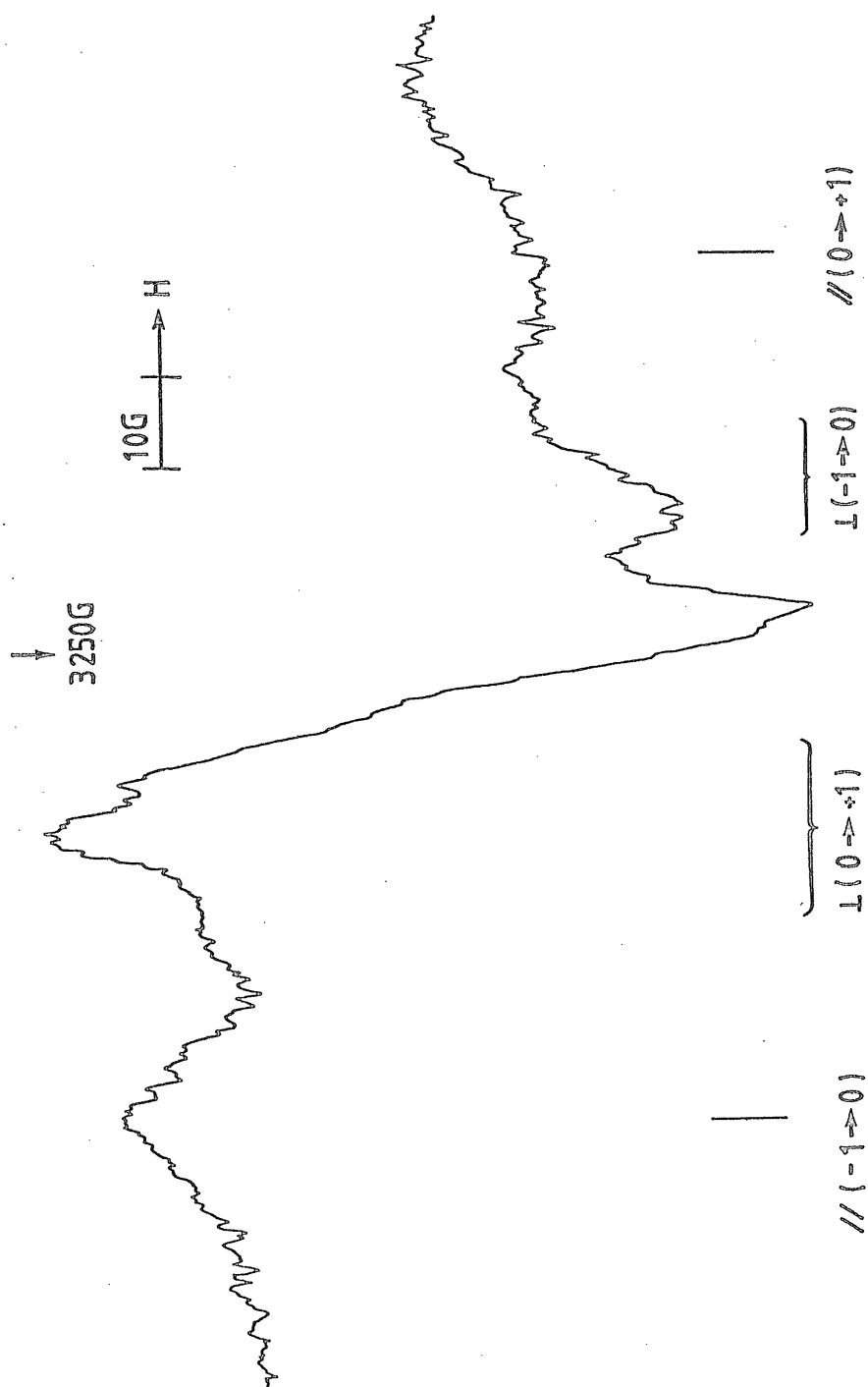




Figure 2.7 (c). First-derivative X-band e.s.r. spectrum of methylcobalamin after annealing. Features are assigned to species B.



defined (Figure 2.7 c) (species B). On further annealing to ca.180 K these features were replaced by those for the normal  $B_{12r}$  (Fig 2.3).

#### Ethylcobalamin

In this case there was no evidence for species A or B, but broadened features for  $B_{12r}$  were detected together with a broad central component which is probably due to ethyl radicals. On annealing these radicals were lost and  $B_{12r}$  features narrowed to their normal widths.

#### CoenzymeB<sub>12</sub>

These results were similar to those of Lowe et al. (197).

#### Acetylcobalamin

No e.s.r. features were resolved after photolysis at 77 K. However on annealing features for  $B_{12r}$  grew in at ca.180 K.

#### Mechanism of photolysis

The e.s.r. parameters for species A (table 2.3) are approximately half those for normal  $B_{12r}$ , except that, in the parallel region, there are extra features, which arise from an extra doublet splitting, indicated in Figure 2.7b. This implies the formation of radical pairs of the type discovered in photolysed persulphates (127, 128). Provided the radical  $R^\bullet$  is trapped at a fixed distance from Co(II) there should be a well defined zero field splitting, and if some orbital overlap is retained, spin exchange should occur, thereby reducing the coupling constants and  $\Delta g(g_{\text{exp}} - 2.0023)$  values by a factor of 2, as observed. In order to explain the extra high field parallel features (Figure 2.7b) a fine structure

Table 2.3 Experimental e.s.r. parameters for radical species formed on photolysis of methylcobalamin

Radical	Nucleus	Hyperfine coupling constants(G) <sup>a</sup>	g-values	2D <sub>  </sub>
		A <sub>z</sub> A <sub>x</sub> A <sub>y</sub>	g <sub>  </sub> g <sub>⊥</sub>	
B <sub>12</sub> r	<sup>59</sup> Co	108 NR NR <sup>b</sup>	2.003 ca.2.32	-
	<sup>14</sup> N	18 NR NR		
B <sub>12</sub> r{c pair}	<sup>59</sup> Co	56 NR NR	2.003 ca.2.16	ca.100 G
	<sup>14</sup> N	ca.9 NR NR		
R <sup>•</sup> pair <sup>d</sup>			2.0025(Av)	ca.100 G
•CD <sub>2</sub> OD <sup>e</sup>	<sup>2</sup> H	ca 3 G	2.0025(Av)	
•CH <sub>3</sub>	<sup>1</sup> H	22.5 (Av)	2.0025(Av)	

(a) = 0.1 mTelsa

(b) NR = Not resolved

(c) Data for the B<sub>12</sub>r component of the radical pair (data for <sup>14</sup>N estimated from line widths)

(d) Data for the radical component (•CD<sub>2</sub>OD?) of the radical-pair

(e) Identical with the normal values for these radical-pair

splitting of ca.100 G ( $2 D_{\parallel}$ ) is needed. This is strongly supported by the fact that the centre of these two sets of cobalt parallel features is then close to 2.0023 as is normally found for Co(II) ( $d_z^2$ ) complexes. This value need not be a principal value of the zero-field splitting since the powder spectra are dominated by the cobalt features. If this postulate is correct, there should be an equal zero-field splitting for the other component of the pair, namely,  $R^{\bullet}$ . This suggests that the signals assigned to species B are mainly due to this component. These features are very broad and no hyperfine coupling can be extracted; however they are of the form expected for a zero field splitting, provided  $2D_{\parallel}$  is in the region of 100 G. The perpendicular features are poorly defined and probably split, but are largely concealed by a central free radical component. The fact that this value is equal to the value derived from the cobalt features means that the principal (parallel) axis for the zero field splitting is the same as that for the parallel cobalt splitting, namely,  $z$ , the direction normal to the corrin. In that case the mean separation between  $R^{\bullet}$  and Co(II) must be ca.8.3 Å from the normal eq 2.10 where

$$D' = \frac{3\beta(3\cos^2\theta - 1)}{R^3} \quad (2.10)$$

$R$  is the mean separation between the spins (129). Thus the following mechanism is proposed. On light absorption a ligand electron moves into the Co( $d_z^2$ ) sigma\*-orbital, and the methyl

radical moves away along the z-axis. This pathway is clear of organic substituents so the major opposition to this motion will be from solvent molecules. Some of these "hot" radicals react with the first  $\text{CD}_3\text{OD}$  molecule encountered to give  $^*\text{CD}_2\text{OD}$ , trapped by hydrogen bonds to the rigid lattice. Alternatively, some methyl radicals may slow and stop in the  $8 \text{ \AA}$  region. Unfortunately, lines are so broad that one cannot rule out the presence of an 11 G (1:3:3:1) splitting from such a trapped methyl radical, but this is unlikely. Some methyl radicals escape this initial barrier and are either trapped (giving the normal methyl features) or react with solvent giving normal  $^*\text{CD}_2\text{OD}$  features (Figure 2.7a).

Although there is no alternative explanation, this conclusion may be treated with caution for two reasons; one is that it is surprising that there should be such precise trapping always in the  $8.3 \text{ \AA}$  region, and the other is that, for such a large separation, that there should be fast spin-exchange. The latter observation surely requires that there should be no intervening solvent molecules which would provide an efficient barrier for electron exchange. Another reason for preferring the idea that the R component of the pair is  $^*\text{CD}_2\text{OD}$  rather than  $^*\text{CH}_3$  is that this will be held away from cobalt by hydrogen bonds whereas the latter, with no intervening solvent, would surely be able to return to its original site.

For ethyl cobalamin, the ethyl radical, being less reactive, is unable to extract deuterium from the solvent, but

escapes and remains trapped in the region of  $15-20 \text{ \AA}$ , thereby giving only spin-spin broadening. On annealing the ethyl radicals diffuse away and react, leaving normal  $B_{12r}$ .

For the acetyl derivative, escape also occurs, but the mean trapping distance is shorter, so that the line broadening is so extensive that no signals are detected. Again on annealing the acetyl radicals move away and react, leaving normal  $B_{12r}$ . For  $CoB_{12}$ , these results agree with Lowe *et al.* (107). At 77 K bond fission occurs, but the large  $dACH_2$  radical cannot escape, and back reaction is complete. At higher temperatures, these radicals move away but, as with the ethyl derivative, the spectra are broadened. Ultimately, on annealing, complete separation occurs and the spectrum of  $B_{12r}$  becomes clear.

Finally, the significance of these results in relation to the results on electron-addition to alkylcobalamins (95) can be considered. Two alternative mechanisms are currently considered for electron addition, one giving  $Co(I)$  and  $R^\bullet$  and the other giving  $Co(II)$  and  $R^-$ . Since there was no trace of methyl radicals for the methyl derivative, and since the present results clearly establish that good signals from the methyl radicals can be obtained from these systems, one can firmly exclude the former mechanism. In fact, these results favour initial electron addition into the corrin  $\pi^*$  orbital followed ultimately by loss of  $R^-$  probably protonation occurs in the transition state.

#### Conclusions about the photolysis studies

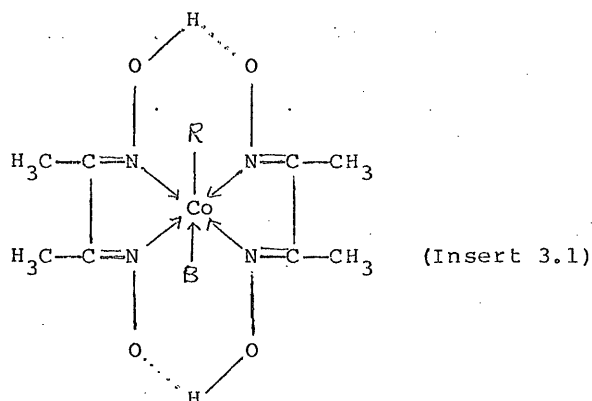
In all the systems studied, photolysis results in homolysis of

the Co-R bond, but these results suggest that the direct consequences vary markedly with the size of the resulting alkyl radicals. For  $R = CH_3$  some radicals can escape and become trapped, with the unequivocal e.s.r. detection of both  $^{\circ}CH_3$  and  $B_{12r}$ . However, they also react with suitably placed solvent molecules ( $CD_3OD$ ) and a precise Co(II) ...  $CD_2OD$  radical-pair is the dominant species. Ethyl radicals seem to be less reactive and also less mobile so that a range of radical-pairs are formed with a relatively large average separation so that broadened signals are obtained.

The same occurs for the acetyl derivative except that the mean separation is reduced, and the e.s.r. features are excessively broadened. For the  $CoB_{12}$  however, the separation at 77 K is not large enough to prevent efficient cage-back reaction, and no photolysis is observed. At higher temperatures photolysis does occur, but pairwise trapping again broadens e.s.r. features.

CHAPTER 3COBALOXIMESINTRODUCTION

In 1964, Schrauzer and Kohnle (130) reported that the reactions of the cobalt atom in  $\text{CoB}_{12}$  can be simulated with much simpler, bis(dimethyl-glyoximato) cobalt(III) complexes (insert 3.1). These complexes resemble  $\text{CoB}_{12}$  so closely in



their chemical properties that they were introduced as coordination chemical models of  $\text{CoB}_{12}$  and were named "cobaloximes" to stress their similarities to cobalamins. In the ensuing years numerous papers appeared in the literature suggesting a number of other cobalt complexes as alternative models(131-133). But it eventually became clear that the simple cobaloximes simulate the reactions of cobalamins qualitatively. Some of the recent studies have shown that

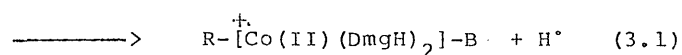
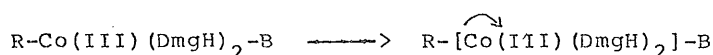


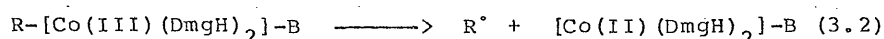
cobaloximes are more stable than corrins. Cobaloximes have a formal -1 charge on the tetradentate ligand. The corrin in coenzyme has a formal -2 charge. Cobaloximes also have a strong Co-C bond and high axial-base binding constant. The symmetry properties of the HOMO of <sup>The</sup> polyene skeleton in cobaloximes differ from those of the  $\pi_{17}$  orbital of the corrin (which is involved in the so called "strain orbital") (134-138). In spite of some differences observed between cobaloximes and cobalamins the similarities dominate (131, 139, 140) and hence they served as useful models of several enzymatic systems (3, 4). In the following section, a brief review is made as an introduction to the results presented in this chapter, and also to compare with those of the cobalamins presented in chapter 2.

The Co-C bond of alkylcobaloximes can be dissociated by homolysis or heterolysis according to eq. 1.7, 1.8 and 1.9.

#### Homolysis of Co-C bond

Only photoreduction (cf eq. 2.2) will be discussed in this chapter. Photolysis of alkylcobaloximes have been extensively studied by Gionnotti and co-workers (103, 104). They suggest that photolysis of methyl and benzyl (pyridine) cobaloximes results in an electron transfer reaction according to eq 3.1. However, ethyl-, n-propyl- and isopropyl (pyridine) cobal-





oximes at 103 K gave homolysis products of the Co-C bond i.e., Co(II) "base-on" species and alkyl radicals(eq,3.2). At 77 K all of them gave electron transfer reactions according to eq,3.1. Photolysis of alkylcobaloximes in the presence of oxygen greatly increased the rate of cleavage of the Co-C bond leading to alkyl peroxy complexes (141-144). When methyl(py)cobaloxime was photolysed in presence of B<sub>12</sub>r methylcobalamin was obtained(141).

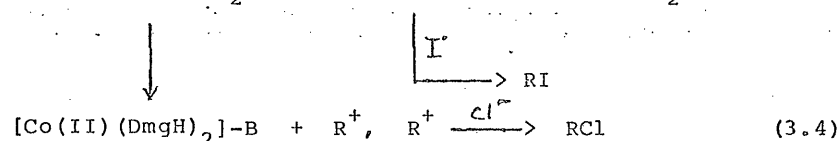
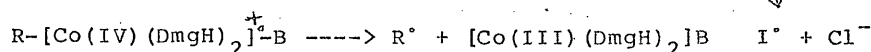
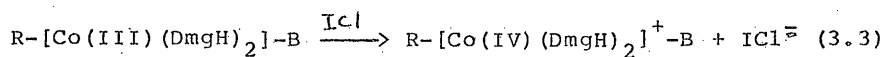
#### Nucleophilic attack on Co-C bond.

Alkylcobaloximes are readily attacked by mercaptide ions to produce cobaloxime(I) or cobaloxime(II) and the respective dialkylsulphides. Thus the reaction of methylcobaloxime with homocysteine in a mildly alkaline solution(pH ~ 10) gave methionine(145). Similar methyl transfers to other alkylsulphide anions have been reported.

#### Electrophilic attack on the Co-C bond: Decomposition by halogens.

Dealkylation of alkylcobaloximes by halogens has been studied in several laboratories(146-148). Cleavage of the Co-C bond of the alkylcobaloximes by chlorine, bromine and iodine occurs with inversion of configuration. The dealkylation of simple alkyl cobaloximes with iodine monochloride yields alkyl iodides, suggesting that these reactions involve an SE<sub>2</sub> open-type intermediate. However, the dealkylation of sec-alkyl cobaloximes by ICl yields alkyl iodides and alkyl chlorides.

Kitchin and Widdowson(149) suggest that dealkylation by ICl involves an initial one-electron oxidation to a cobalt(IV) cationic complex, which dissociates according to eq 3.3 and 3.4.



#### Reductive cleavage of Co-C bond

Polarographic studies of alkylcobaloximes showed that the reduced species produced in the first reduction step spontaneously decayed due to Co-C bond cleavage. The bond cleavage of the reduced species is expected to be dependent on the nature of the orbital that an excess electron occupies(133,134). Hashino et al.(150) have shown that radiolysis of methyl(py)cobaloxime at 77 K resulted in an intermediate with the electron localised in the metal  $d_{z^2}$  orbital. Upon annealing above 77 K, it is thought to give a Co(I) derivative and a methyl radical. Benzyl(py)cobaloxime and chloro(py)cobaloxime gave the corresponding anion-radicals which dissociated into Co(II) species and the corresponding anions of axial ligands.

The primary objectives of these studies were as follows;

(1) Since earlier attempts to study the spin-distribution in the metal-carbon sigma\*-orbital of methylcobalamin did not succeed(cf,chapter 2),it was decided to study methyl(py)cobaloxime using methyl labelled with  $^{13}\text{C}$ (-carbon).(2) To study the effect of higher alkyl groups on the Co-C bond cleavage.(3) To see if methyl(py)cobaloxime gave a Co(II)...radical pair similar to methylcobalamin(cf,chapter 2).(4) To measure the spin distribution between Co and the hydrogen (and deuterium) axial ligand.(5) To compare these results with cobalamins.

As described in chapter 2,photolysis and radiolysis methods have been used to generate paramagnetic species of cobaloximes.The first part of this chapter deals with radiolysis and second part with photolysis results.

#### EXPERIMENTAL

Alkyl(py)cobaloximes were prepared according to the method of Schrauzer and Windgassen(139).A typical preparation is as follows:

297 mg(1.25 mMole) of  $\text{CoCl}_2 \cdot 6 \text{H}_2\text{O}$  and 290 mg(2.5 mMole) of DMgH were stirred in 3.3 ml of methanol in a nitrogen atmosphere.After 30 mins.0.2 ml of 50% sodium hydroxide and 0.1 ml of pyridine(1.25 mMole) were added and the solution was cooled to between  $-10$  to  $-20^\circ\text{C}$  in an ice-salt sludge bath.1.8 mMole equivalent of alkyl iodide was added while stirring.This was followed by the addition of 0.1 ml of 50% sodium hydroxide and 3.7 mg sodium borohydride in 0.02 ml water.The reaction was stirred for 15 mins and then was

allowed to warm up gradually to room temperature. After an hour the methanol was evaporated, and the sample washed with water, recrystallised from hot water and dried in vacuo. All operations were done in a nitrogen atmosphere.

$\text{CD}_3$ -methyl(py)cobaloxime and  $^{13}\text{CH}_3$ -methyl(py)cobaloxime were prepared using methyl iodide with corresponding labels. Ethyl iodide was used for the preparation of the ethyl derivative and propyl-, isopropyl-, and isobutyl(py)cobaloximes were prepared by using the corresponding iodides.

Chloro(py)cobaloxime and Chloro(trph)cobaloxime.

Both these complexes were prepared by the method of Schrauzer (151). 500 mg (2.1 mMoles) of  $\text{CoCl}_2 \cdot 6\text{H}_2\text{O}$  and 550 mg (4.7 mMole) of DMgH were suspended in 20 ml 95% ethanol and heated with stirring. 4.3 mMole equivalent of pyridine or trph was added and the mixture cooled to room temperature. Air was blown through the solution for 30 mins and it was left for 60 mins at room temperature. The precipitated complex was filtered, washed with water, ethanol, ether and dried in vacuo at room temperature.

Hydrido(trph)cobaloxime and deuterio(trph) cobaloxime.

These complexes were prepared by the method of Schrauzer and Holland (31). 100 mg of chloro(triphenylphosphine) cobaloxime was suspended in 50 mM sodium phosphate buffer pH 7.0 containing 50% methanol. 30 mg of sodium borohydride in 0.5 ml water was added over a period of 4 mins. During the addition of the last drops, the sample was transferred to a

nitrogen atmosphere and left there for 2 hours. The black ppt was filtered and washed with water, dried in vacuo at 75°C for 4 hours. Sodium borodeuteride and deuterated solvents were used for the preparation of deuterio analog.

CHN analysis for the cobaloximes are given below;

	calculated			found		
	C	H	N	C	H	N
Methyl(py)						
cobaloxime	43.41%	6.77%	18.08%	43.20%	6.00%	18.11%
<sup>13</sup> CH <sub>3</sub> (py)						
cobaloxime	44.02%*	5.77%	18.22%	43.57%*	5.72%	18.23%
CD <sub>3</sub> (py)						
cobaloxime	43.76%	5.79%*	18.22%	43.29%	5.74%*	18.13%
Ethyl(py)						
cobaloxime	45.35%	6.09%	17.63%	44.96%	5.95%	17.58%
n-propyl(py)						
cobaloxime	46.71%	6.33%	17.03%	46.81%	6.10%	16.98%
Isopropyl(py)						
cobaloxime	46.71%	6.33%	17.03%	45.94%	5.96%	17.03%
Isobutyl(py)						
cobaloxime	48.00%	6.63%	16.46%	47.78%	6.55%	16.69%
Chloro(py)						
cobaloxime	38.67%	4.74%	17.35%	38.62%	4.79%	17.45%
Chloro(trph)						
cobaloxime	53.21%	4.98%	9.55%	53.15%	5.05%	9.22%
Hydrido(trph)						

cobaloxime 56.52% 5.47% 10.14% 55.85% 5.33% 9.37%

Deutero(trph)

cobaloxime 56.42% 5.48%\* 10.13% 55.85% 5.33%\* 9.37%

\* includes the corresponding isotope.

Samples for radiolysis experiments were prepared in 2-MTHF or  $CD_3OD$  as described in chapter 2. Samples for photolysis were prepared by dissolving the complex in the above solvents, degassing in a supracil e.s.r. tube and sealing. Photolysis was carried out at 77 K using a 100 W high pressure Hg lamp for 90 mins. UV light was filtered using a quartz cell containing dust-free water. E.s.r. spectra were recorded as described in chapter 2. In order to trap "base-on" cobaloxime (II) (this species dimerises when formed at 77 K) formed during photolysis, the samples were prepared in 1M pyridine or by admitting air into the e.s.r. tube. A dipyridyl derivative was obtained in the former and a superoxo-derivative was obtained in the latter case.

## RESULTS AND DISCUSSION

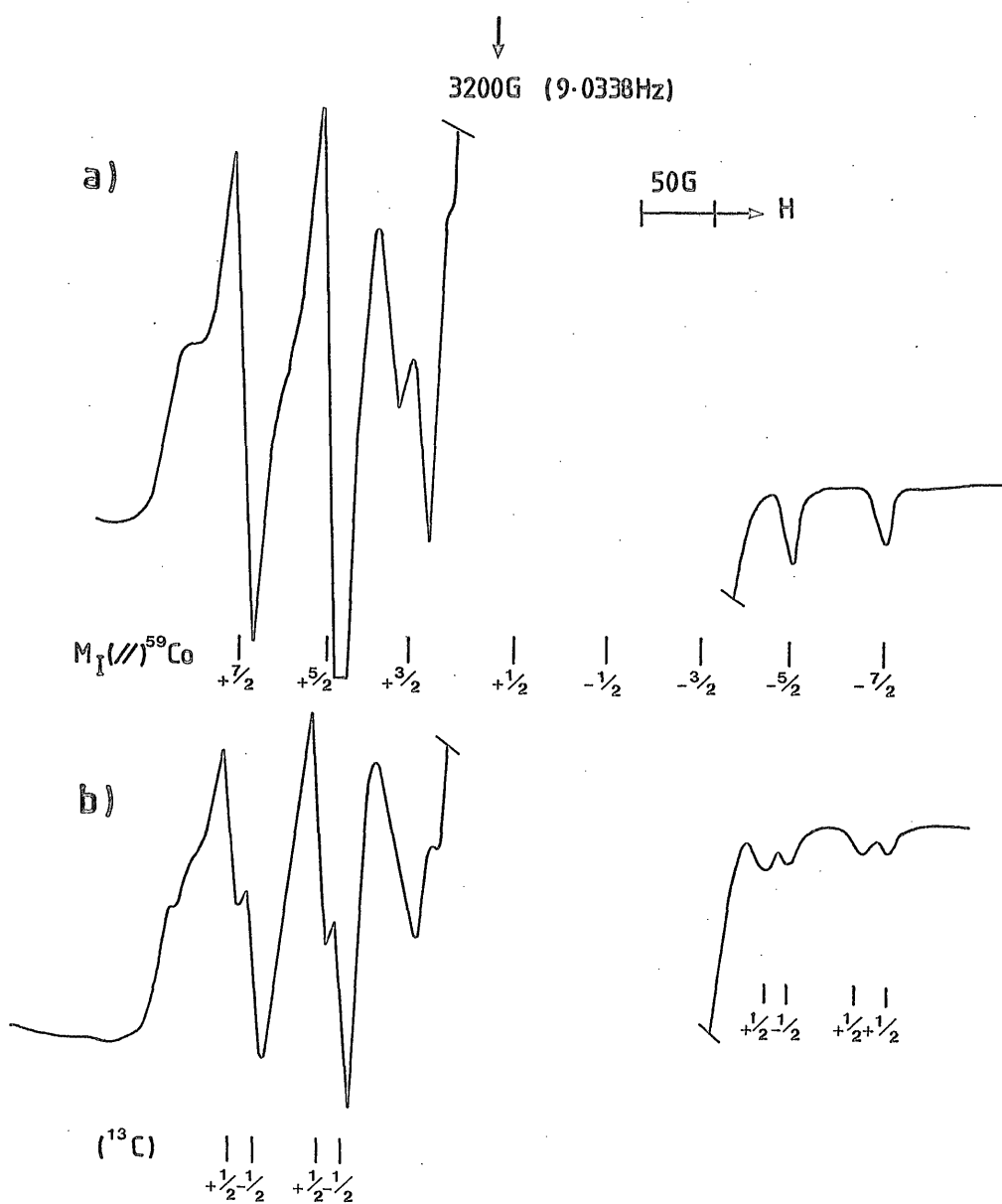
### RADIOLYSIS WORK

In general these results using  $CD_3OD$  or MTHF glasses were similar, and some attention is drawn to the differences in the following;

#### Alkyl(py)cobaloxime

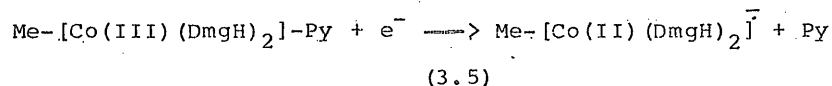
The spectrum was similar to that published by Hashino et al. (Fig 3.1a) (150), when  $CH_3$  was replaced by  $CD_3$  there was no

Figure 3.1 First-derivative X-band e.s.r. spectra of methyl-(py) cobaloxime. Features are assigned to the anion complex (a) using  $^{12}\text{CH}_3$ -methyl (b)  $^{13}\text{CH}_3$ -methyl.





significant change, but  $^{13}\text{CH}_3$  gave clear extra doublet splitting assigned to hyperfine coupling to  $^{13}\text{C}$  nuclei (Fig 3.1b, Table 3.1). This result strongly supports the  $\text{Co}-\text{CH}_3$  sigma\* structure postulated by Hashino et al. but the absence of  $^{14}\text{N}$  structure from the pyridine ligand suggests its loss (eq 3.5) rather than a strong confinement of the SOMO to the C-Co bond. This agrees with the complete absence of any



$^{14}\text{N}$  coupling. Since delocalisation on to the methyl group is relatively low (see below), one would have expected  $^{14}\text{N}$  coupling of at least 10 G had the ligand been retained. Similarly had the electron been captured into the cobalt  $d_{x^2-y^2}$  orbital, as could have been expected in terms of the M.O. scheme of Green et al. (152), one would have expected considerable hyperfine coupling to the four  $^{14}\text{N}$  nuclei of the oxime ligands. Also the form of the  $g$  tensor component is in fact better according to the  $(d_z^2)^1$  formulation.

The hyperfine coupling constants are used to give values for A and 2B (purely dipolar part), and then converted into approximate orbital populations in the usual manner (129), the results are listed in table 3.2. The 2B value for  $^{13}\text{C}$  is approximate. If there has not been extensive flattening at carbon (i.e.  $\text{sp}^3$  hybridisation is retained), a total spin density of ca. 6% on the methyl group was obtained.

Table 3.1 E.s.r. parameters for various Co(II) cobaloxime derivatives

Cobaloxime	Nucleus	Hyperfine coupling constants/G <sup>a</sup>			g-values		
R-, [R-(DmgH) <sub>2</sub> ]-	A <sub>Z</sub>	A <sub>X</sub>	A <sub>Y</sub>	g <sub>Z</sub>	g <sub>X</sub>	g <sub>Y</sub>	
CH <sub>3</sub>	59Co	62.5	<u>ca.42</u>	<u>ca.42</u>	2.002	<u>ca.2.099</u>	<u>ca.2.099</u>
(CD <sub>3</sub> )							
13C	13C	19	<u>ca.17</u>	<u>ca.17</u>			
R	59Co	62.5	<u>ca.42</u>	<u>ca.42</u>	2.002	<u>ca.2.099</u>	<u>ca.2.099</u>
CH <sub>3</sub> /py <sup>b,d</sup>	59Co	58.4	-	-	2.002	2.11	2.11
? <sup>e</sup>	59Co	38.5	25.0	25.0	2.002	2.002	2.002
O <sub>2</sub> /py <sup>b</sup>	59Co	20	15	15	2.06	2.002	2.002
(py) <sub>2</sub>	59Co	88	<u>ca.40</u>	<u>ca.40</u>	2.008	<u>ca.2.11</u>	<u>ca.2.11</u>
	14N	16	12.5				
Cl <sup>-</sup> /py <sup>b</sup>	59Co	105	<u>ca.45</u>	<u>ca.45</u>	2.002	<u>ca.2.16</u>	<u>ca.2.16</u>
	14N	22	<u>ca.18</u>	<u>ca.18</u>			
Cl <sup>-</sup> /py <sup>d</sup>	59Co	18	16	16	2.140	2.252	2.252
PPh <sub>3</sub> <sup>b</sup>	59Co	100	f/g		2.002	g	g
	31P	138	120	120			

(a) = 0.1 mTelsa

(b) Axial ligands, py = pyridine, PPh<sub>3</sub> = triphenylphosphine.

(c) R = Alkyl. (d) Ref.150

(e) Unidentified species alpha (see text)

(f) A<sup>35</sup>Cl ca.20 G before annealing. (g) Not clearly defined.

Table 3.2 Approximate ligand orbital populations, estimated from  $A_{iso}$  and  $2B^a$  (%)

Ligand	Nucleus	$a_s^2$	$a_p^2$	$a_s^2 + a_p^2$	
-CH <sub>3</sub>	<sup>13</sup> C	1.7	ca. 2.0	≥ 3.7	
-(py) <sub>2</sub>	<sup>14</sup> N	2.5	7	9.5	
-py	<sup>14</sup> N	3.5	8	11.5	
-PPh <sub>3</sub>	<sup>31</sup> P	3.6	6	9.6	

(a) Using the atomic parameters given in ref 129.

For  $^{59}\text{Co}$  hyperfine coupling data there is a sign ambiguity since isotropic spectra could not be obtained. If like signs are used, an extremely low density results. However using unlike signs gives  $A_{\text{iso}}(^{59}\text{Co}) \approx (-)7 \text{ G}$  and  $2B \approx +70 \text{ G}$ , the signs being those required for  $d_z^2$  configuration. The small value of  $A_{\text{iso}}$  suggests considerable admixture of 4s character to reduce the magnitude from the usual value of ca.  $-80 \text{ G}$ .

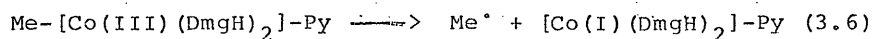
However this gives a total spin-density on cobalt of ca. 50%.

~~It is necessary~~  
So ~~to~~ account for a substantial missing fraction.

Delocalisation on to equatorial ligands cannot account for very much of this, in view of the absence of  $^{14}\text{N}$  hyperfine coupling. Therefore there must be some admixture of the outer,  $4p_z$  cobalt orbital. Such admixture can reinforce the wave function in the non-bonding region vacated by the pyridine ligand thereby reducing the carbon-cobalt antibonding interaction. The anisotropic coupling for the  $4p_z$  population is of the same form as that for the  $3d_z^2$  contribution, but is smaller because of the more diffuse nature of the 4p orbitals. An approximate estimate shows that about equal population of the  $d_z^2$  and  $p_z$  orbitals is required to account for the missing spin-density. The unusually small positive g-shifts for the alkyl derivatives may reflect a negative contribution from p-orbital population. This model helps to explain the low spin density on carbon. This result is surprising in the light of the results for the structurally similar hydrides  $[\text{H-Ni}(\text{CN})_4]^{2-}$  and  $[\text{H-Pt}(\text{CN})_4]^{2-}$ , for which

delocalisation onto hydrogen was ca.30 % (153,154). The coupling to  $^{195}\text{Pt}$  for the latter nicely accounted for the remaining spin-density as a  $d_{z^2}$  contribution, there being no need to postulate  $p_z$  admixture. However for both types of complex, the g-values are close to free-spin indicating an unusually isolated SOMO.

Hashino *et al.* showed conclusively that Co(II) complexes are not formed from methyl(py) cobaloxime adduct on further annealing. In order to accommodate the electro-chemical results (eq 3.6) which show that the cobalt-carbon bond



is broken under their conditions, they postulated a break-down to give  $^\bullet\text{CH}_3$  and a Co(I) complex (eq 3.6). Since  $^\bullet\text{CH}_3$  radicals were not detected also since the pyridine ligand has been lost, the incentive for such a reaction is unclear.

The absence of detectable  $^1\text{H}$  hyperfine coupling suggests that it must be small. It can be concluded that it will generally be necessary to use the  $^{13}\text{C}$  hyperfine coupling to detect the presence of alkyl groups in these complexes.

The results for the other alkyl derivatives (Table 3.1) were very similar to those for the  $^{12}\text{CH}_3$  derivative, so one can safely conclude that they all have essentially the same electronic structure.

In the particular case of methyl(pyridine)cobaloxime in  $\text{CD}_3\text{OD}$  solvent, after gamma-irradiation and annealing to the softening point of the glass and recooling to 77 K, a novel spectrum was obtained (Fig 3.1c), this species (alpha-) has  $g_{\parallel} \approx g_{\perp} \approx 2.0023$ , with rather small coupling to  $^{59}\text{Co}$  ( $A_{\parallel} = 38.5 \text{ G}$ ,  $A_{\perp} = 25 \text{ G}$ ). The free-spin g-values suggest a species having major spin density on one of the ligands, however like-signs for the cobalt coupling gives  $A_{\text{iso}} = 29.5 \text{ G}$  and  $2B = 9$ , It seems probable that one of the parent complexes has trapped an alkyl radical ( $\text{R}^\bullet$  or  $^\bullet\text{CD}_2\text{OD}$ ), but the precise structure of this centre is not known.

#### Other Cobaloximes

A brief study was made of various other derivatives in order to gain experience of electron addition to cobaloximes. The chloro(pyridine)cobaloxime was previously studied by Hashino et al. (150) who obtained an e.s.r. spectrum which was typical of the "perpendicular" region of cobalt(II) complexes, the parallel feature being too broad to detect. The small low field splittings assigned by them to the parallel  $^{59}\text{Co}$  coupling are better described as coupling to ligand nuclei ( $^{14}\text{N}$ ). In fact these spectra are better defined (Fig 3.2) and some of the expected high field parallel lines were detected. In MTHF solvent the ligand hyperfine features are complicated, and there is a weak residual interaction with  $^{35/37}\text{Cl}$  nuclei. However, on annealing or directly using  $\text{CD}_3\text{OD}$  solvent, a better defined set of lines were obtained, showing triplet splittings for coupling to

Figure 1.1(c). First-derivative X-band e.s.r. spectrum of an unknown radical ( $\alpha$ pha) obtained after annealing methyl(py)cobaloxime above 200 K.

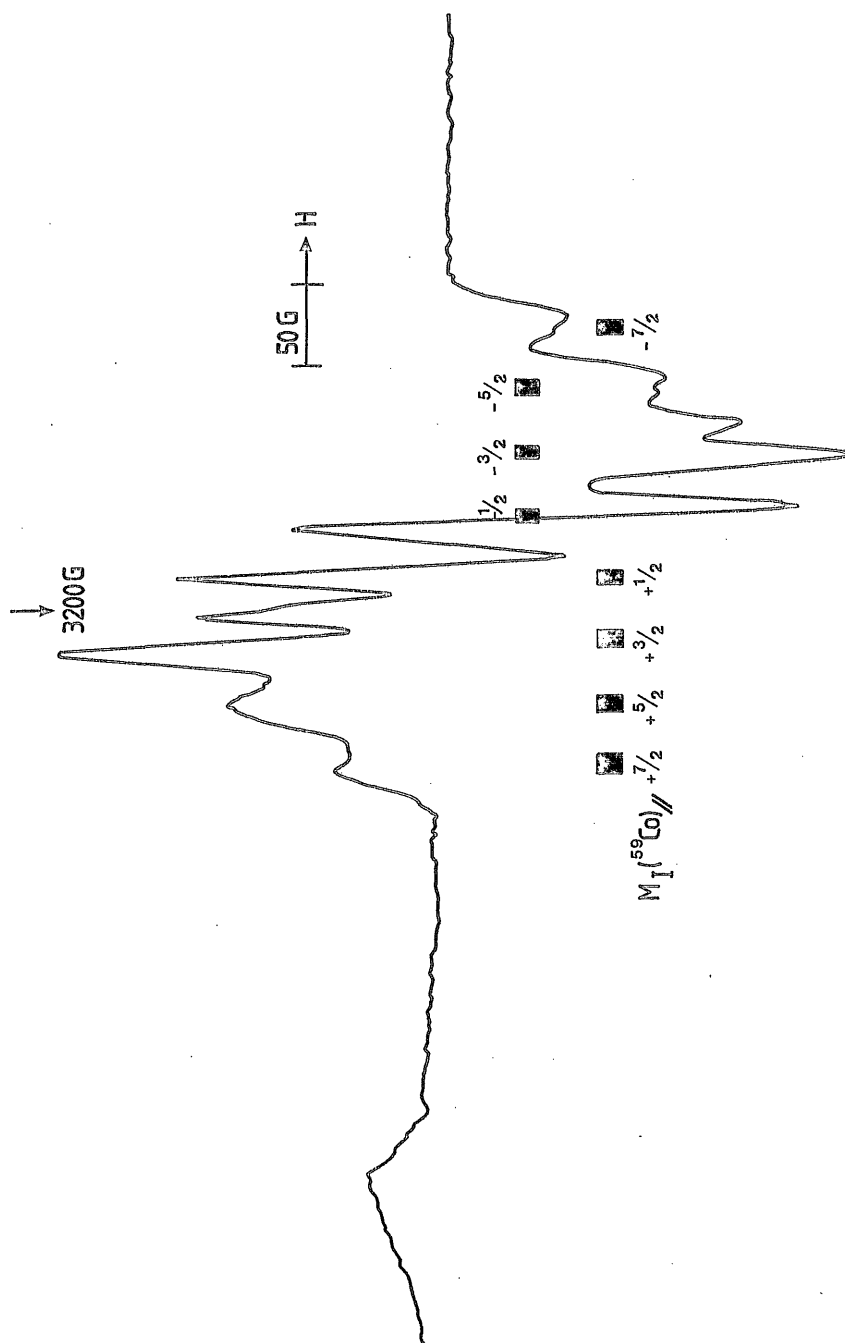


Figure 3.2 (a). First-derivative X-band e.s.r. spectrum of  $\text{Co}(\text{DmgH})_2$  py

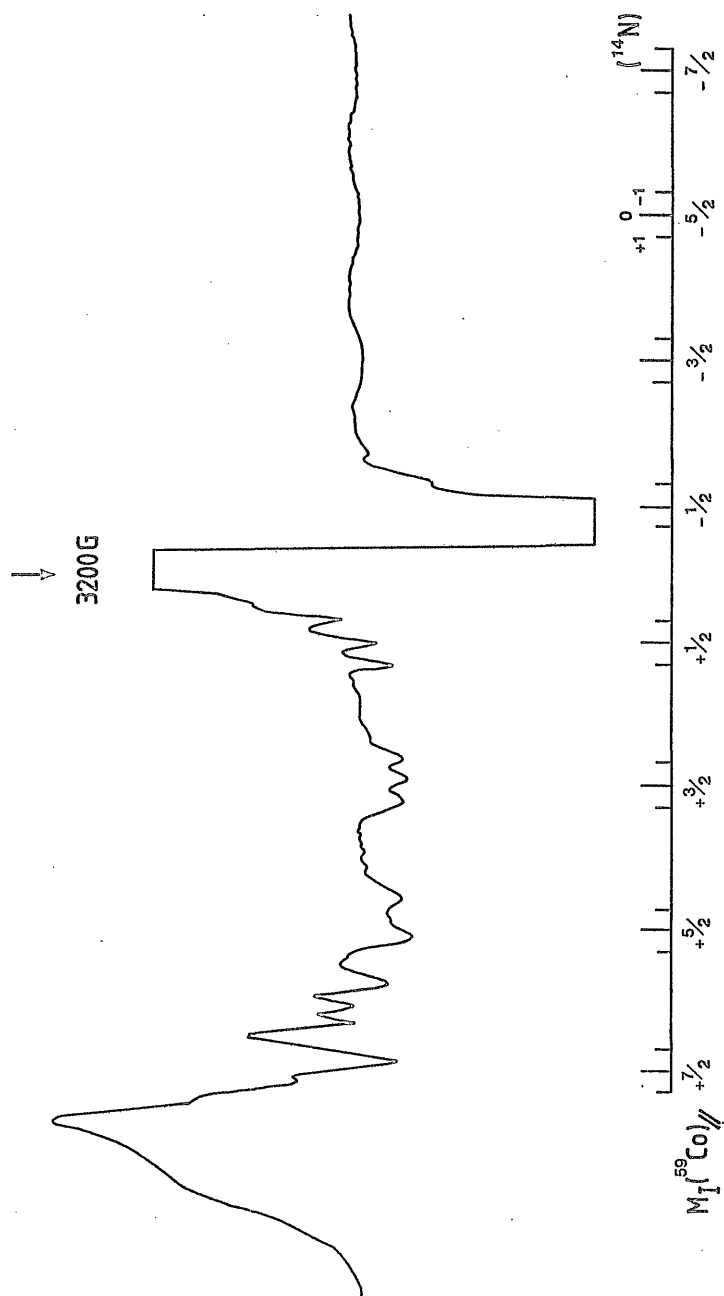
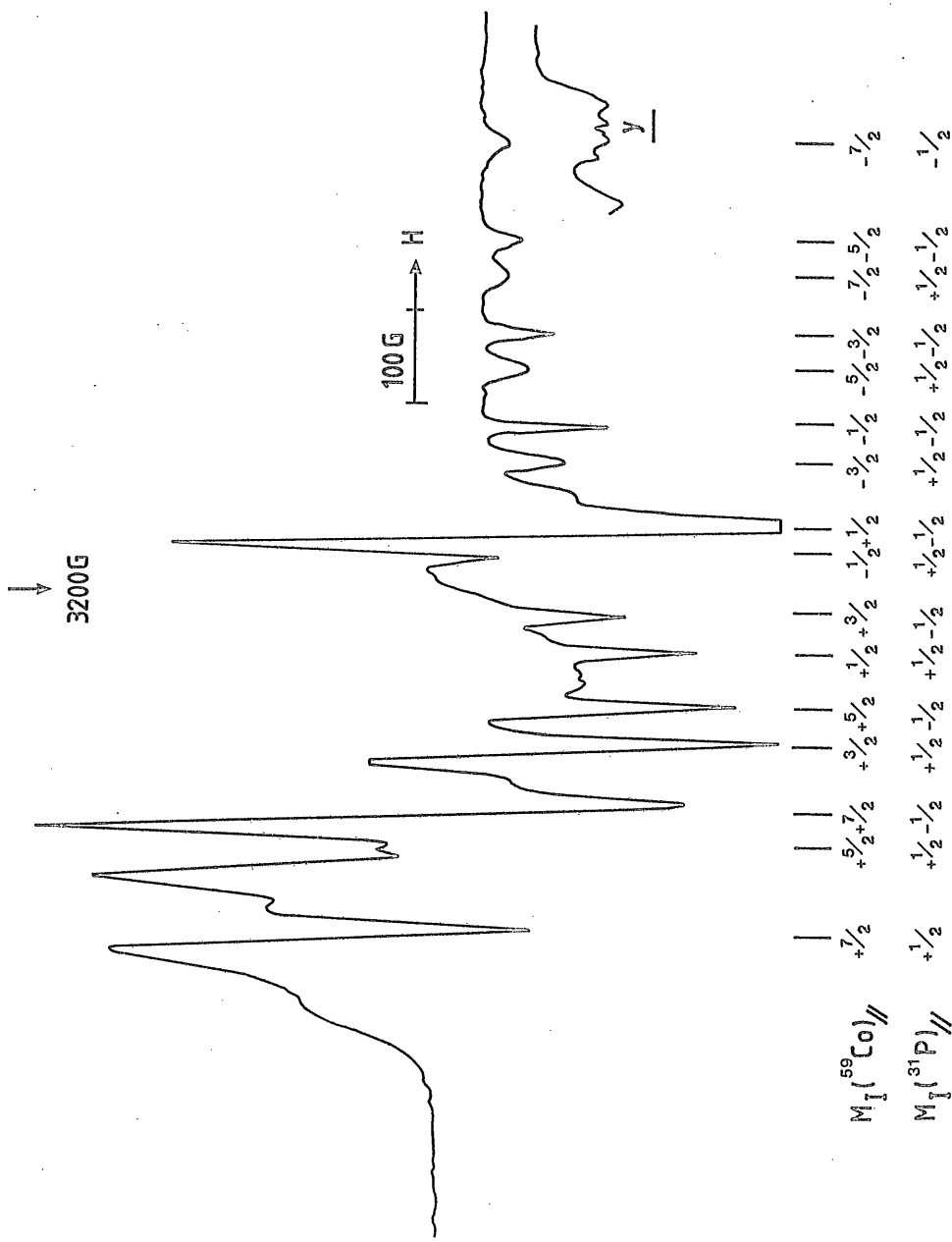




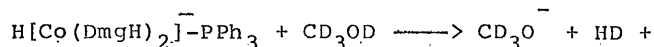
Figure 3.2.2 (b) First-derivative x-band e.s.r. spectrum of  $^{\circ}\text{Co}(\text{DmgH})_2\text{PPh}_3$ .



$^{14}\text{N}$  nuclei. Thus  $\text{Cl}^-$  is readily lost. The e.s.r. parameters show that, as usual for cobalt(II) complexes, the electron is in the  $3d_{z^2}$  orbital on cobalt. The data are in fact quite similar to those for  $\text{B}_{12}\text{r}$ . Some studies were also made on the triphenyl phosphine derivative with chlorine or hydrogen in the other axial site. The former behaved similar to the pyridine complex. Initially a poorly resolved e.s.r. spectrum was obtained, with some indications of weak chlorine coupling as with the chloro(py)cobaloxime, but on slight annealing the spectra shown in Fig 3.2b was obtained, showing a large doublet splitting assigned to  $^{31}\text{P}$  hyperfine coupling. Evidently the chlorine ligand is readily lost as  $\text{Cl}^-$  after electron addition.

The coupling to  $^{31}\text{P}$  is normal for such  $\sigma^*$  complexes (155, 156). Analysis in the usual way results in ca. 3.6% 3s and ca. 6% 3p orbital populations. Thus the spin density on the  $\text{Ph}_3\text{P}$  ligand is greater than that on the methyl group in the methyl derivative. Indeed, the g-value and  $^{59}\text{Co}$  parameters for  $\text{Co}(\text{DmgH})_2\text{py}$  and  $\text{Co}(\text{DmgH})_2\text{PPh}_3$  complexes are similar, as is the delocalisation on to pyridine or  $\text{PPh}_3$ , but they both differ strongly from those for the alkyl derivatives which are clearly unique. There is no need to invoke major p-orbital population on cobalt for these derivatives. It was expected that the hydride derivative would give the  $\text{H-Co}(\text{DmgH})_2$  complex with a loss of  $\text{PPh}_3$ . In fact the reverse occurred, both the proton and deuterium derivatives giving spectra similar to that assigned to the  $\text{Co(II)trph}$  derivative. The loss of  $\text{H}^-$  under these conditions was unexpected but some alternative

mechanisms must be found. As for the chloride derivative, the initial spectra were less well defined than those after annealing, but there was no proton splitting. The best results were obtained for solutions in  $\text{CD}_3\text{OD}$  solvent and for these the reactions are shown in eq 3.7 & 3.8.



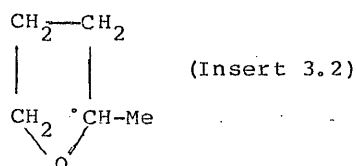
#### Comparison with electron addition and alkyl cobaloximes

These results make an interesting contrast with those for the alkylcobalamins (chapter 2). In this study the e.s.r. evidence suggested initial electron addition into a  $\pi^*$  corrin orbital showing no appreciable interaction with the  $^{59}\text{Co}$  nucleus. On annealing the electron moved onto the metal, but the  $d_{x^2-y^2}$  orbital was favoured over the  $d_{z^2}$  orbital. Thus these complexes, normally considered to be very similar, gave quite different results in the initial stages of electron addition. The choice of pathway must depend on quite subtle issues.

#### PHOTOLYSIS WORK

Alkyl(pyridine)cobaloximes; Alkyl radicals.

In all cases organic radicals were detected after photolysis at 77 K (Table 3.3). No radicals were detected in the absence of the cobalt derivatives. For MTHF glasses the dominating species was always the normal MTHF radical (insert 3.2) but for  $\text{CD}_3\text{OD}$  glasses well resolved features for the



alkyl radicals  $\text{R}^\cdot$ , derived from the complexes were obtained in addition to those for  $\cdot\text{CD}_2\text{OD}$  radicals (Fig 3a). There was no evidence for the formation of trapped hydrogen atoms during these reactions. The solvent radicals are almost certainly formed by reaction with "hot"  $\cdot\text{R}$  radicals, before trapping. These results establish conclusively that important photolysis pathway is cobalt-carbon bond homolysis.

#### Co(II) centres

In all cases, broad features assignable to Co(II) centres were also obtained. However, these were formed in far greater yield than that of the alkyl radicals, and there was usually a poorly defined doublet splitting on the major perpendicular features which is not present for the Co(II) (py) species, and which was lost on annealing (Fig 3.3b). At high powers, central doublet features were also obtained in some cases, reminiscent of features assigned to triplet-state pairs in these studies

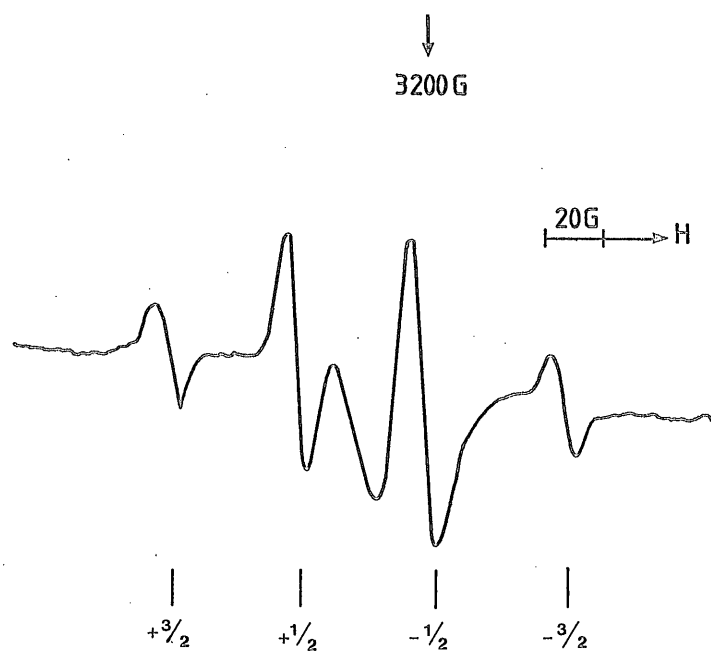


Figure 2.2 a. First-derivative X-band e.s.r. spectrum of methyl radicals obtained after photolysis of methyl(py) cobaloxime

Figure 3.3.(b) First-derivative e.s.r. spectrum showing features assigned to t-butyl radicals and broadened features for CO(II) complex.

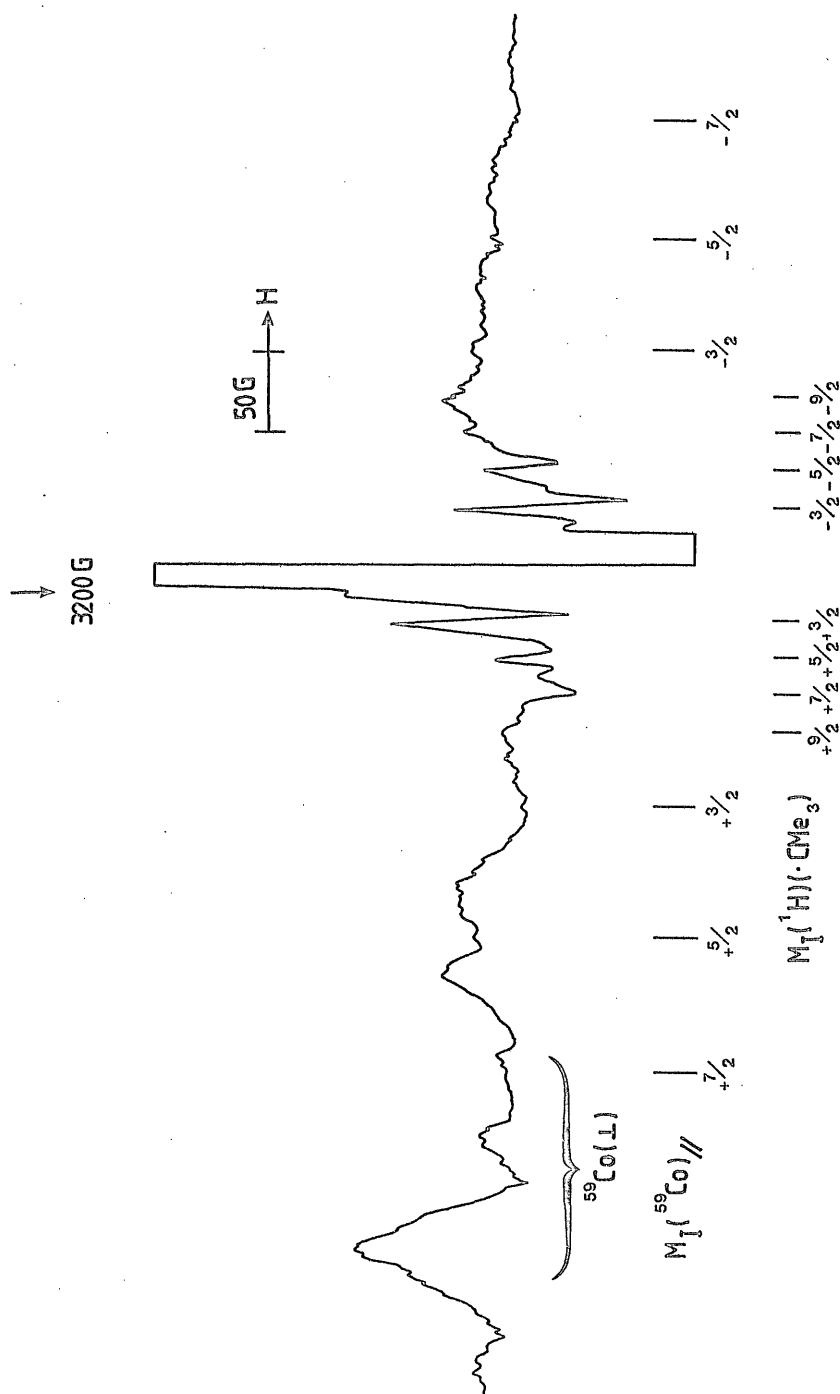


Figure 3.3. (c) First-derivative X-band e.s.r.spectrum of superoxo cobaloxime.

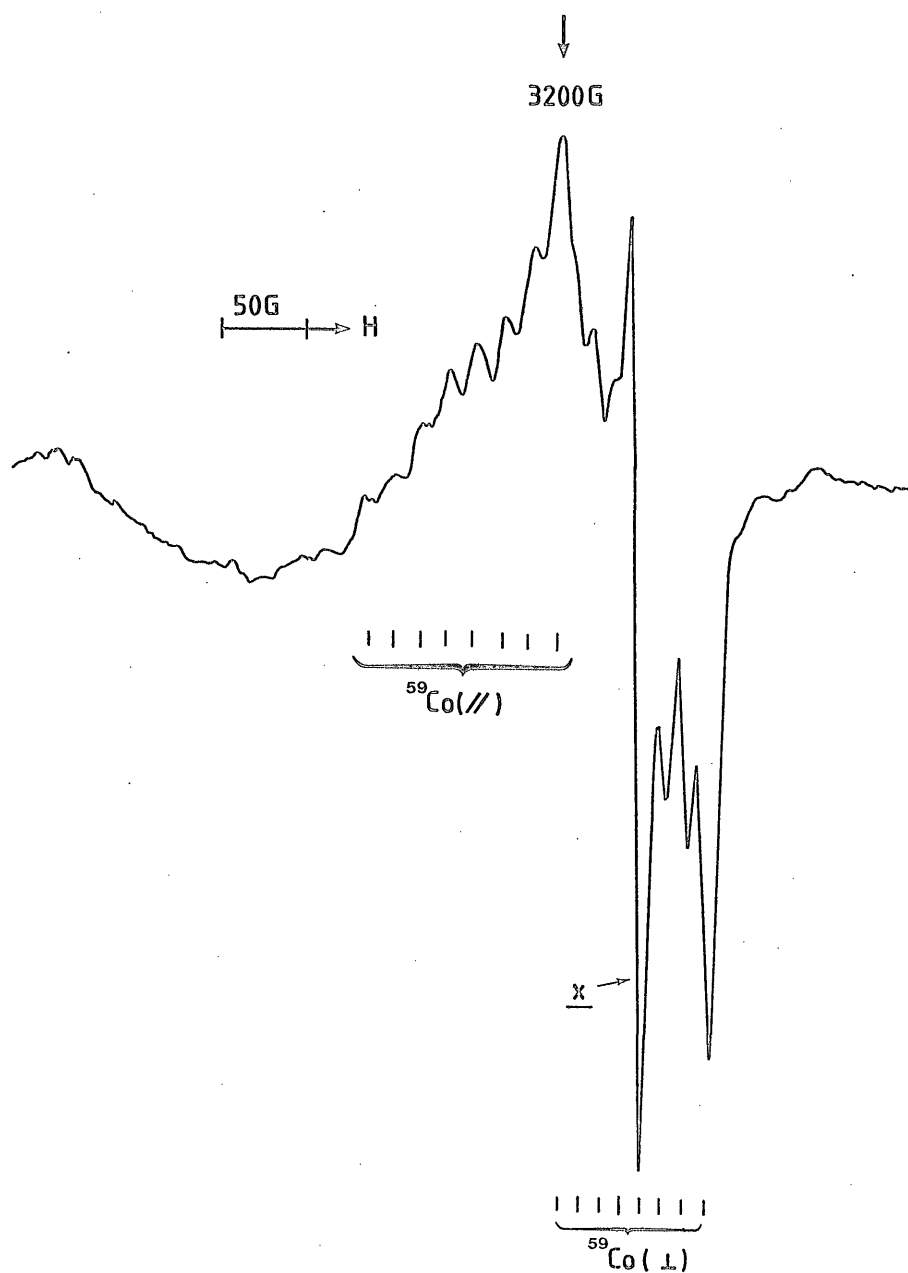


Figure 3.3 (d) First-derivative X-band e.s.r.spectrum of dipyridyl cobaloxime

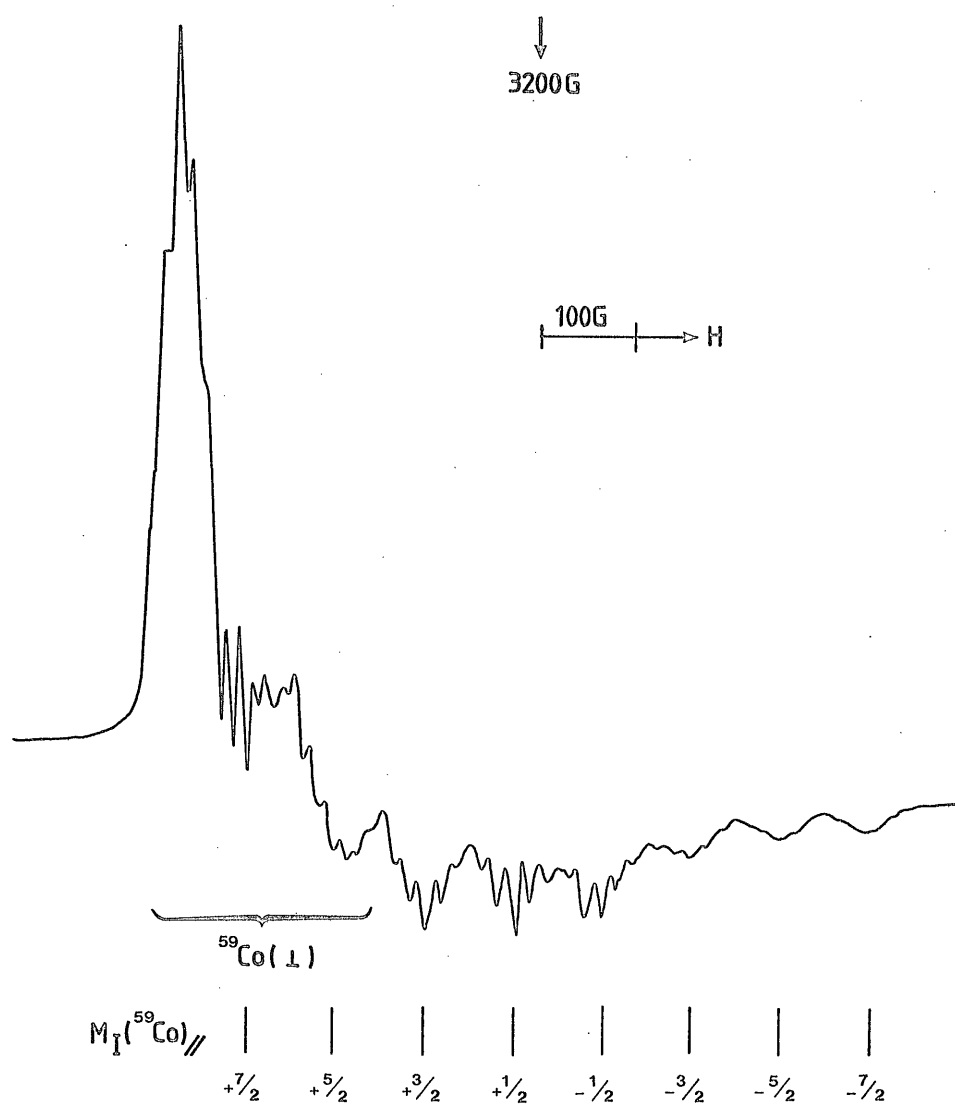




Table 3.3 Radicals detected by e.s.r spectroscopy after photolysis of dilute solutions of alkyl cobaloximes;

R-Co(DmgH)<sub>2</sub>-B

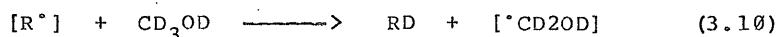
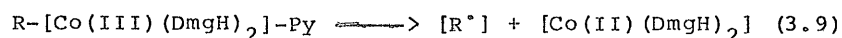
Ligand R	Solvent	Radicals	Other products
-CH <sub>3</sub>	CD <sub>3</sub> OD	<sup>•</sup> CH <sub>3</sub> <sup>•</sup> CD <sub>2</sub> OD	Co(II) + Broad "pair" features <sup>a</sup>
	MeTHF	<sup>•</sup> MeTHF <sup>b</sup>	Co(II) (Broadened)
-CD <sub>3</sub>	CD <sub>3</sub> OD	<sup>•</sup> CD <sub>3</sub> <sup>•</sup> CD <sub>2</sub> OD	Co(II) (Broadened)
- <sup>13</sup> CH <sub>3</sub>	CD <sub>3</sub> OD	<sup>13</sup> CH <sub>3</sub>	
-C <sub>2</sub> H <sub>5</sub>	CD <sub>3</sub> OD	<sup>•</sup> CH <sub>2</sub> CH <sub>3</sub>	Co(II) + (Broadened features)
	MeTHF	<sup>•</sup> MeTHF <sup>b</sup>	Co(II) (Broadened)
-CH <sub>2</sub> CH <sub>2</sub> CH <sub>3</sub>	CD <sub>3</sub> OD	<sup>•</sup> CH <sub>2</sub> CH <sub>2</sub> CH <sub>3</sub> <sup>c</sup>	Co(II)
-CH(CH <sub>3</sub> ) <sub>2</sub>	CD <sub>3</sub> OD	<sup>•</sup> CH(CH <sub>3</sub> ) <sub>2</sub>	Co(II)
-CH <sub>2</sub> CH(CH <sub>3</sub> ) <sub>2</sub>	CD <sub>3</sub> OD	<sup>•</sup> C(CH <sub>3</sub> ) <sub>3</sub>	Co(II)

(a) Ill defined broadening, with no resolved zero field splitting, assigned to weak Co(II)....Radical coupling.

(b) Normal MeTHF radicals.

(c) Broad, poorly defined features: Could be a mixture of <sup>•</sup>CH<sub>2</sub>CH<sub>2</sub>CH<sub>3</sub> + <sup>•</sup>CH(CH<sub>3</sub>)<sub>2</sub> radicals.

of the photolysis of alkylcobalamins (chapter 2). Therefore the reaction sequence 3.9-3.11 is proposed where the brackets represent cage trapping. The caged triplet-state pairs



probably include  $R^\bullet$  and solvent radicals. These are the major products at 77 K, but since the e.s.r. spectra are very sensitive to separation, the lines are very broad. Only those radicals that escape the cages and move well away from the Co(II) complexes gave well resolved spectra. On annealing all signals were rapidly lost. However if oxygen was not removed, well defined features for superoxo cobaloxime were detected.

#### Comparison with alkylcobalamins

These results are very similar to those reported for alkylcobalamins (96). In the particular case of methylcobalamin pair-trapping was sufficiently precise to permit the extraction of the zero-field splitting parameters, for which a mean separation of  $\text{ca. } 8.3 \text{ \AA}$  was determined. Probably the separations are comparable in this study, but the spectra are too poorly defined to warrant any attempt at analysis. Thus, although they differ markedly with respect to electron addition, the alkylcobaloximes closely resemble the cobalamins in photolysis.

### Comparison with the active enzyme radicals

In view of the current interest in the doublet e.s.r. spectrum obtained from the  $\text{CoB}_{12}$ -enzyme complex during reaction with substrates, it seemed of interest to compare these results for pair-trapping with those which are ascribed to pair-trapping when enzyme- $\text{CoB}_{12}$  complexes with substrates such as diols or ethanolamine are frozen at 77 K. Two e.s.r. features result (47). A broad resonance at  $g=2.3$  is clearly due to the  $\text{Co(II)}$  complex, but there has been considerable controversy regarding the cause of an asymmetric doublet feature in the free-spin region. It now seems to be reasonably well established that these features are due to  $\text{R}^{\bullet} \cdots \text{Co(II)}$  pairs probably  $\text{ca. } 10 \text{ \AA}$  apart. However the normal spin-spin dipolar contribution to the spectra is apparently small (simulations for which this term is omitted are still reasonably accurate), the major contribution to the doublet splitting coming from the exchange term. Thus these spectra differ markedly from the triplet-state centers studied herein, despite the fact that in both the cases  $\text{R}^{\bullet} \cdots \text{Co(II)}$  pairs are postulated. In this work there can be little doubt that the normal dipolar features are seen. These are for transitions  $|-1 \rightarrow 0\rangle, |0 \rightarrow -1|$  within the triplet manifold split by the zero-field coupling. However it seems that the active enzyme doublet features are singlet-triplet transitions for systems in which the exchange term,  $J$ , is quite small.

CHAPTER 4COBALT PORPHYRINS, COBALT PHTHALOCYANINS, COBALT-PEPTIDE  
COMPLEXES AND MANGANESE PORPHYRINSINTRODUCTION

In this chapter some of the results on the cobalt complexes of biologically relevant ligands such as porphyrins, phthalocyanins and peptides have been presented and their implications in biological systems are discussed.

Co(II) forms low spin ( $d^7$ ) complexes with porphyrins, phthalocyanins, corrins and related systems. The unpaired electron in a  $d_{z^2}$  orbital in the ground state offers a sensitive system to study axial perturbations of the metal. In contrast, Co(II) forms a high spin complexes with peptides and proteins. Although it is a disadvantage that these complexes must to be studied by e.s.r. spectroscopy at liquid helium temperatures, it has been shown that the spectra are extremely sensitive to low-symmetry configurations of the ligand field (157). Co(II) has been widely used to study cobalt substituted zinc proteins (158-163).

This chapter is broadly classified into the following sections:

- (1) Cobalt porphyrins
- (2) Cobalt phthalocyanins
- (3) Cobalt peptide complexes
- (4) Cobalt carnosine complexes
- (5)  $\text{Co}(\text{EHPG})^-$  and  $\text{Mn}(\text{EHPG})$

## (6) Manganese porphyrins

EXPERIMENTAL

TPP, proto-porphyrins, EHPG and peptides were obtained from Sigma chemicals. Cobalt phthalocyanin was supplied by Kodak Ltd.

Co(III) protoporphyrin IX

This was prepared in the form of pyridyl adduct according to the procedure of Yonetani *et al* (164,165). A typical preparation is as follows: 100 mg of cobaltous acetate was dissolved in 100 ml of glacial acetic acid in a beaker. The mixture was heated to 80-85°C under a stream of nitrogen gas. Similarly 100 mg of proto-porphyrin was dissolved in 40 ml of glacial acetic acid and 15 ml of pyridine. The mixture was like-wise heated to 80°C under a stream of nitrogen. The heated porphyrin solution was gradually added to the cobalt solution. After 15 mins the reaction mixture was cooled and evaporated to dryness in a vacuum rotary evaporator. The dried material was dissolved in py;chloroform;water;octane(10;5;5;5 v/v) and chromatographed on silica gel. The dipyrityl derivative of cobalt TPP was eluted and evaporated to dryness. The purity of the preparation was checked by optical spectroscopy. Co(II)TPP was prepared by the method of Walker (166). Purified Mn(III) TSPP was supplied by Dr. A. Harriman and the procedure is described in ref. 167.

Co(III)peptide complexes

Co(III) (gly-gly)<sub>2</sub>.6H<sub>2</sub>O

$\text{Co(III)(gly-L ala)}_2$

$\text{Co(III)(L ala-L ala)}_2$

These complexes were prepared from the corresponding dipeptides and cobalt carbonate(168). A typical procedure is as follows: 60 mg of cobalt carbonate(0.5 mMole) was suspended in a solution of dipeptide (1 mMole equivalent) in 20 ml water. It was warmed to 60°C with stirring. 8 ml of hydrogen peroxide (6%) was added dropwise allowing the vigorous effervescence to subside. During this the colour of the solution changed to red and it was cooled overnight, filtered and rotoevaporated at 40°C. Inorganic salts and unchanged peptide were separated by sephadex G-10 filtration and the product was freeze-dried. Crystalline complexes were not obtained for the last two complexes.

CHN results for  $\text{Co(III)(gly-gly)}_2 \cdot 6 \text{ H}_2\text{O}$ , (calculated) C 22.2%, H 5.5%, and N 12.9%. (found) C 21.8%, H 4.7% and N 12.6%.

Sodium glycylglycinato trinitro cobaltate(III)

This was prepared by the method of Celap and Solujic(169). 2.38 g of cobalt chloride (in 10 ml water) was mixed with a solution of sodium nitrite(2.07 g in 10 ml water). To this 1.32 g of gly-gly and 0.36 g sodium hydroxide dissolved in 20 ml water was added. Air was passed through the reaction mixture for 3 hours and it was rotoevaporated at 40°C. The product was washed with ethanol, ether and finally recrystallised from hot water. Purity of the sample was checked by optical spectroscopy (Fig 4.1a).

CHN results are: (calculated) C 14.04%, H 2.06% N 20.48%,

(found) C 14.01%, H 2.10% N 18.6%

Ethylenediamine glycyglycinato nitro cobalt(III)

This was prepared from sodium glycyglycinato trinitro cobaltate(III) (169). To a solution of 1.86 g (5 mMole) of this complex in 10 ml of water, 0.5 ml ethylenediamine was added. The reaction mixture was heated at 60°C for 2 hours and then left overnight at room temperature. The product was filtered, washed with ethanol, ether and dried in vacuo. Purity of the sample was checked by optical spectroscopy (Fig 4.1b).

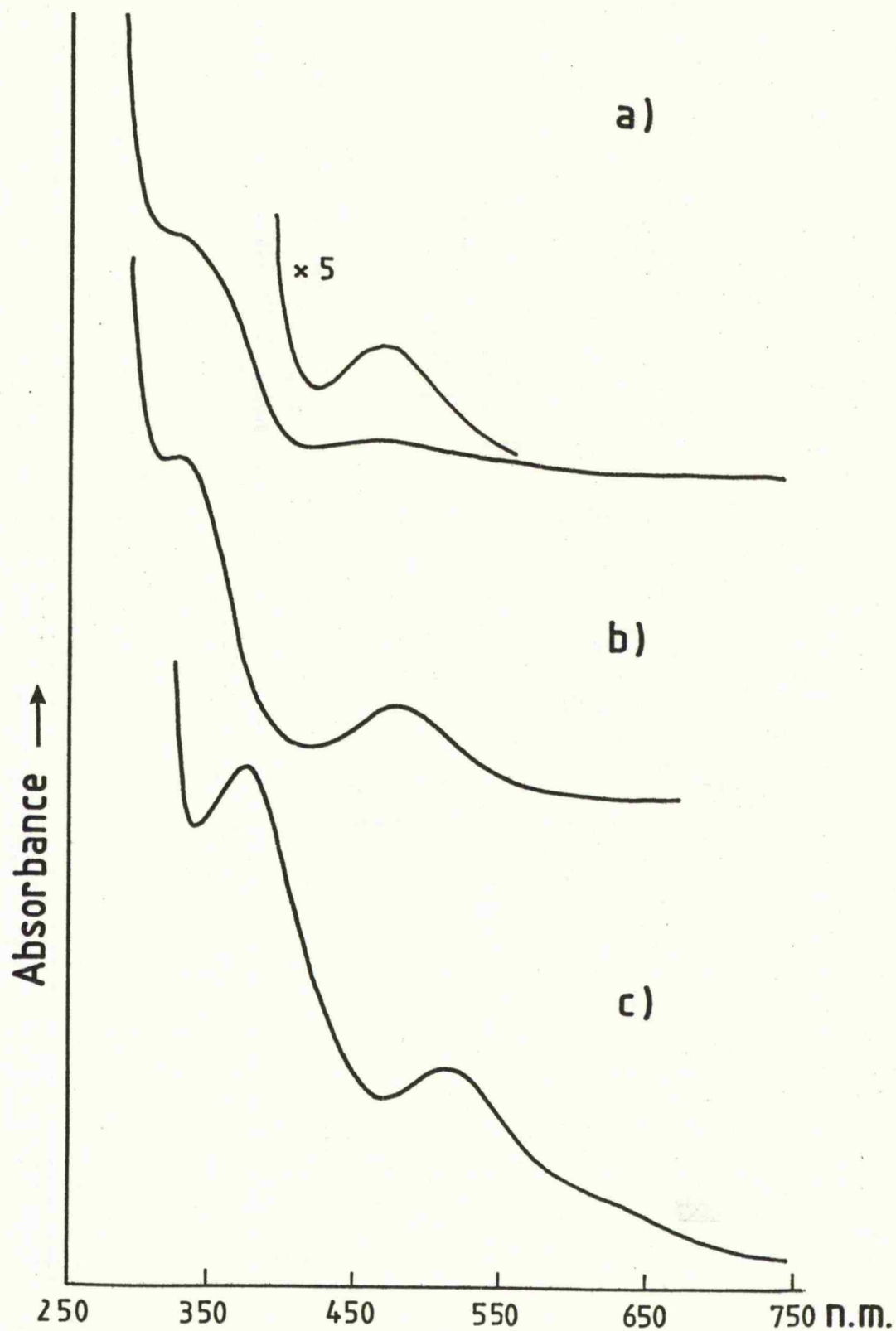
Co(EHPG) and Na[MnEHPG] were prepared by the method of Patch et al. (163). EHPG was recrystallised from acetone in a nitrogen atmosphere.

Co[EHPG] was prepared by mixing 8 mMole of  $\text{CoCl}_2 \cdot 6 \text{H}_2\text{O}$  and 8 mM equivalent of EHPG in 10 ml of 1.5M ammonium hydroxide. The dark brown solution was stirred for 3 days. A small amount of 3% hydrogen peroxide was added to oxidize any Co(II) to Co(III) complex. The product was filtered and rotoevaporated to dryness. It was taken up in methanol and purified on a silica gel column. Purity of the preparation was checked by optical spectroscopy (fig 4.1c).

Na[Mn(EHPG)]  $1.5 \text{H}_2\text{O}$

720 mg EHPG was suspended in 5 ml of water through which nitrogen was passed for 30 mins. About 180 mg sodium hydroxide was added, stirred and nitrogen gas was passed for 1.5 h until all the solid EHPG was dissolved. 536 mg of Mn(III) acetate was added and left stirring overnight. It was filtered and the filtrate concentrated by rotoevaporation.

Figure 4.1. Optical spectra of (a)  $\text{NaCo(III)(gly-gly)(NO}_2)_3$  (b)  $\text{Co(III)(gly-gly)en NO}_2$  (c)  $\text{Co(III)EHPG}^-$ . All spectra were recorded in water.





The product was recrystallised from 50% ethanol/water and was dried in vacuo. Purity of the sample was checked by optical spectroscopy (Fig 4.1d).

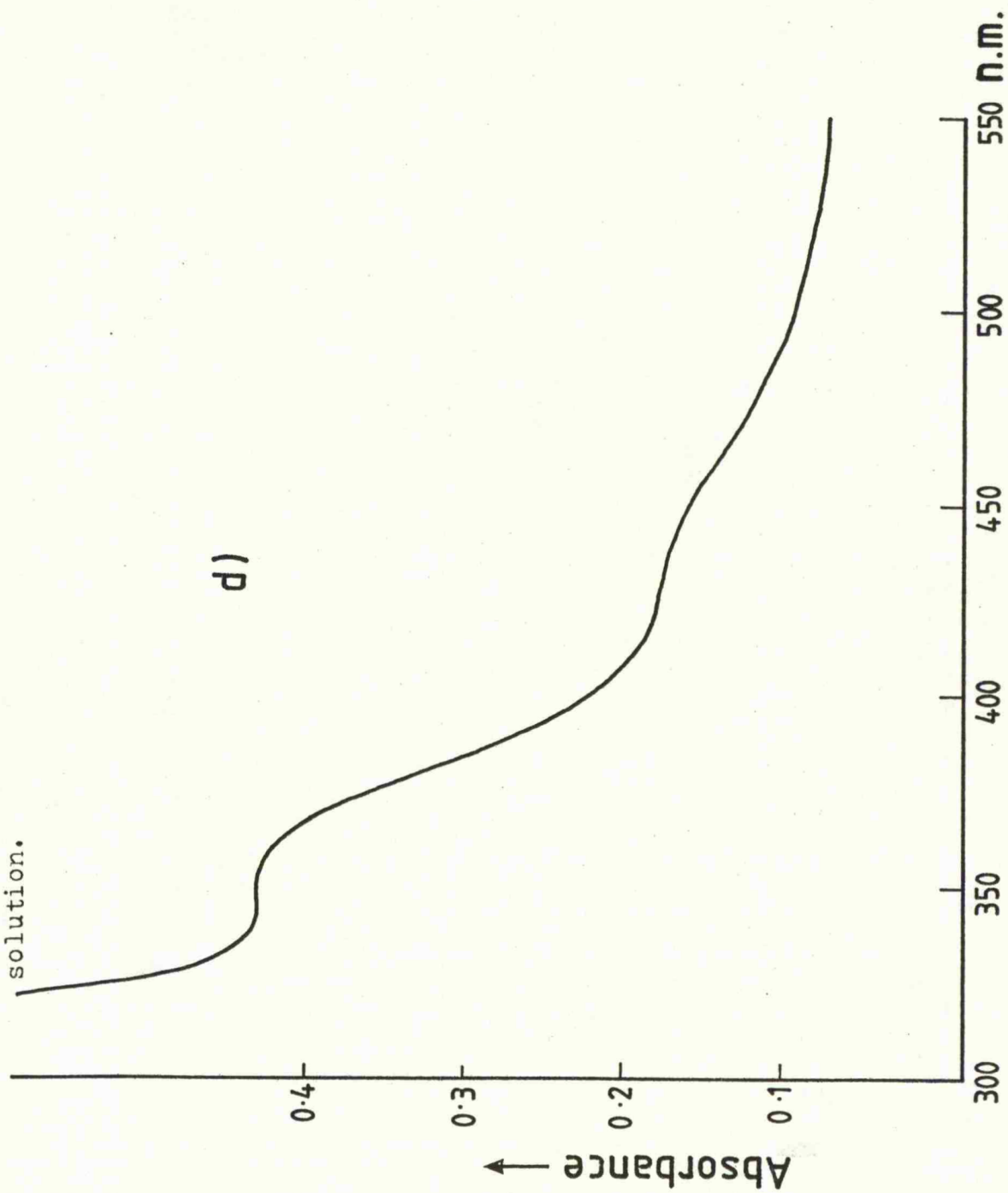
Samples of Co-peptides, Co-EHPG and Mn-EHPG complexes were also prepared in  $\text{CD}_3\text{OD}$  and  $\text{D}_2\text{O}$ . Adducts of Co-PTP and Co-PTH were prepared in  $\text{CH}_3\text{OH}$  and benzene respectively. Cobalt complexes of L-carnosine, gly-L his, and L-homocarnosine sulphate were prepared by mixing 10 mM cobaltous chloride with the peptide in ethyleneglycol-water so that the final concentration was in the desired molar ratio. The pH of the solution was adjusted with aliquots of 10 mM HCl or 10 mM sodium hydroxide. Glassy-beads were made as described in chapter 2 and the samples were irradiated to a dose of 1 Mrad. E.s.r. spectra were recorded as described in chapter 2.

## RESULTS & DISCUSSION

### Co-TPP and Co-PTP

Co(II) porphyrins and related low spin Co(II) complexes have received considerable attention because of their ability to form reversible dioxygen complexes. They also function as one electron donor or two electron acceptors in reaction with ligands such as  $\text{CO}$ ,  $\text{SO}_2$ , amines and phosphines (166, 170-174). Because of oxygen binding properties of Co(II) porphyrins, they have been used in substituted myoglobin and haemoglobin as model complexes to understand the mechanism of oxygenation in haemoglobin (175). This section describes the reactions of simple heterocycles (containing two nitrogens) or thiazole (containing a nitrogen and a sulphur atom in

Figure 4.1 d. Optical spectrum of  $\text{Mn(III) EHPG}^-$  in water/ethanol solution.

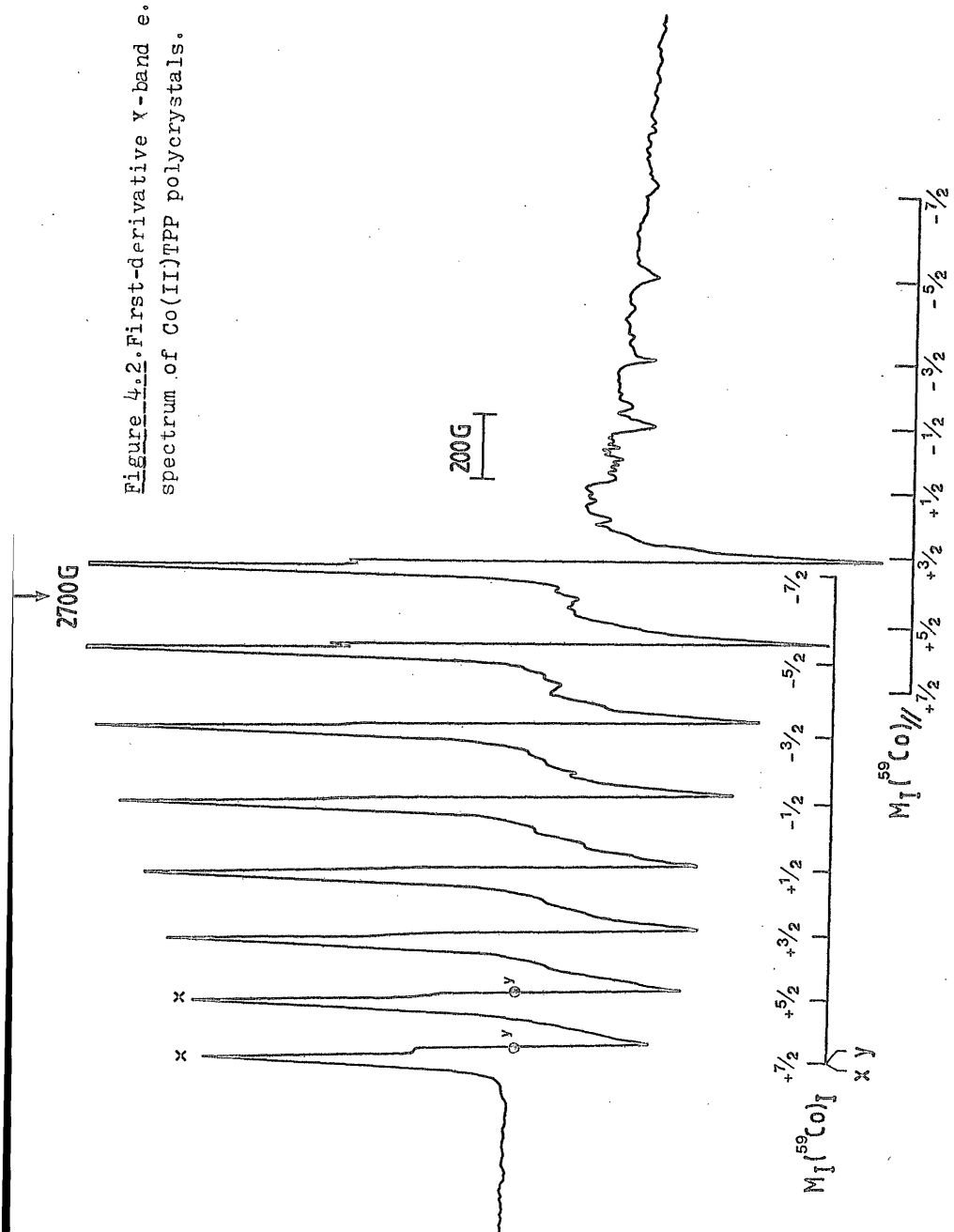


the ring) with CoTPP.

An e.s.r.spectrum of poly crystalline CoTPP is shown in figure 4.2. This spectrum shows well defined features from cobalt perpendiculars as shown for Co-PTH (176). Cobalt parallels are relatively much weaker and this is similar to the observation of Walker (166). When CoTPP is dissolved in benzene or similar solvents strong features due to the well known superoxo CoTPP are seen (table 4.1).

Co(III)PTP prepared by the method of Yonetani et al. (164,165) was in the form of dipyridyl derivative. Radiolysis of dipyridyl Co(III)PTP gave the Co(II) derivative (Fig 4.3a). This spectrum is similar to that for dipyridyl TPP reported by Walker (166). Shf interaction with two axial nitrogen is broadened due to phase separation in excess pyridine. On annealing above 77 K, it gave mono pyridyl Co PTP (Fig 4.3b). In the presence of oxygen it gave superoxo cobalt PTP. Similar results were obtained with dipyridyl CoPTP dissolved in 20% pyrazine. In presence of 20% thiazole or 20% pyridazine, CoPTP gave slightly different spectra (Fig 4.3c) but still retained both the axial ligands. Thiazole is bonded through nitrogen and not sulphur. Annealing (in presence of oxygen) above 77 K lead to the formation of superoxo CoPTP, this suggests that one of the heterocyclic ligands is displaced by oxygen. This observation is similar to that for bipyridyl cobaloximes (cf, chapter 3, photolysis work). The e.s.r.spectra of  $\text{Co}(\text{L}_4)\text{B}_2$  and  $\text{Co}(\text{L}_4)\text{B}$  are characteristic of a low spin Co(II) complex with the unpaired electron in  $3d_{z^2}$  orbital. Superoxo PTP has similar e.s.r.parameters as that

Figure 4.2. First-derivative  $\gamma$ -band e.s.r. spectrum of  $\text{Co(II)TPP}$  polycrystals.



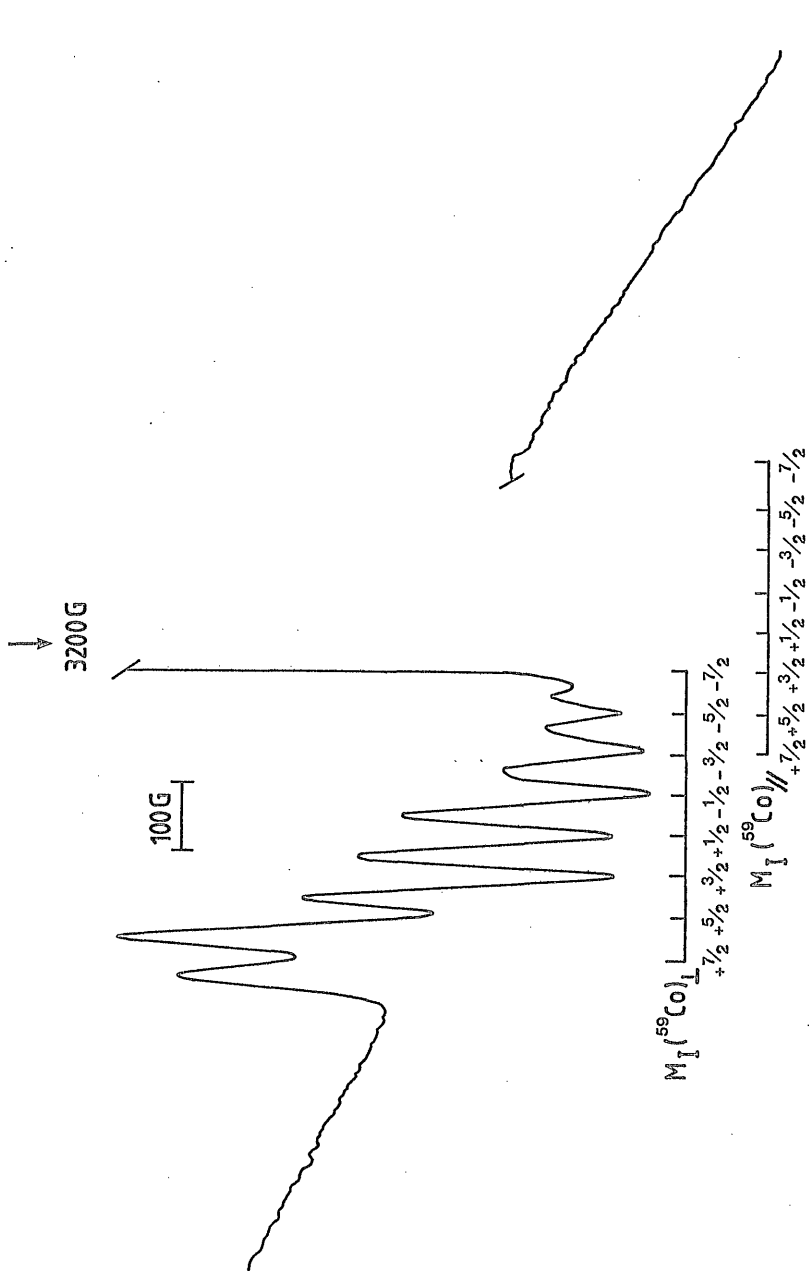
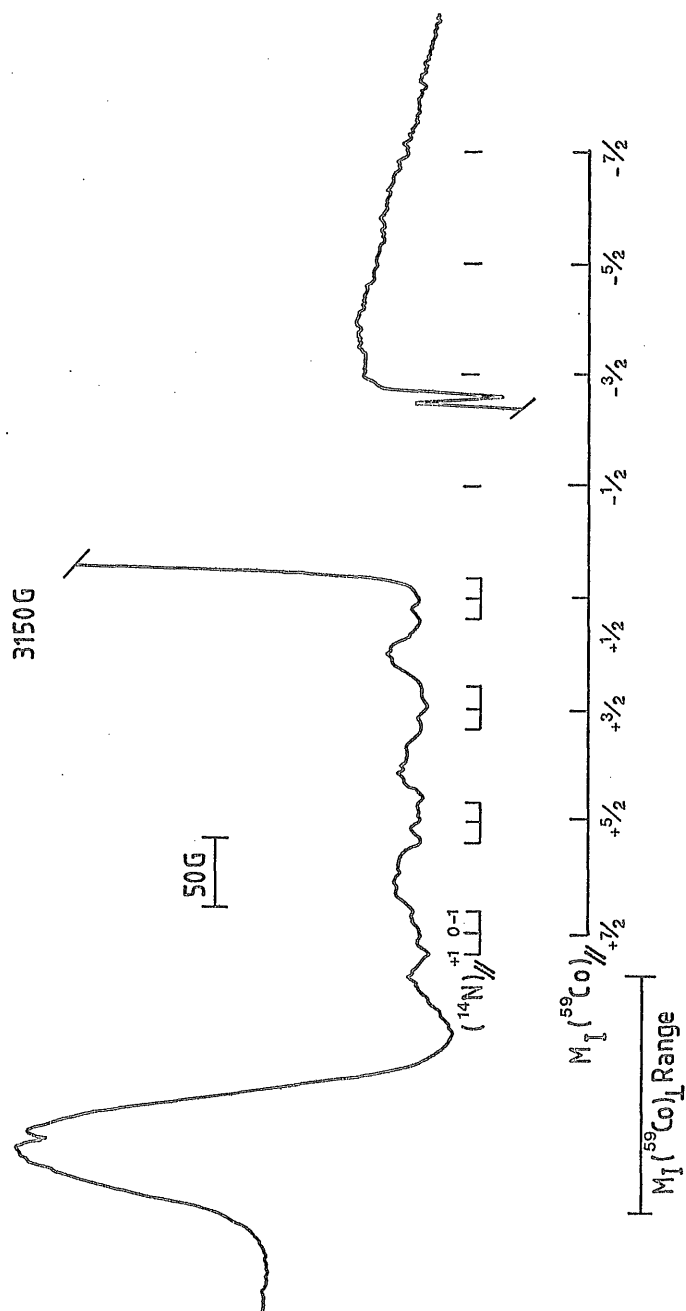


Figure 4.3 a. First-derivative X-band e.s.r.spectrum of dipyrrolyl adduct of Co(II) protoporphyrin-IX in methanol.

Figure 4.3 b. First-derivative X-band e.s.r. spectrum obtained after annealing dipyrrolyl adduct of Co(II) protoporphyrin-IX and recooling back to 77 K.



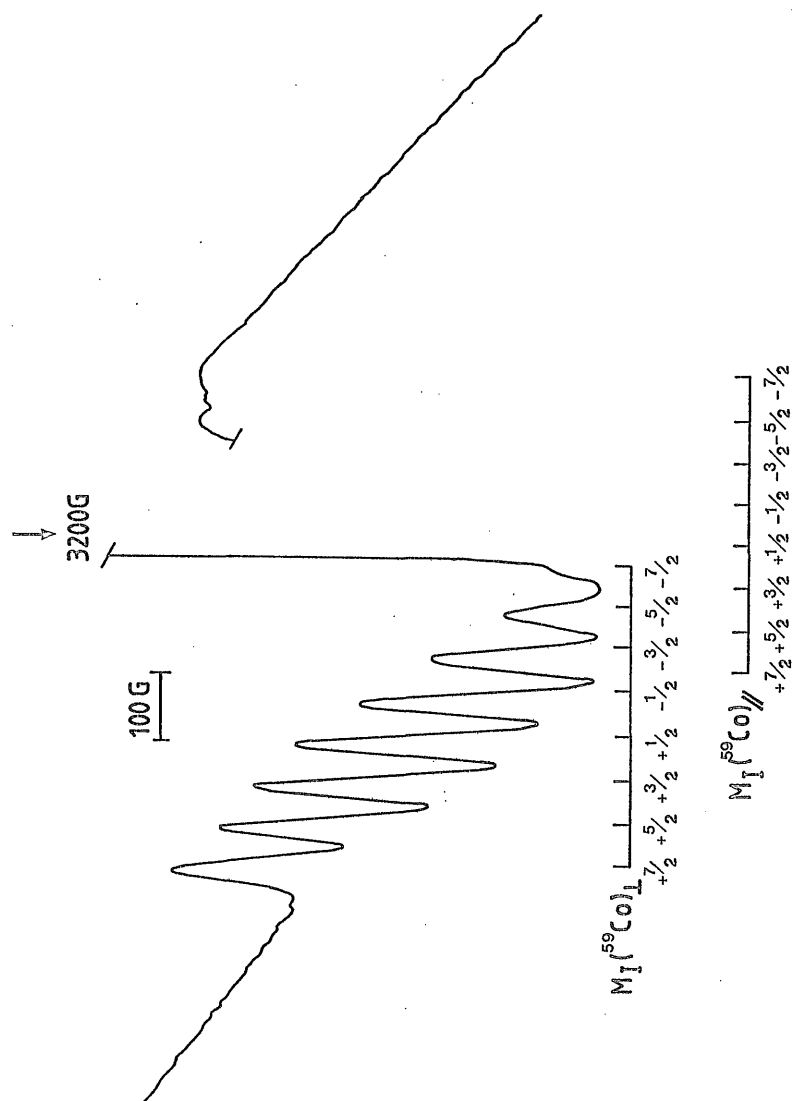


Figure 4.3 c. First-derivative X-band e.s.r. spectrum of Co(II) protoporphyrin-IX in the presence of 20% thiazole.

Table 4.1 E.s.r parameters for some cobalt complexes

Complex	Nucleus	Hyperfine coupling constants/Ga		g-values	
		$A_{\perp}$	$A_{\parallel}$	$g_{\perp}$	$g_{\parallel}$
CoTPP Polycrystals	$^{59}\text{Co}$	220	220	3.25	1.94
Co(p-Ome)TPP <sup>b</sup>	$^{59}\text{Co}$	422	157	3.28	1.79
Co(p-Ome)TPP + 2py <sup>b</sup>	$^{59}\text{Co}$	61	64	2.216	2.047
	$^{14}\text{N}$	-	12		
Co(p-Ome)TPP-O <sub>2</sub> <sup>b</sup>	$^{59}\text{Co}$	11.4	17.8	2.002	2.077
CoPTH + 2 py <sup>c</sup>	$^{59}\text{Co}$	NR	83	2.268	2.016
	$^{14}\text{N}$	-	12		
CoPTP + 2 py	$^{59}\text{Co}$	ca.60	ca.60	2.202	2.002
	$^{14}\text{N}$	-	NR		
CoPTP + 1 py	$^{59}\text{Co}$	ca.60	ca.60	2.202	2.018
	$^{14}\text{N}$	-	16		
CoPTH + 2 Thiazole	$^{59}\text{Co}$	ca.43	89	2.24	2.018
	$^{14}\text{N}$	-	14		
Co(gly-gly) <sub>2</sub>	$^{59}\text{Co}$	-	-	5.24	2.26
Co(gly-gly) <sub>2</sub> (NO <sub>2</sub> ) <sub>3</sub>	$^{59}\text{Co}$	ca.62	NR	2.18	2.18
Co(gly-gly) <sub>2</sub> en	$^{59}\text{Co}$	NR	NR	2.18	-
Co(EHPG)	$^{59}\text{Co}$	NR	NR	5.26	-

(a) = 0.1 mTelsa (b) Ref 11

(c) Ref, J.M.Assour J. Am. Chem. Soc. 87, 4701 (1965). (d) NR = Not resolved.



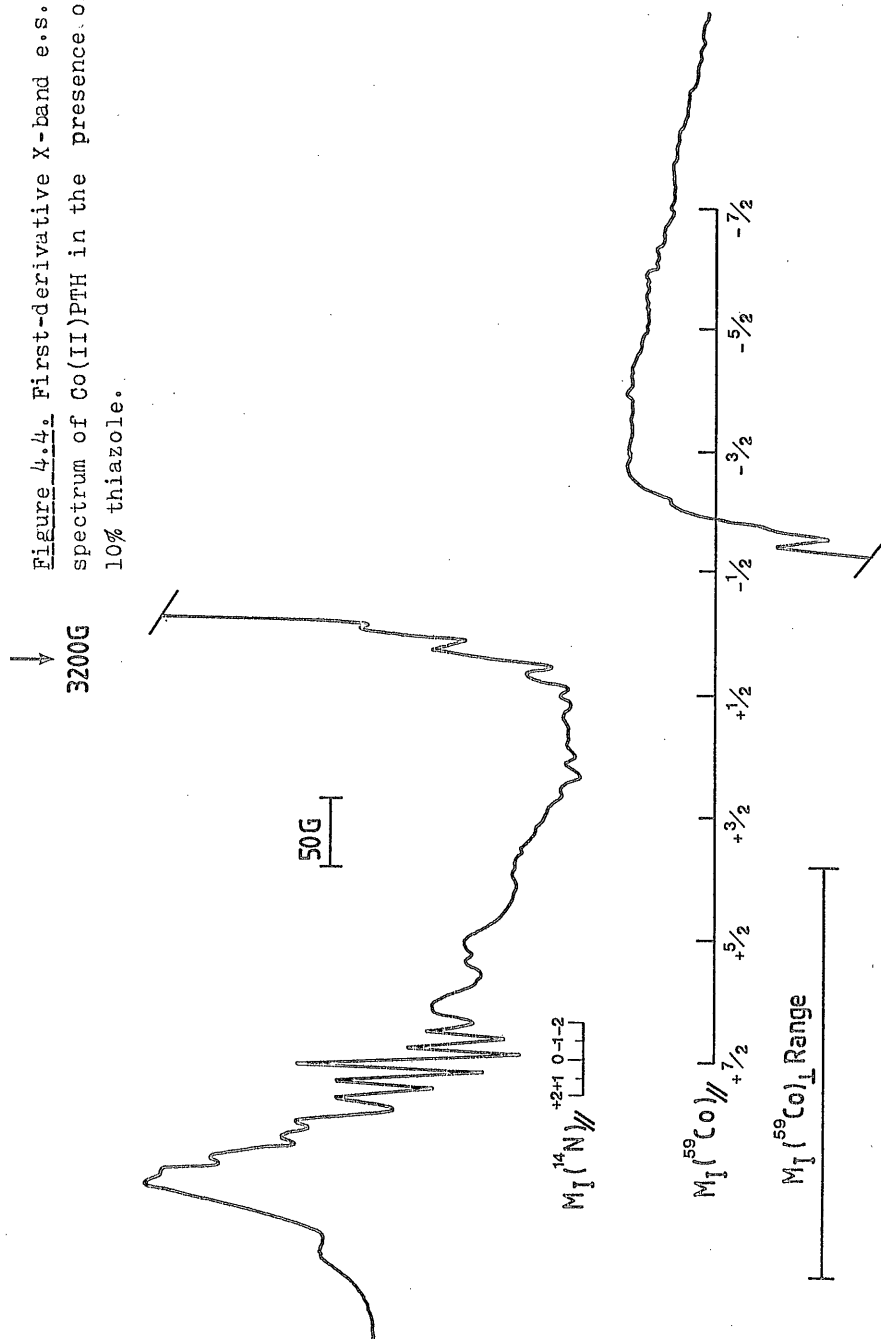
for superoxo cobalamins and superoxo cobaloximes(cf chapter 2 & 3) (table 4.1).

#### Co PTH

Phthalocyanins,owing to their planar porphyrin-like structure,great stability,intense colour and electronic and catalytic properties,have been the subject of growing interest (176-178).Although Co PTH are not reversible oxygen carriers,they do form adducts with pyridine and related ligands.PTH are known to exist in three different polymorphic forms.The beta-form is the most stable polymorph.Co(II)PTH, prepared and sold by Kodak laboratories have been used in this study. Co(II)PTH is insoluble in most organic solvents but sparingly soluble in benzene.Co-PTH solutions in benzene containing 20% pyridine gave the dipyridyl derivative with well defined shf lines for two axial nitrogens( $A_{||} = 15$  G) (Fig 4.4).Identical product was obtained in the presence of 10% thiazole.After annealing above 77 K no change in the e.s.r. spectra was observed.This suggests that dipyridyl derivative or dithiazole derivative is stable unlike the corresponding derivative of Co(II)PTP.It does not form superoxo phthalocyanins when annealed in presence of oxygen.This is one of the major differences between Co PTH and other cobalt complexes such as cobalt porphyrins, cobaloximes and cobalamins.E.s.r.parameters are characteristic of low spin  $d^7$ -configuration with the unpaired electron in a  $d_{z^2}$  orbital(table 4.1).

#### Co(III)dipeptide complexes

Figure 4.4. First-derivative X-band e.s.r. spectrum of Co(II)PTH in the presence of 10% thiazole.

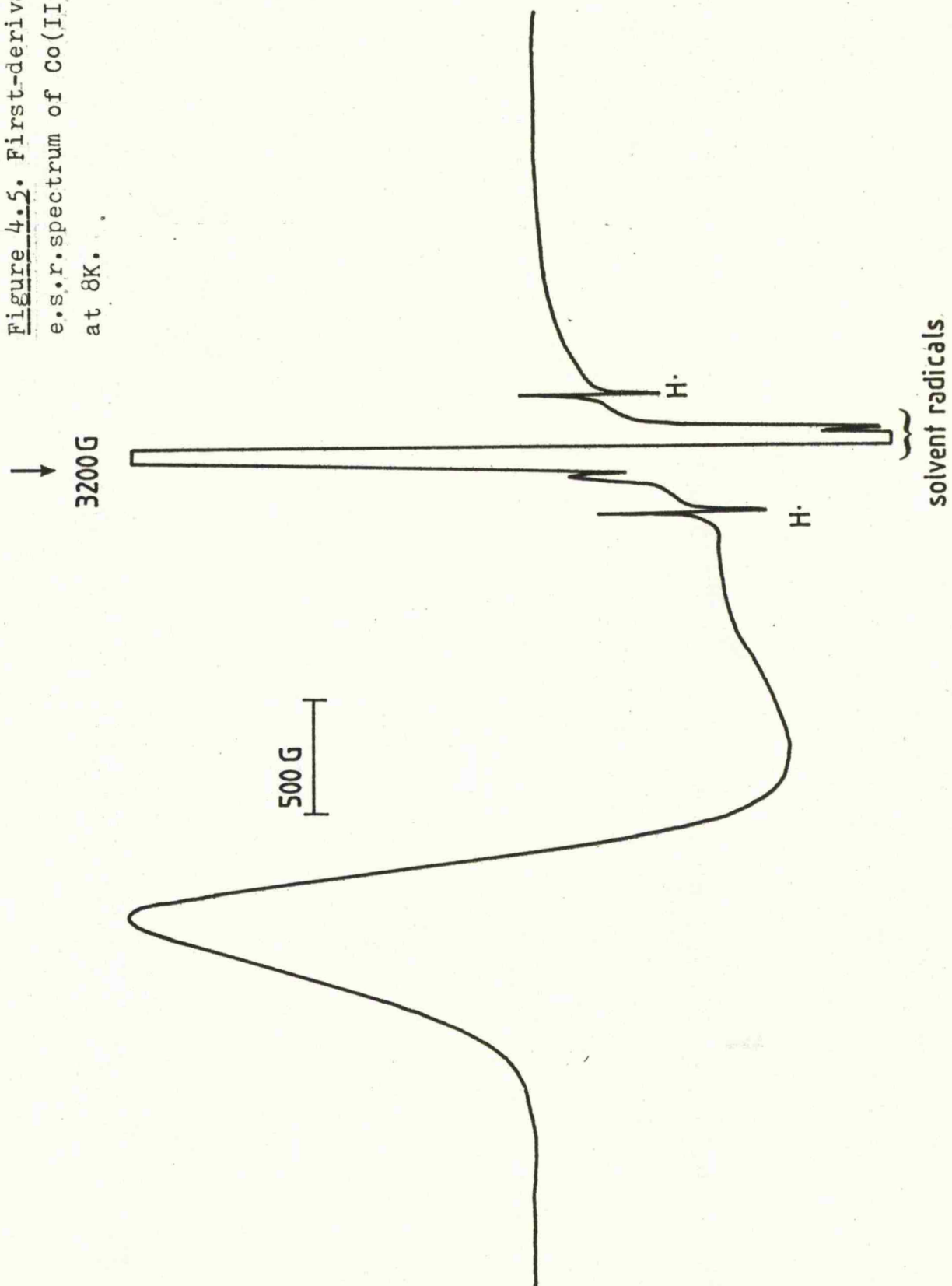


Cobalt porphyrins and cobalt corrins, when incorporated into proteins, bind proteins through their fifth coordination site. The sixth coordination site may be left open for catalysis. In contrast to this Co(II) forms high spin complexes when substituted for other metals in metallo-enzymes. Co(II) is largely used with Zn containing proteins since the  $Zn^{2+}$  ion is magnetically and optically silent (158-161). The potential liganding centres for metals in a protein are carboxylates, imidazoles, thiolates and phenolates. These groups have high pK and are ineffective ligands for divalent metals (179).

In this section a few Co(II) (di-peptide)<sub>2</sub> complexes have been studied as model complexes for cobalt substituted Zinc proteins. The e.s.r. spectrum of Co(gly-gly)<sub>2</sub> is shown in fig 4.5.

Similar spectra were obtained for Co(II) (gly-L ala)<sub>2</sub> and Co(II) (L ala-L ala)<sub>2</sub>. All the complexes exhibited a symmetrical peak of  $g = 5.2 - 6.0$ . The large line-widths contains the unresolved  $^{59}Co$  hyperfine coupling.  $g_x'$  and  $g_y'$  are too broad to be seen probably because of unresolved  $^{59}Co$  hyperfine coupling and also additional broadening effects arising from a variability in the precise co-ordination geometry induced by discontinuities in the frozen medium (157). The  $g_x'$  values correspond to the model complexes such as dibromodip-methoxyaniline cobalt(II) and other complexes shown in ref 161. Evaluation of parameters such as  $\gamma$ ,  $\delta$ , and  $\beta^2$  could not be done due to the lack of precise  $g_y'$  and  $g_z'$  values. It has been shown however, (161) that values in

Figure 4.5. First-derivative X-band  
e.s.r. spectrum of  $\text{Co(II)(gly-gly)}_2 \cdot 2\text{H}_2\text{O}$   
at 8K.



the range of 4-17  $\text{cm}^{-1}$  are associated with tetra coordinated species whilst higher values of 50-81  $\text{cm}^{-1}$  are associated with penta coordination. Intermediate values are associated with a trigonal bipyramidal structure wherein a fifth axial ligand is far removed and almost behaving as trigonal pyramidal structure (161).

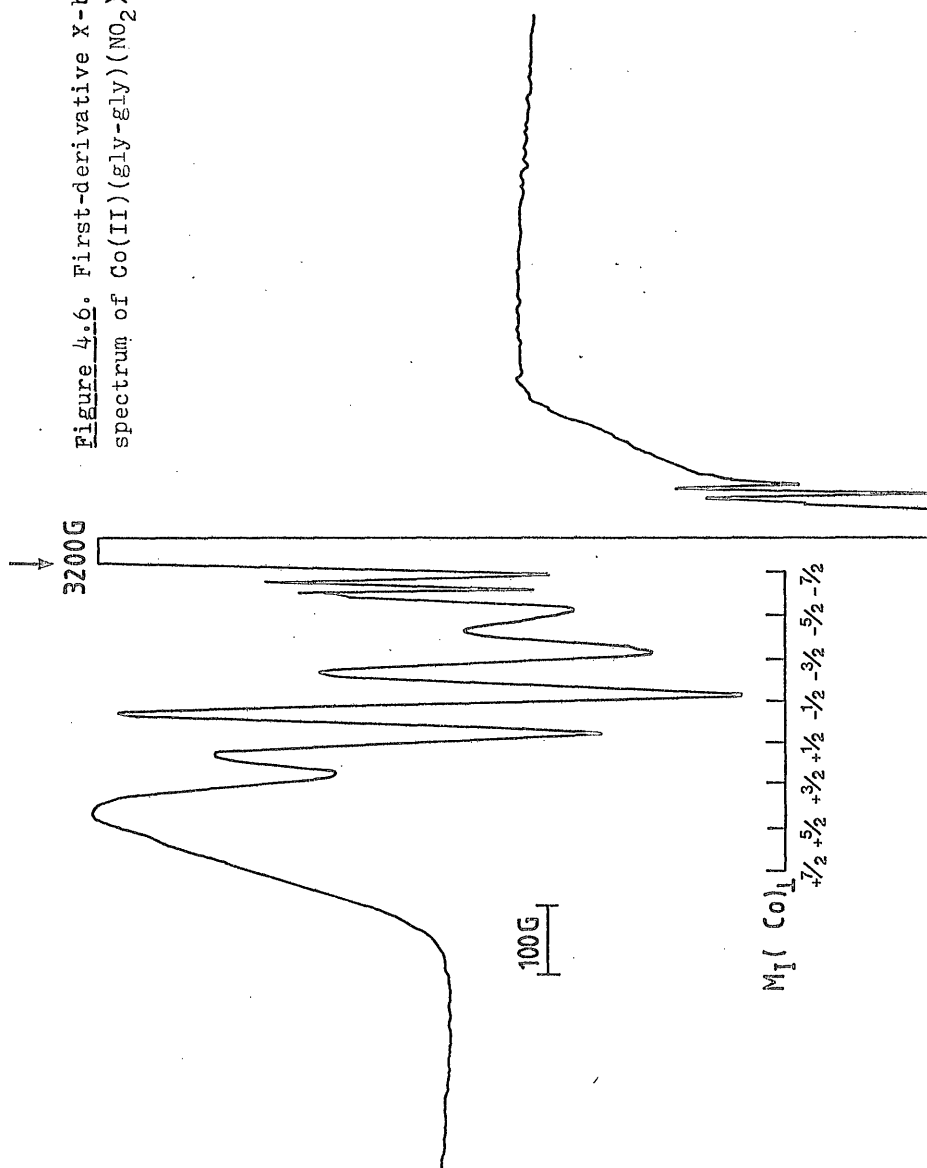
Low spin cobalt peptide complexes were prepared by incorporating ligands such as  $\text{NO}_2$  and en. Fig 4.6 shows the e.s.r. spectrum of  $\text{Co(II)(gly-gly)(NO}_2)_3$

#### Co(II)carnosine complexes

Carnosine(beta-alanyl-L-histidine) is a dipeptide which forms a low spin superoxo cobalt complex in the presence of oxygen (180,181).  $\text{Co(II)}$  and enzyme carnosinase is present at highest concentration in the kidney(182,183). Carnosine is the substrate of this enzyme and it binds  $\text{Co(II)}$  to function as a reversible oxygen carrier. Since the kidney monitors the oxygen tension of blood(184,185) superoxo cobalt complex of carnosine has an important physiological role. In this section some of the results obtained from cobalt complexes of carnosine and its structural analogs like gly-L-his and homo-L carnosine are presented.

Cobaltous chloride forms superoxo complex with carnosine and its structural analogs under appropriate conditions(Fig 4.7a). Gly-L-his and homo-carnosine formed superoxo cobalt complex at pH ca.9.0 when the metal to ligand ratio was 1;10 or 1;20(Fig 4.7b). Carnosine however gave superoxo cobalt complex even when the metal to ligand ratio was 1;1000(181).

Figure 4.6. First-derivative X-band e.s.r. spectrum of  $\text{Co(II)(gly-gly)(NO}_2)_3$  at 77 K.



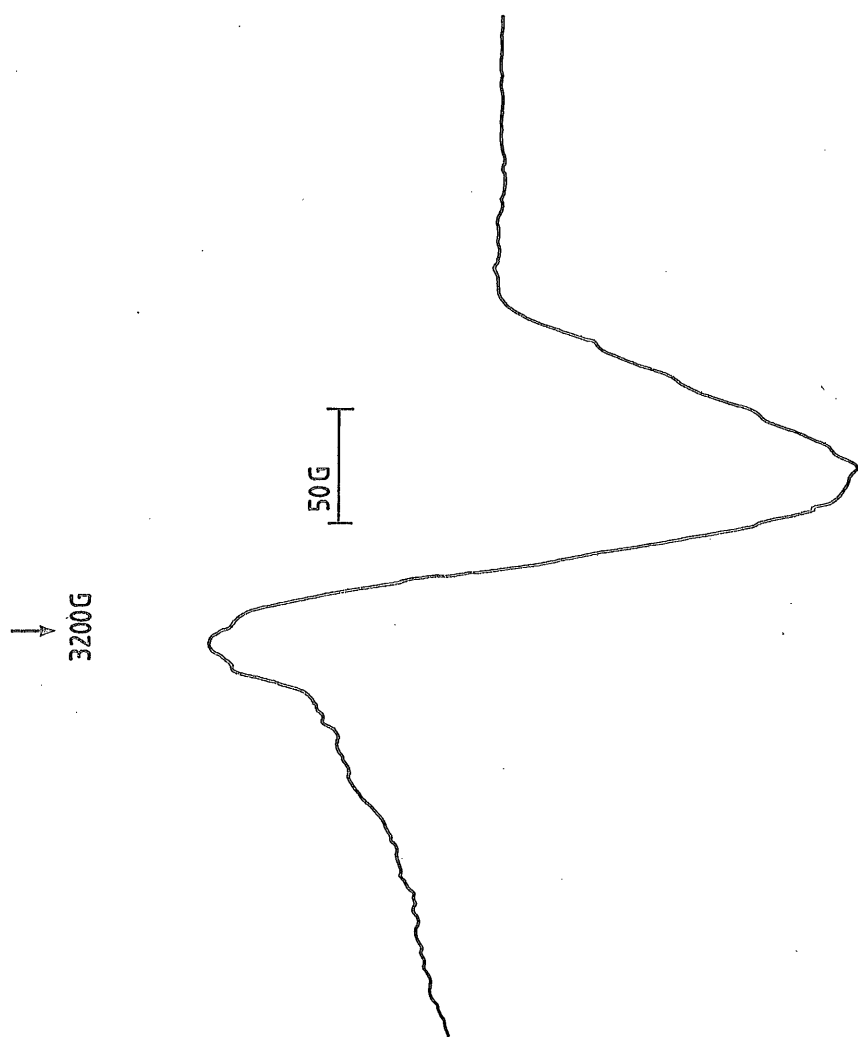
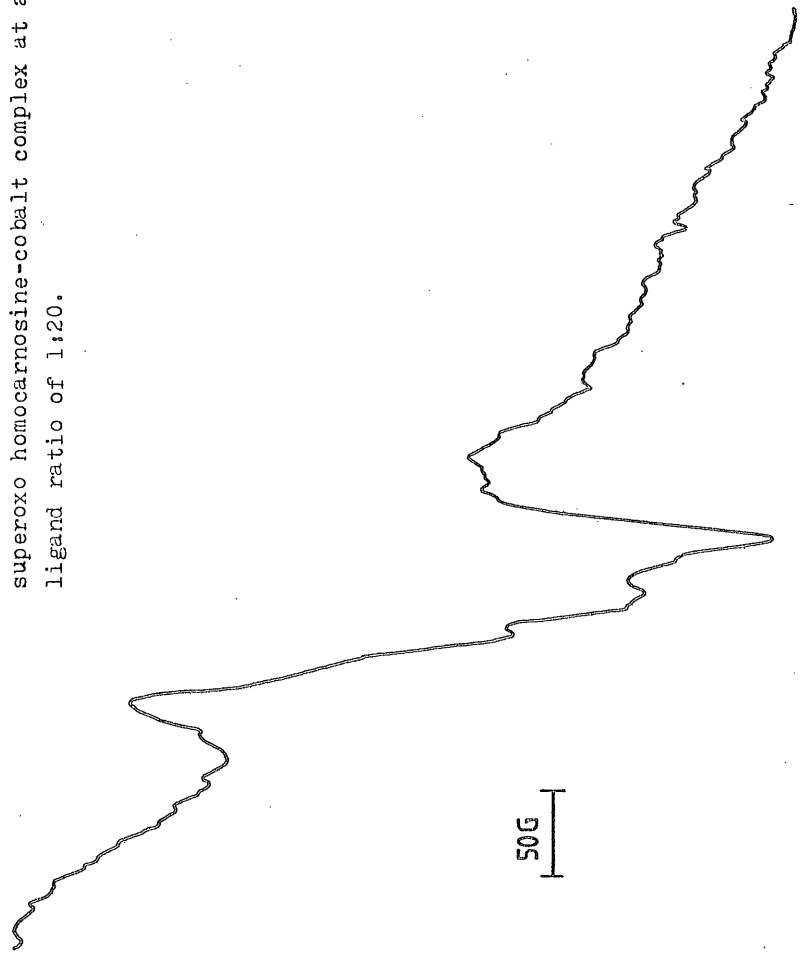


Figure 4.7 a. First-derivative X-band e.s.r. spectrum of superoxo cobalt-carnosine complex at a metal to ligand ratio of 1:20.

↓  
3200G

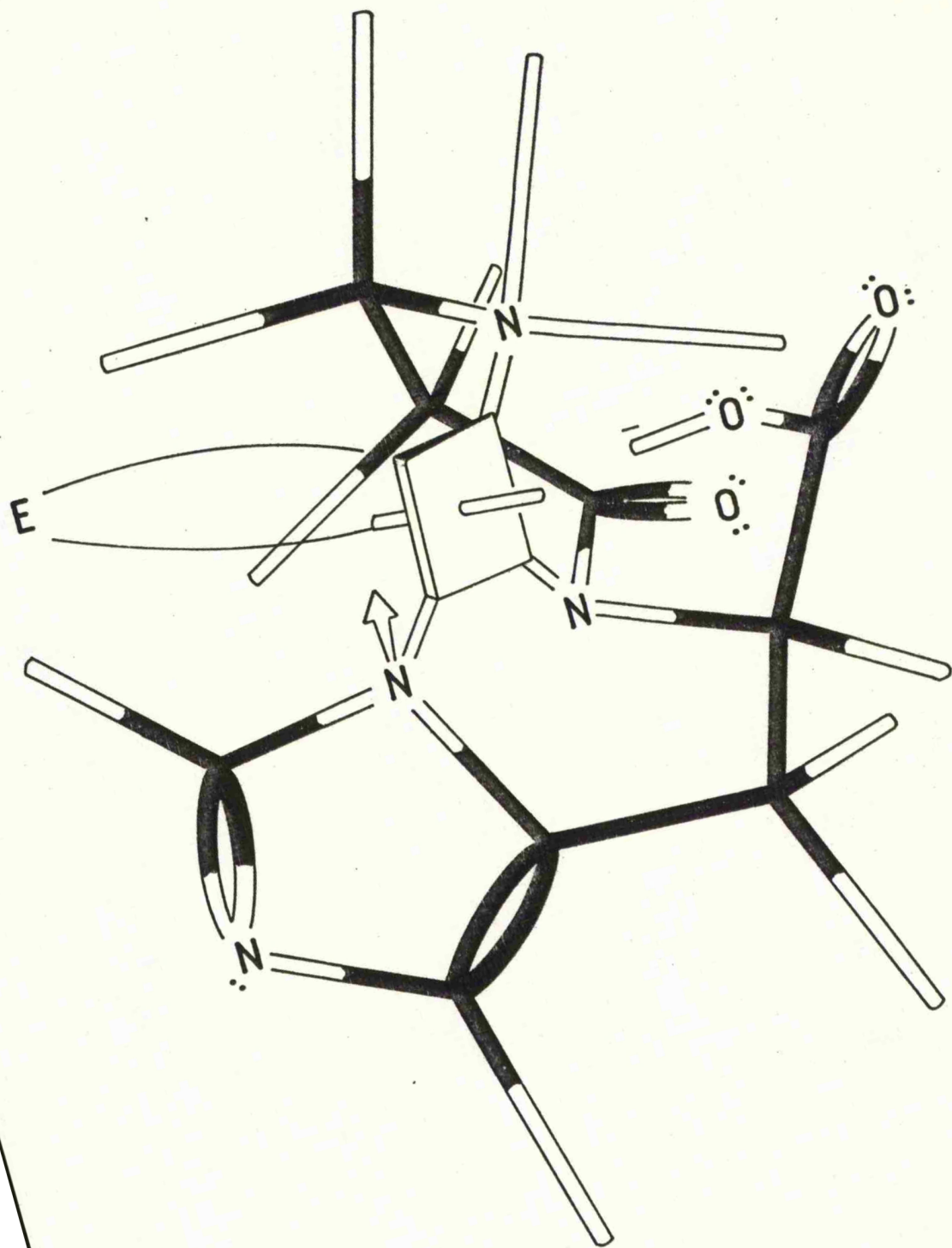
Figure 4.2 b. First-derivative X-band e.s.r. spectrum of superoxo homocarnosine-cobalt complex at a metal to ligand ratio of 1:20.



50G



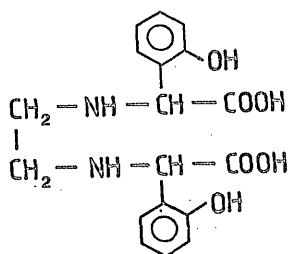
Figure 4.8. Structure of Co(II)-carnosine complex when metal to ligand ratio is one (reproduced from ref 181).



Brown and Antholine have proposed a structure of cobalt -carnosine complex at an equimolar metal to ligand concentration (181) (Fig 4.8). The e.s.r. spectra clearly show the characteristics of a low spin complex with oxygen bonded in the axial position and probably water or a solvent molecule coordinated at sixth coordinating site. This work shows that superoxo cobalt complex is also formed with structural analogs, gly-L-his and homo L-carnosine. In the absence of oxygen, no e.s.r. signal was observed with any of these ligands, however, upon exposing the solution to air, the colourless solution changed to brownish yellow which gave an e.s.r. spectrum of superoxo cobalt complex.

Co(III)EHPG, Mn(III)EHPG and Mn porphyrins

Serum transferrin, a glycoprotein of 80,000 MW is present in the blood of all mammalian systems. It has several functions of clinical importance. An important role of this enzyme is the transport of iron from sites of absorption to the site of utilisation. It also functions as a "buffer" of metal concentration in blood and acts as an anti-bacterial agent (186, 187). Thus this protein is required to have structural features which are efficient in binding a metal at the site of absorption and releasing it at the site of utilisation. Several models have been proposed (163, 188) and one of the successful models is the metal complex of ethylene bis(o-hydroxy phenyl)glycine (Insert 4.1). The ligand itself contains the same type of donor groups implicated in the protein (186).



(4.1)

In the following section some of the results on Co(III)EHPG and Mn(III)EHPG are presented. This work was carried out with the following objective. (i) To study the nature of two complexes and (ii) to test that radiolysis (electron addition) at 77 K is useful to reduce Mn(III) complexes to paramagnetic Mn(II) form and to extend this work to study chloroplasts. Mn(III)TSPP is another complex studied for this purpose.

EHPG contains a mixture of meso and racemic isomers and no attempt was made to separate these isomers, however they were recrystallised. Table 4.1 shows the e.s.r. parameters for the cobalt EHPG complex. It is evident that this complex forms a high spin complex.  $g_y'$  and  $g_z'$  are too broad to be seen, hence no structural parameters could be deduced. In contrast to this, Mn(III)EHPG gave a high spin ( $S=5/2$ ) Mn(II) complex with near cubic symmetry. In addition to the main six hyperfine components intermediate lines due to formally forbidden transitions are also apparent. Broadening of the hyperfine lines from low to high field indicates a small D component. In the case of Mn(II)TSPP two types of species were observed (fig 4.9). In addition to intense signals from the solvent radicals, a broad resonance appeared in the region of  $g = 6.0$

Figure 4.2. First-derivative X-band e.s.r. spectrum of Mn(II)PSP : (a) species A  
(b) species B.



which was just resolved into six hyperfine components from coupling to  $^{55}\text{Mn}$  nuclei ( $I = 5/2$ ) (species A). After annealing to remove solvent radicals, two sets of lines from  $^{55}\text{Mn}$  in the  $g = 2$  region were detected. One set, characteristic of  $\text{Mn(II)}$  with only a small zero-field splitting, grew in intensity on annealing (species B). At the same time, the other set, assigned to species A decayed slightly and became less well resolved.

#### Species A

Because of the great width of the e.s.r. features, the data given in the table 4.2 have large error limits (189, 190). These results are typical of high spin ( $S=5/2$ )  $d^5$  systems with large tetragonal zero-field splitting parameters ( $D$ ). The results require that  $D$  be greater than the microwave energy ( $\text{ca. } 0.3\text{cm}^{-1}$ ) (191). Because of the absorption of the species B, it was difficult to obtain details of the expected "parallel" features in the  $g = 2$  region, but extra features giving " $g_{\parallel} \sim 2$  and  $A_{\parallel} \sim 78\text{ G}$ " could be picked out. The  $g = 2$  features are far weaker than the  $g = 6.0$  features for such complexes and the hyperfine splitting is usually isotropic. The quoted values of  $g_{\parallel}$  and  $g_{\perp}$  are nothing to do with the true  $g$ -tensor components, but simply serve to identify transitions within the  $S = 5/2$  manifold that are intense at X-band frequencies (160). In fact, the values of  $g$  must be nearly isotropic at  $g = 2.00$ .

#### Species B

The e.s.r. spectrum of this species is typical of high spin ( $S=5/2$ )  $\text{Mn(II)}$  complexes. Although this species is clearly a

Table 4.2 E.s.r. parameters for some Mn complexes

Complex      Apparent g values       $^{55}\text{Mn}$  Hyperfine coupling constants/G<sup>a</sup>

	$g_{\parallel}$	$g_{\perp}$	$A_{\parallel}$	$A_{\perp}$
Mn(II)EHPG	2.00	-	ca. 79	-
Mn(II)TSPP <sup>b</sup>	ca. 2.00	$5.9 \pm 0.1$	ca. 78	$78 \pm 1$
Mn(II)TPP/py <sup>c</sup>	2.00	5.96	74	74

(a) = 0.1 mTelsa

(b)  $D > 0.3 \text{ cm}^{-1}$

(c)  $D \approx 1.2 \text{ cm}^{-1}$

product of irradiation, it seems unlikely that it is formed directly from MnTSPP, since this would require the ejection of manganese from the porphyrin ring and resolvation. This is extremely unlikely under these conditions (192) and species B is probably formed from some Mn(III) impurity. These results clearly establish that Mn(III) complexes which do not involve manganese clusters can be readily reduced by ionizing radiation, and the resulting Mn(II) can be detected.

Preliminary experiments with chloroplasts were not successful. This may be because manganese pairs are present, as suggested by recent work of Dismukes and Siderer (193).

CHAPTER 5BIO-ORGANIC RADICALSINTRODUCTION

The radical chemistry of thiols, sulphides and disulphides is of considerable complexity and importance. The radical intermediates have been extensively studied by optical (194-196) and e.s.r. (197-199) methods. It is now clear that well defined e.s.r. features originally assigned to  $RS\cdot$  radicals are not due to such radicals (200). It has been suggested that the species concerned is an adduct of  $RS\cdot$  and  $R_2S$  or  $RSH$  molecules ( $RS\cdot SR_2$ ) but Hadley and Gordy prefer to identify this species as  $RSS\cdot$  radical (201). Because of this ambiguity, this species is referred to as X (198). It seems possible that these  $RS\cdot SR_2^-$  and  $RSS\cdot$  species have similar e.s.r. spectra, since there are cogent reasons for accepting one or other structure under different conditions (198, 202). It has been shown that  $RS\cdot$  radicals, which are expected to have variable g tensor components depending on their environment, can be characterised by their spectra in dilute solutions at 77K (198). Disulphide radicals are of two types,  $(RSSR)^+$  cations with  $\pi^*$ -structure, and  $RSSR^-$  with a  $\sigma^*$ -structure (198, 199, 201, 203, 204). These can be readily formed from  $RSSR$  molecules by the use of ionizing radiation, and they both have well defined, characteristic e.s.r. tensors. Yet another important class of  $\sigma^*$ -radicals are the  $RSSR_2^+$  cations, formed by the addition of  $R_2S^+$  cations [also characterised by e.s.r.



spectroscopy (205)] to an  $R_2S$  molecule(198,199,206).When simple RSSR molecules in dilute solution such as  $CD_3OD$  are exposed to gamma-rays at 77 K,electrons ejected from the solvent molecules add efficiently to give  $RSSR^-$  sigma\*-anions.These are characterised by their g-tensor components (g<sub>1</sub> ca.2.020,g<sub>2</sub> ca 2.002) and often also by their proton hyperfine coupling constants(fig 5.1).When the features are broad,they are sufficiently distinctive to be taken as being characteristic of  $RSSR^-$  radicals.Disulphides play a major structural role in certain enzymes and proteins,and one aim of this study was to examine the possibility that electrons might selectively add to these units during radiolysis of dilute solutions at 77 K.Since electrons react with amide units and other protein components under these conditions,it was by no means certain that selectivity would be observed.The other aim was related to this.Previous studies of certain metalloproteins under these conditions have shown that electron capture at metal centres can be efficient(207-209).It was interesting to discover whether this selectivity is particular to metal centres.Previous studies of sulphur radicals in proteins includes the pioneering work of Singh and Ormerod(210) and Stratton(211).

#### EXPERIMENTAL

The proteins,enzymes,and peptides used in this study were purchased from Sigma chemicals and used as supplied.Dilute

solutions of solute were prepared either in water/ethylene glycol mixtures or  $\text{CD}_3\text{OD}/\text{D}_2\text{O}$  (ca, 1; 4v/v). Samples were prepared and e.s.r. spectra were recorded as described in chapter 2.

#### RESULTS AND DISCUSSION

These results are remarkably simple for a wide range of proteins and related compounds containing S-S linkages listed in table 5.1. Good spectra were obtained for  $\text{RSSR}^-$   $\sigma^*$ -anions. In all cases, dilute aqueous glasses were used at 77 K, and hence the only major reaction expected for the proteins was electron addition. The efficient formation of these anions was independent of the site of the S-S linkages and of the number of such linkages in each molecule. The yields (for solutions ca. 10 mM) were linear with a dose of ca. 1 Mrad, but tended to level off when the dose was increased. Typical e.s.r. spectra are shown in figs 5.1 and 5.2. The only variations were minor differences in  $g_x$  and  $g_y$ , and in a small additional yield of radicals with  $g$  values close to 2.0023. In each case, it was possible to anneal the glasses to temperatures at which the solvent radicals fell to zero with no apparent loss in signals from protein molecules.

Proteins devoid of S-S linkages appeared to add electrons with roughly the same efficiency, but it is not possible to detect any clear structure in the broad features at ca. 2.0023 so one cannot identify these radicals from these spectra. The presence of RSH units made no difference and in particular,

Figure 5.1. First-derivative X-band e.s.r. spectrum of cystine radical anions together with feature alpha assigned to carbon centered radicals.

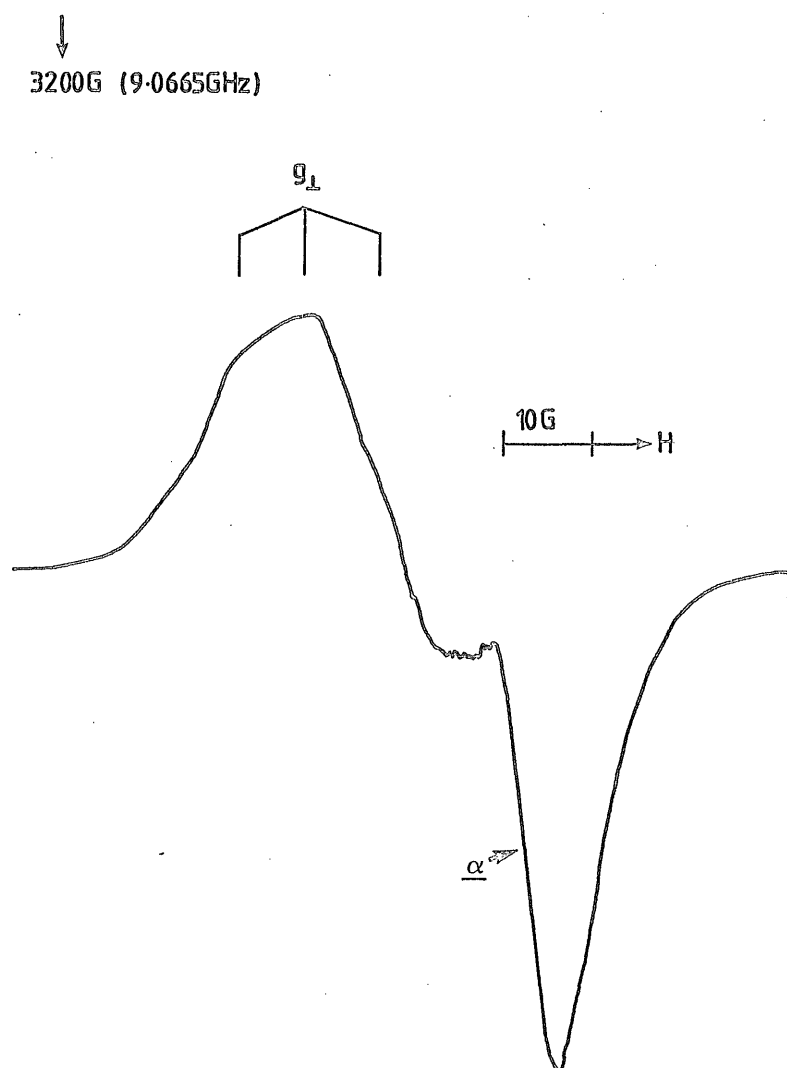
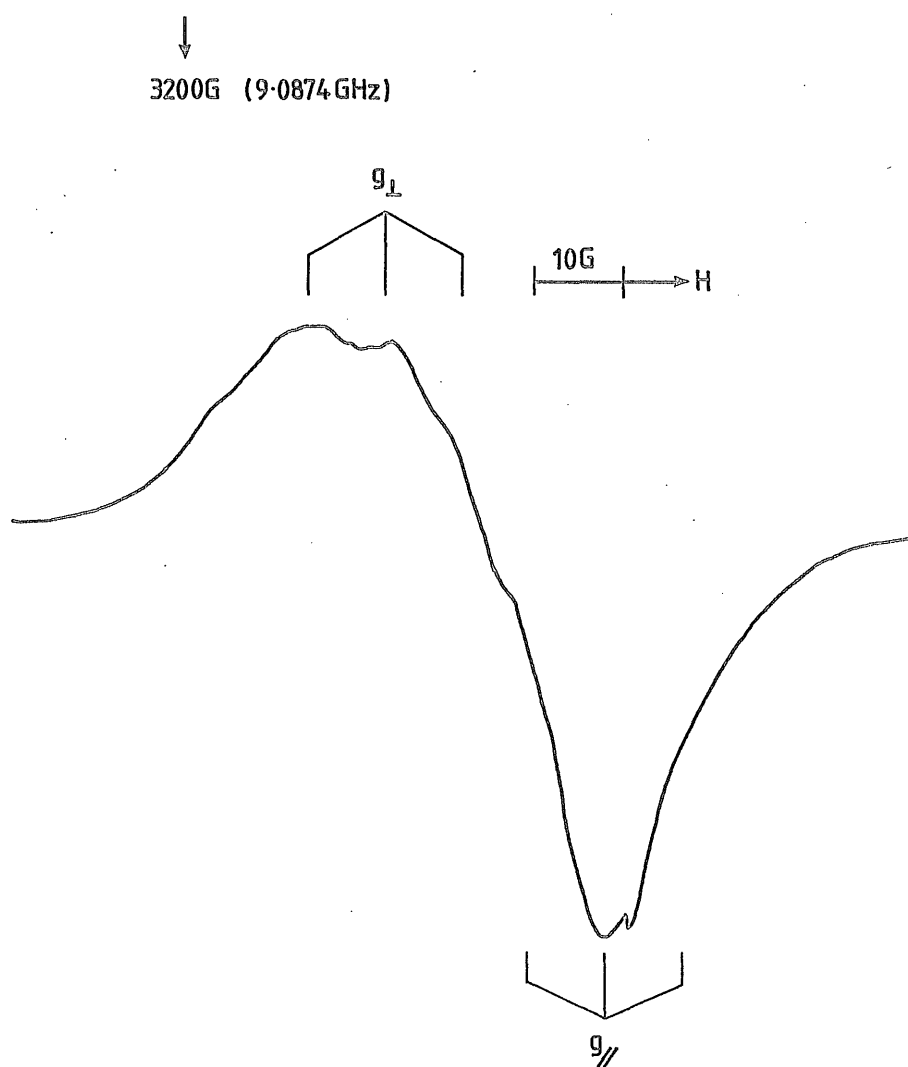


Figure 5.2. First-derivative X-band e.s.r. spectrum of lysozyme.  
Features are assigned to RS•SR radical anions.



there was no evidence for the formation of  $RS^\bullet$  radicals. It is remarkable that cystine and homocystine actually gave higher yields of carbon-centered radicals than the proteins listed in table 5.1, as can be judged by comparing figs 5.1 and 5.2. This probably reflects the fact that ammonia is a good leaving group, and hence deamination competes with electron capture at the S-S bond. Such terminal groups are of course, rare in high MW protein residues. One significant observation was that if oxygen was not scrupulously removed, signals characteristic of  $RO_2^\bullet$  radicals grew in at very low doses prior to the growth of any other radicals. Further investigation on the source of these radicals is necessary, but they are not necessarily formed from protein radicals by the addition of oxygen. In the absence of oxygen, the rate of growth of radicals for equal concentrations of proteins was about the same in the absence or presence of disulphide linkages. This result is of considerable significance. The simplest explanation seems to be that once an electron has "entered" a protein molecule it can move around and selectively seek out the S-S bonds, at which it is preferentially trapped. In the absence of S-S bonds or other electron scavengers, it reacts with aromatic rings, or probably amide linkages to give anions, or dissociative electron capture (eq 5.1 and 5.2) (212). It may also seek out terminal  $NH_3^+$  units. All such radicals contribute to the free-spin

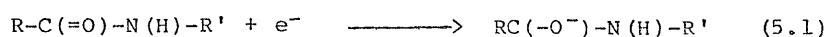
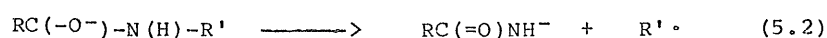


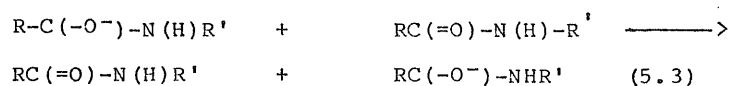
Table 5.1 E.s.r.data for electron addition products formed by radiolysis of dilute solutions of proteins and related compounds in  $\text{CD}_3\text{OD}/\text{D}_2\text{O}$  (1:4v/v) glasses after annealing to ca.180 K to remove signals from solvent radicals.

Protein	Source	Proton hyperfine coupling(G) <sup>a</sup>	g-tensor components		
			g <sub>x</sub>	g <sub>y</sub> <sup>c</sup>	g <sub>z</sub>
-----					
Alcohol					
dehydrogenase(Yeast)		9.5	2.019	ca.2.019	2.002
Glutathione					
(Oxidised)(Synthetic)		b	2.017	2.017	2.002
alpha-Chymo-					
trypsin(Bovine pancreas)		8.0	2.021	2.014	2.002
alpha-Lact-					
albumin(Bovine milk)		9.5	2.020	ca 2.020	2.002
Conalbumin(Hen's egg)		b	2.020	ca.2.020	2.002
Insulin(Bovine pancreas)		9.0	2.020	ca.2.020	2.002
Venom(Formosan cobra)		7.5	2.020	ca.2.020	2.002
Oxytocin(Synthetic)		8.0	2.020	ca.2.020	2.002
Lysozyme(Hen's egg)		9.0	2.020	2.017	2.002
Glutathione					
reductase(Yeast)		8.0	2.024	2.015	2.002
Lipoamide dehydro-					
genase(Porcine heart)		8.0	2.024	2.015	2.002
Thyroglobulin(Bovine)		b	ca.2.018	ca.2.018	2.002
Albumin(Bovine serum)		11.0	2.018	2.018	2.002
Ribonuclease					
(Bovine pancreas)		9.0	2.019	2.019	2.002
Homocystine(Synthetic)		8.5	2.019	2.019	2.002
Cystine(Synthetic)		8.5	2.019	2.019	2.002
Cystine.HCl <sup>d</sup> (Crystal)		10.3 + 7.2	2.0178	2.0174	2.0024

(a) = 0.1 mTelsa. In all cases for which proton hyperfine coupling was resolved, a broad triplet similar to that observed for cystine anions was observed. (b) = Very broad components : Hyperfine coupling was not resolved. (c) = In most cases,  $g_z$  and  $g_y$  were not sufficiently defined for us to draw a clear distinction. (d) = Ref 199.



signals observed in the absence of disulphide linkages. This aspect of the work is worthy of more extensive study but, in the mean time, it is provisionally concluded that excess electrons are remarkably mobile within proteins prior to being permanently trapped. This suggests that transport occurs via electron transfer of the type, as eq 5.3. Such transfers will be facile provided they occur more rapidly than the time



required for the radical (eq 5.1) to relax to its equilibrium conformation (probably pyramidal at the radical centre) or to undergo dissociative electron capture (eq 5.2). This result may be of importance in the study of electron-transfer reactions of enzymes.

#### Availability of S-S units

In all cases, electron addition to S-S groups occurred efficiently at 77 K. This result contrasts with results from chemical reduction, in which buried S-S groups are very difficult to reduce, and also radiolytically induced electron transfer from radicals such as  $\text{Me}\dot{\text{C}}\text{HOH}$  or  $\text{CO}_2^-$  (213). In the latter studies for example, ribonuclease gave no  $\text{RSSR}^-$  anions whereas BSA gave good yields, as judged by optical spectroscopy (211). This is because the S-S group in ribonuclease

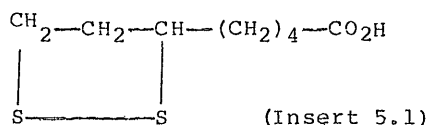
is strongly protected by the surrounding protein molecule.

#### The e.s.r. data

The fact that the sigma\*-orbital is well described as primarily 3p-3p on sulphur has long been established by the  $^{33}\text{S}$  hyperfine coupling (204). The e.s.r. spectra of the radical anion of cystine formed under comparable conditions is characterised by a hyperfine triplet of ca 8.5 G. (table 5.1). It seems that the preferred conformations for these anions are such that only two of the four beta-protons interact strongly with the unpaired electron. The form of the g-tensor components give, in principle, some measure of the degree of twist ( $\theta$ ) of one RS group relative to another. For  $\theta = 90^\circ$ , symmetry requires that  $g_x = g_y$  ( $g_{\perp}$ ) and the structure requires that  $g_{\perp} > g_{\parallel} = 2.0023$ . However when  $\theta$  deviates from  $\theta = 90^\circ$ ,  $g_x \neq g_y$ .

In many spectra, it is difficult to distinguish between  $g_x$  and  $g_y$  so that  $\theta$  must be close to  $90^\circ$ . However, in a few instances (table 5.1) rather large deviations from axial symmetry were observed. Presumably, in these species, the requirements of the protein structure tend to open or close the bond angle. The effect is particularly noticeable for anion-radicals of alpha-chymotrypsin, lysozyme, glutathione reductase and lipoamide dehydrogenase. This hypothesis is nicely verified by results of lipoic acid (insert 5.1). Here the ring structure restricts  $\theta$  to  $60^\circ$ , and the e.s.r. spectrum





for the anion shows a marked deviation from axial symmetry, with  $g_x = 2.020$  and  $g_y = 2.012$ . It is interesting that in this case, only one proton coupling of ca. 10 G was detected (198).

#### Species X

This species (either  $\text{RS}^-\text{SR}_2$  or  $\text{RSS}^\bullet$  as described above) is very well characterised by its e.s.r. spectrum (198). In all studies, a search was made for this species at 77 K and during annealing studies. For the disulphides, the only positive result was for reduced superoxide dismutase (214). If this formulation of this species is correct (198), these results imply a protonation, as in eq 5.4. Clearly this will occur most



readily for S-S units in hydrophilic regions of the protein. This result suggests that the S-S group in superoxide dismutase is unusual in being relatively readily accessible to solvent molecules or other proton donors.

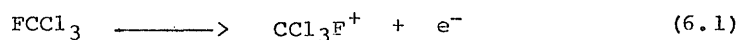
CHAPTER 6RADICAL CATIONSINTRODUCTION

One of the conspicuous missing links in the e.s.r study of simple molecules is spectral data for cation radicals of molecules containing functional groups such as ethers, aldehydes, ketones, esters, amides, nitroalkanes, peroxides, persulphides, and many substituted aromatic and heterocyclic derivatives.

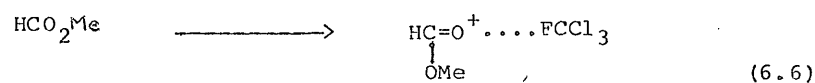
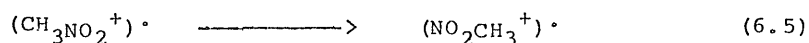
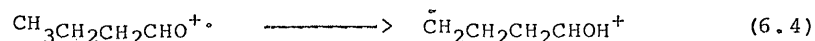
Very early methods of producing radical cations, such as radiolysis of sulphuric acid solutions, had limited applicability because of the insolubility of many compounds or the presence of the acid-labile groups. Both these problems have been overcome by the use of halogenated solvents such as  $\text{CCl}_4$ ,  $\text{FCCl}_3$ ,  $\text{SF}_6$ ,  $\text{CF}_2\text{Cl}_2$ ,  $\text{CHCl}_2\text{CHCl}_2$  etc. These solvents have an additional advantage in that some of them have high i.p. This method was originally used by Shida & Hamil (215) for optical studies. Only recently has this method been used in e.s.r. studies (216-218). Thus it seemed worthwhile to exploit this method to generate radical cations by the action of ionizing radiation on dilute solutions of corresponding neutral molecules. The mechanism of formation of radical cations in a freon matrix occurs by positive charge migration.

When a dilute solution of  $\text{FCCl}_3$  (i.p. 11.9 eV) containing a

solute (whose i.p. is less than that of  $\text{FCCl}_3$ ) is exposed to gamma-radiation, the matrix molecules are ionized resulting in a mobile "hole" (eq. 6.1-6.3). Positive charge migration results in the ionization of solute molecules (this mechanism



is very similar to p typing in semiconductors). Under these conditions, i.e. in a matrix which is sufficiently dilute, intermolecular interactions are avoided and the possible chemical processes likely to interfere with radical cation formation are a hydrogen atom transfer from alkyl chains (219) or rearrangement (220) or formation of a  $\text{FCCl}_3$ -adduct (221) (eq. 6.4-6.6). These processes occur in exceptional cases and



it will be evident from the results presented below that in the

majority of cases only primary radical cations are formed. The concomitantly produced paramagnetic by-products such as trapped holes  $(\text{CCl}_3\text{F}^+)_t$  and electron adducts  $(\text{CCl}_3^+ \dots e^-)$  or their decomposition products  $\text{CCl}_2\text{F}$  and  $\text{Cl}^-$  give practically no e.s.r. signals owing to extreme dipolar broadening of hyperfine interaction. Thus this method offers a convenient procedure to study radical cations.

This chapter is broadly classified into the following sections;

1. Radical cations of aromatic derivatives
2. Radical cations of heterocyclic derivatives
3. Radical cations of aliphatic derivatives
4. Inorganic radical cations

#### EXPERIMENTAL

All materials were of high grade and were used as supplied. A range of solutions containing solute and solvent in the ratio of 1;1000 (w/v) were de-gassed by repeated freeze-thaw cycles and were frozen at 77 K. Samples of  $\text{N}_2\text{O}_4$  were prepared by passing  $\text{NO}_2$  into  $\text{FCCl}_3$  and the solution was frozen at 77 K. All samples were exposed to gamma-radiation to a dose of 1 Mrad. E.s.r. spectra were recorded as described in chapter 2.

#### RESULTS AND DISCUSSION

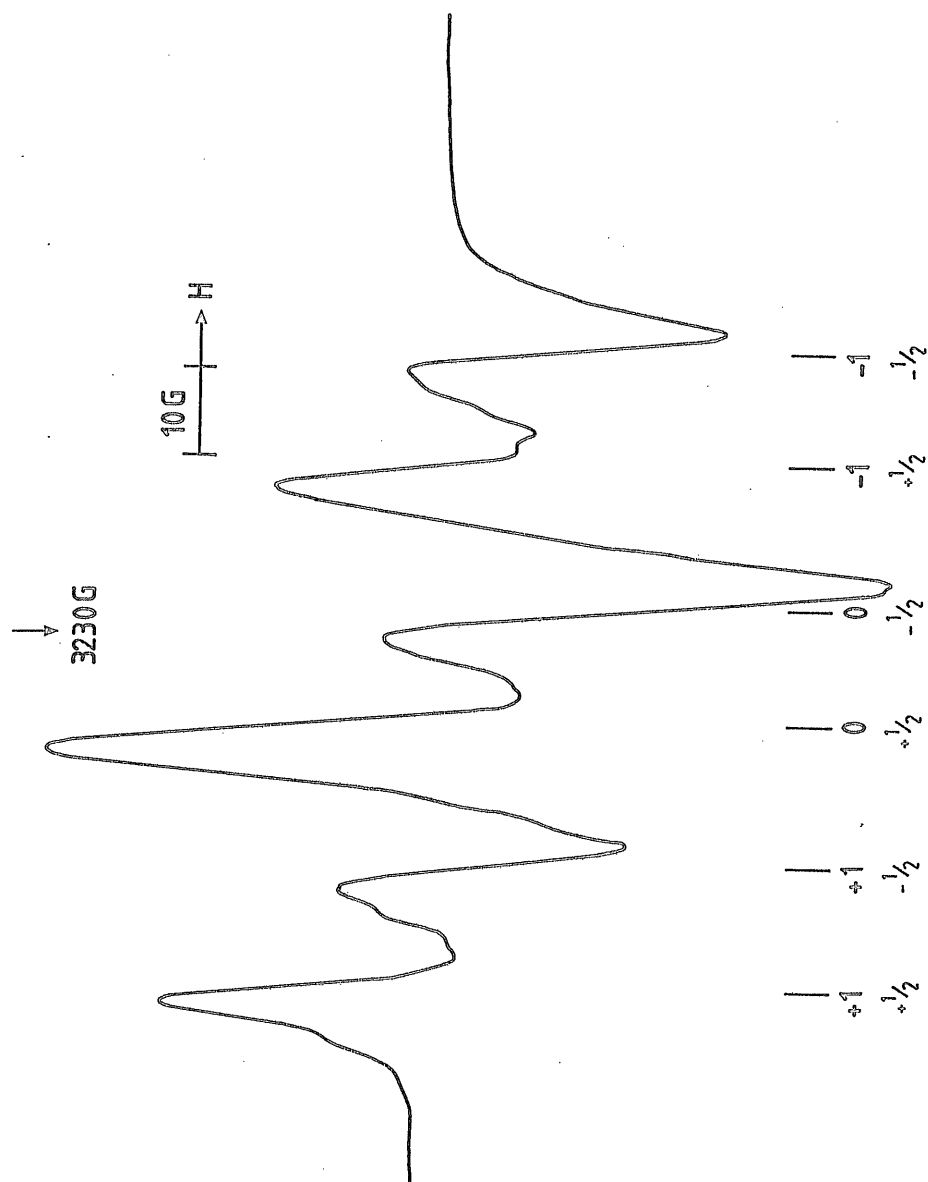
##### (1). Radical cations of aromatic derivatives

The e.s.r. spectra for toluene cations in freon have been published previously (222). Those for ethylbenzene and

p-cymene cations are shown in fig 6.1. That for isopropyl benzene was similar to that for the ethyl derivative. The latter has been analysed in terms of the strongly coupled protons (29 G) and one weakly coupled proton (12 G), as indicated in the stick diagram. Analysis of the isopropyl derivative spectra required the presence of two conformers (Table 6.1) one with small coupling to beta-proton (6 G) and one with a larger coupling (21 G). The latter being favoured for p-cymene, a strong coupling to the p-methyl protons (18 G) together with coupling to one other proton is required to give a satisfactory fit, but three different conformers were formed at 77 K (fig 6.1b and c). One, with zero coupling to the beta-proton was unstable, and was lost irreversibly on annealing. Another, with a large coupling (18 G) grew in intensity simultaneously. All three cations gave averaged spectra reversibly on annealing, the average beta-proton coupling being close to that for the methyl protons of the toluene cation (18.5 G). However, the onset of averaging occurred at ca. 150 K for the ethyl derivative and ca. 130 K for the isopropyl derivatives. The spectra for the t-butyl derivative are more difficult to understand (Fig 6.1d and e). At 77K a broad triplet was obtained ( $A = 13$  G). On warming, this changed to a quartet (Fig 6.1d) and then to the expected 12 G doublet. These changes were reversible. The doublet is clearly due to p-hydrogen; the source of the other splitting is not clear.

Spectra for the silyl derivatives,  $(\text{PhSiH}_3)^+$  and  $(\text{PhSiMe}_3)^+$

Figure 61 a. First-derivative X-band e.s.r. spectrum of ethylbenzene radical-cation.



↓  
3250 G

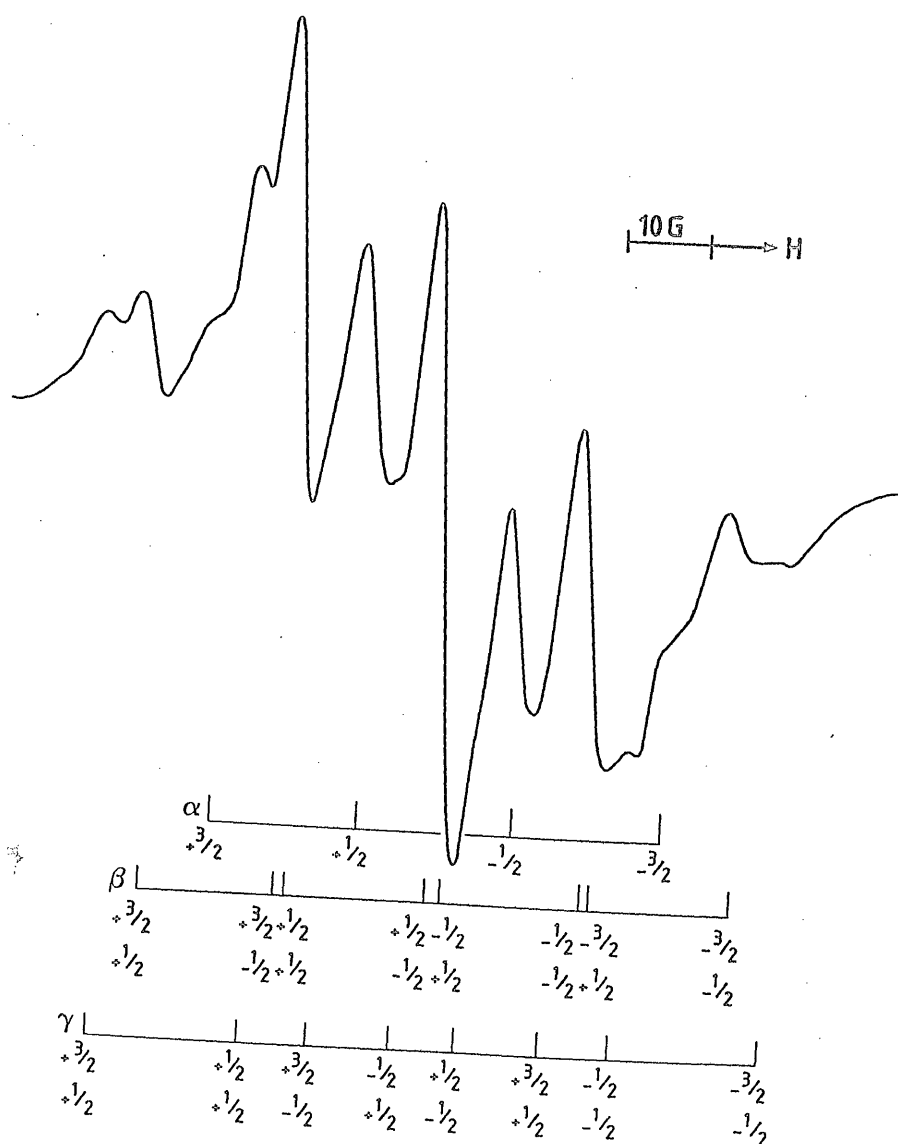
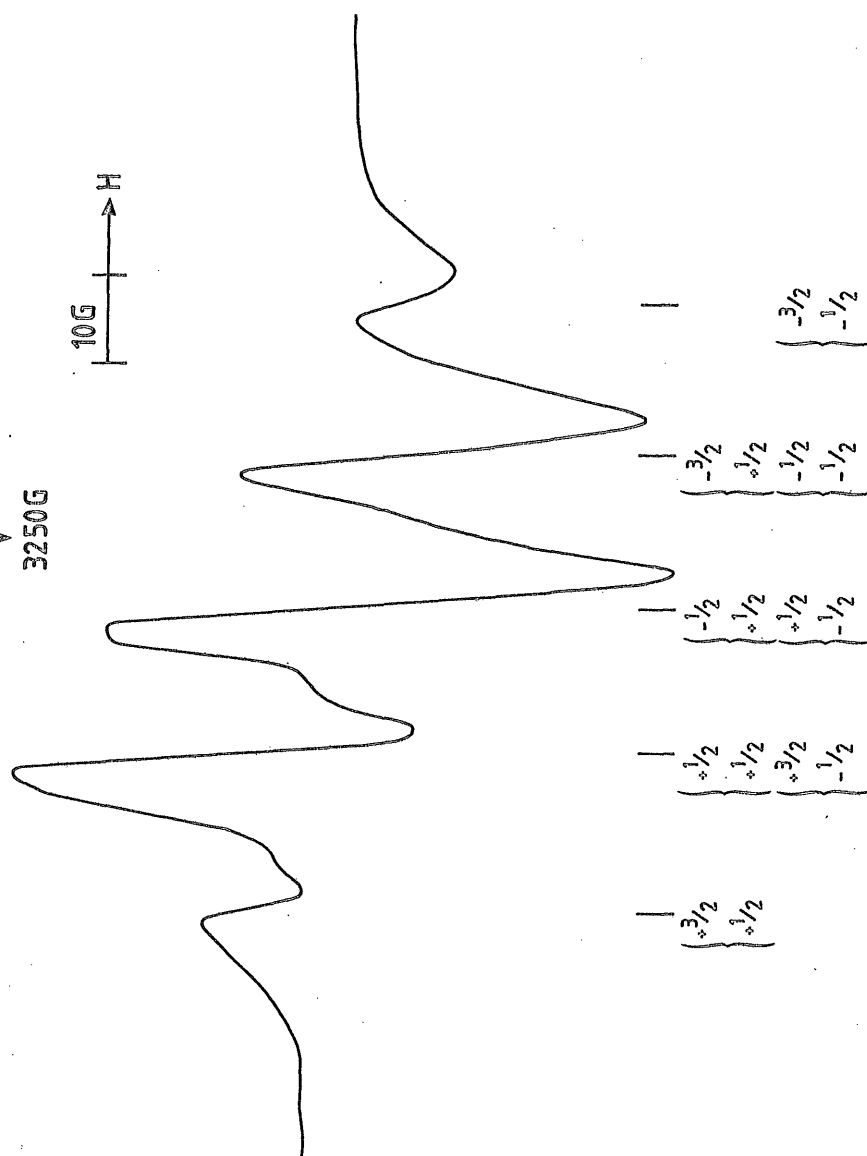


Figure 61. c. First-derivative X-band e.s.r. spectrum obtained from p-cymene in freon at ca 130 K.



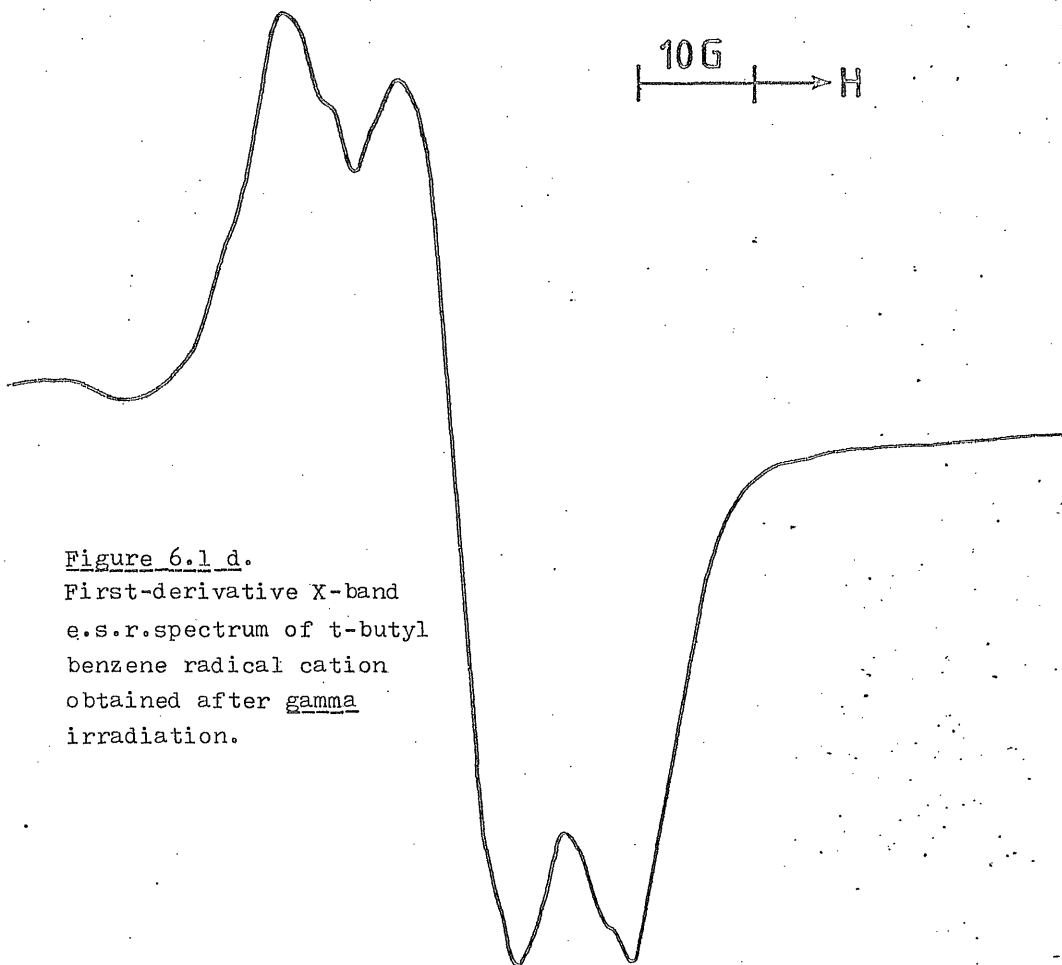


↓  
3230G

10G → H

Figure 6.1 d.  
First-derivative X-band  
e.s.r.spectrum of t-butyl  
benzene radical cation  
obtained after gamma  
irradiation.

+1 0 -1



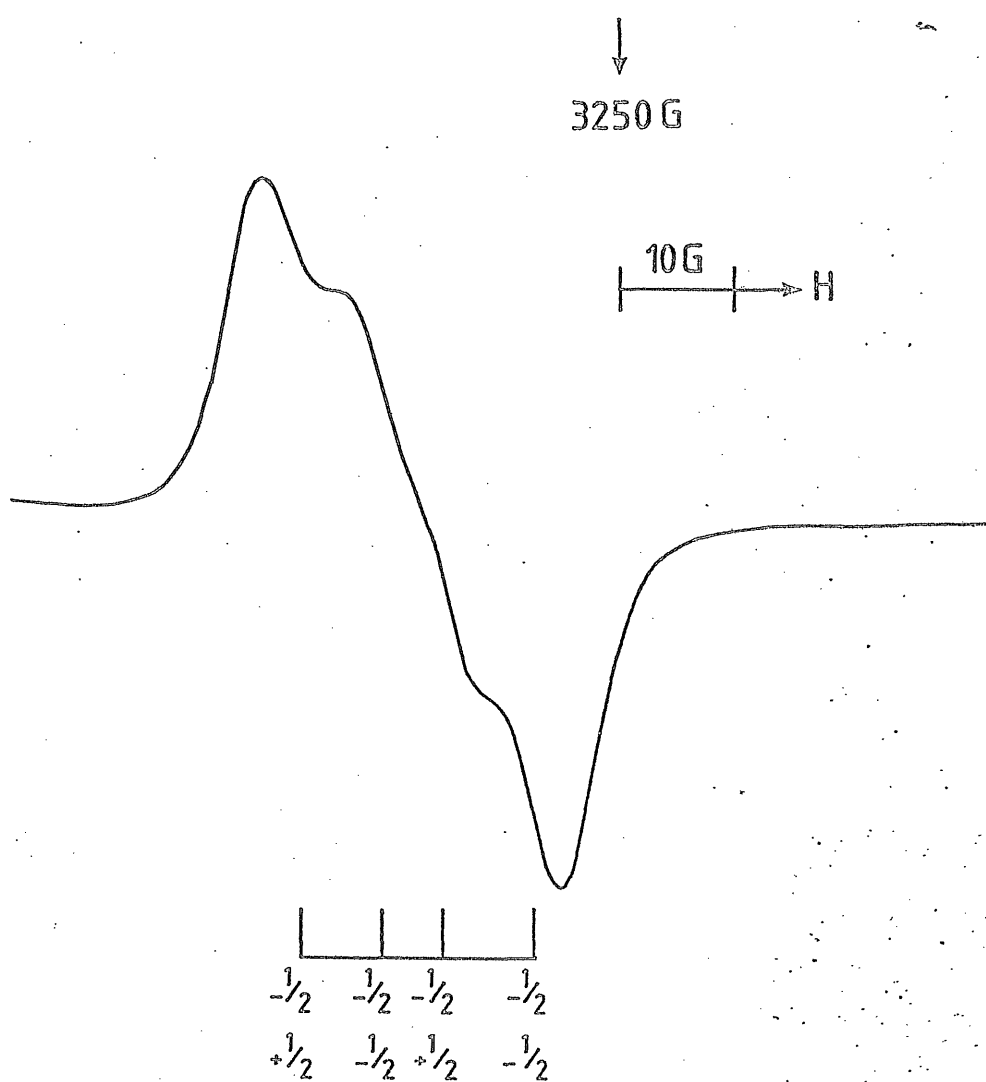


Figure 6.1 e. First-derivative X-band e.s.r. spectrum of t-butyl benzene radical cation obtained after annealing.

$^1\text{H}$ -Hyperfine coupling constants/ $\text{G}^{\text{a}}, \text{b}$

para-hydrogen      substituent-H

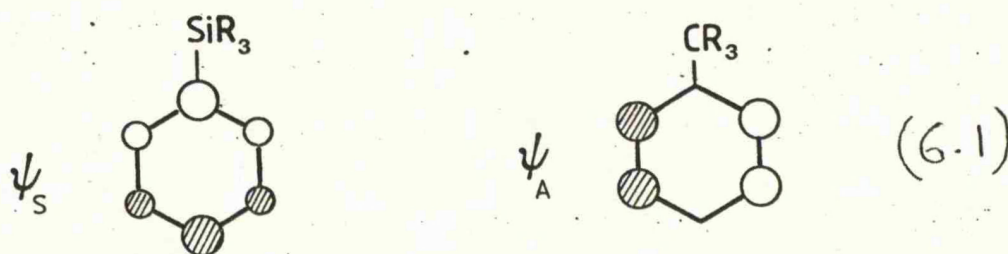
$\text{C}_6\text{H}_5\text{-CH}_3^+$	12	18.5 ( $3^1\text{H}$ )
$\text{C}_6\text{H}_5\text{-CH}_2\text{CH}_3^+$	12	29.0 ( $2^1\text{H}$ )
$\text{C}_6\text{H}_5\text{-CH}(\text{CH}_3)_2^+$	12	(i) 6, (ii) 21; ( $1^1\text{H}$ )
$\text{CH}_3\text{C}_6\text{H}_4\text{CH}(\text{CH}_3)_2^+$	18 ( $\text{CH}_3$ )	(i) 0, (ii) 18, (iii) 28; ( $1^1\text{H}$ )
$\text{C}_6\text{H}_5\text{C}(\text{CH}_3)_3^+$	12	$\underline{\text{C}}$
$\text{C}_6\text{H}_5\text{SiH}_3^+$	11	9 ( $3^1\text{H}$ )
$\text{C}_6\text{H}_5\text{SiH}(\text{CH}_3)_2^+$	11	18 ( $1^1\text{H}$ )
$\text{C}_6\text{H}_5\text{Si}(\text{CH}_3)_3^+$	11	--

$\underline{\text{a}}$  = 0.1 mTelsa

$\underline{\text{b}}$  = All  $\underline{\text{g}}$  values were close to 2.0025. The form of the spectra suggest slight  $\underline{\text{g}}$  anisotropy but this was too small to estimate with confidence.

$\underline{\text{c}}$ , Structure of unknown origin was observed at 77 K but was lost on annealing.

are shown in fig 6.2. The former comprises a quintet (ca. 10 G) due to four nearly coupled protons, each feature resolving into a triplet (3 G) on annealing (2a). That for the  $-\text{SiMe}_3$  derivative is a simple doublet ( $A = 11$  G), whilst for the  $-\text{SiHMe}$  derivative two dissimilar doublet splittings are required (11 & 18 G) to explain the spectrum. These results are best interpreted in terms of symmetric SOMO,  $\psi_s$  (insert 6.1). Thus the unique proton splitting of ca. 12 G region for the

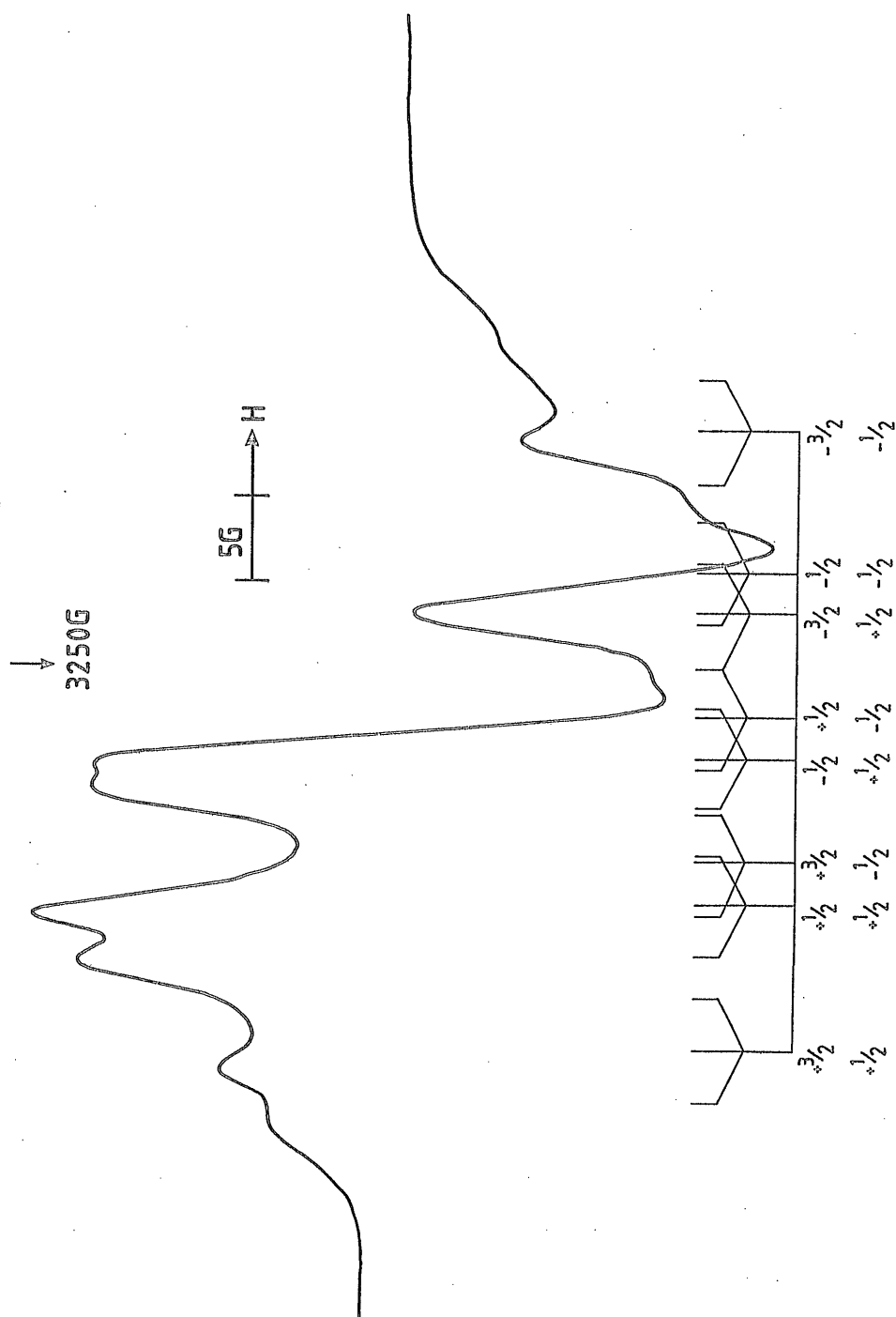


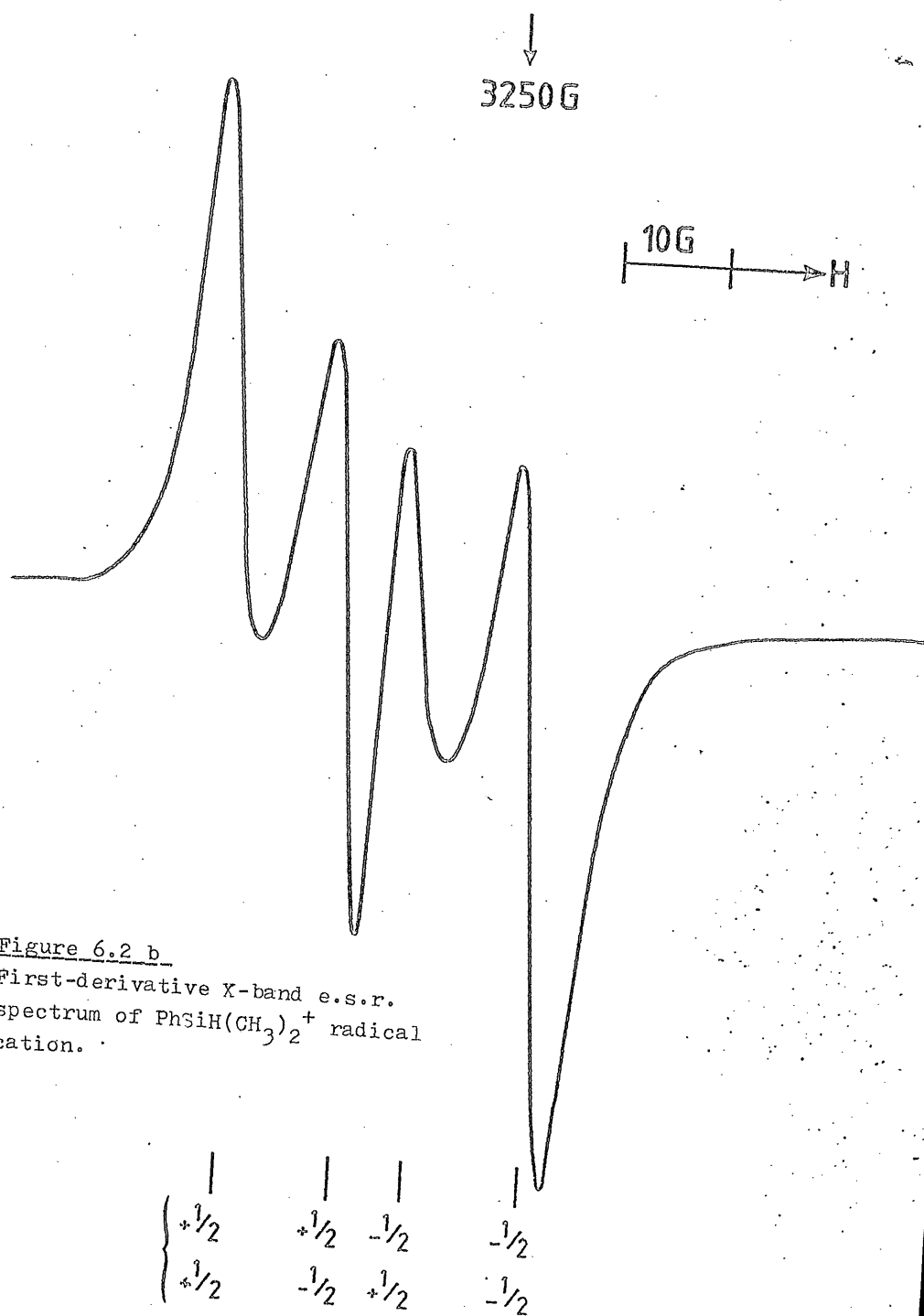
alkyl derivatives is assigned to the para-ring proton. These coupling constants are appreciably larger than that reported for the  $D_{2h}$  form of the benzene cation (8.2 G) despite delocalisation onto the substituents. One possible reason for this is given below. Coupling to the remaining ring proton is in the region of 2-3 G, but this was only clearly resolved for the silyl derivative, for two of the four protons, which are expected to be equivalent in pairs.

Results for the ethyl benzene is noteworthy in that coupling to the equivalent protons (29 G) is very much greater than that (18.5 G) observed for the toluene cation (222). This result requires that the conformation shown in insert 6.2 is adapted. This is surprising, since it is



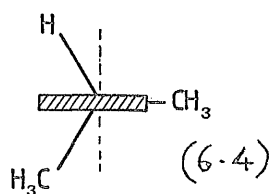
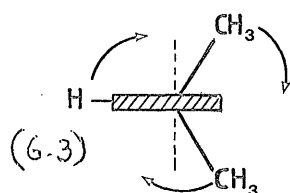
Figure 2 a. First-derivative X-band e.s.r. spectrum of phenylsilane radical-cation.





sterically the least favoured conformer. This suggests that by hyperconjugation, electron release for the sigma-bond is markedly more favourable for this cation than is that for the C-CH<sub>3</sub> bond, and that this outweighs the steric barrier caused by the in-plane methyl group, however for anions that some structure of lower symmetry is not adapted. The spectra change quite sharply for a rotating ethyl group in the 150-160 K region ( $A = 18.5$  G).

For the isopropyl derivatives (cumene and p-cymene) there seems to be an almost complete balance between the steric and hyperconjugation forces. Thus rotation is less hindered than for the ethyl derivative, and different conformations have comparable stabilities. At 77 K, one of the two major first formed species for p-cymene showed only an 18 G quartet due to hyperfine coupling to the methyl protons. However, this form was lost irreversibly on annealing. The other two species had beta-proton splittings of ca. 18 G and 28 G respectively, and were both re-formed from the averaging species on recooling to 77 K. This suggests that the species with  $A(^1\text{H}) \approx 0$  has conformation 6.3, this being the sterically favoured form

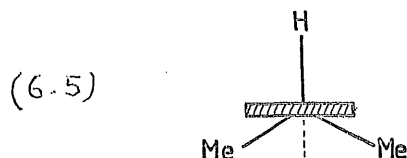


of the parent molecules. The species with  $A(^1\text{H}) = 28$  G must then have structure 6.4, with the conformer having  $A(^1\text{H}) \approx 18$  G being between these two structures. Clearly these structures

have comparable stabilities, which explains why "free" rotation sets in reversibly on annealing.

For the silyl derivative, the proton coupling for the  $-\text{SiH}_3$  group (9 G) is approximately half that obtained for the toluene cation (18.5 G). It is noteworthy that this reduction by a factor of two is exactly that observed on going from oxygen to sulphur for the typical ether and sulphide cations (223, 224). In the present case, the major factor contributing to this fall is due to relatively poor orbital overlap for the Si-H orbital relative to the C-H orbital. However, for the ether and sulphide cations it is mainly the difference in the effective electron affinity of the ether 2p and sulphur 3p orbitals that causes the reduction, so the similarity in these changes observed may be coincidental.

For the  $(\text{PhSiHMe}_2)^+$  cation, the coupling of 18 G is assigned to the Si-H proton. The large coupling can be understood in terms of the conformer (insert 6.5) giving maximum sigma-pi overlap, and hence double the average of 9 G observed for



the Si-H derivative. Therefore, as with carbon, electron release from the Si-H bond is more favourable than that from the Si-Me bonds. Nevertheless, it is clearly less than that for C-H bonds. For this cation hyperconjugation wins over steric factors, which are greatly reduced because of the size of



the silicon atom. No change in the conformation was observed on warming this species in marked contrast with the  $(\text{PhCHMe}_2)^+$  cation.

The reason why the p-proton coupling is so much greater than that found for benzene cations at 4 K must be discussed. This is not thought to be caused by slight admixture of  $\Psi_A$  into  $\Psi_S$  structure of ethane cation, and clearly such admixtures for the substituted cations would require that the pure  $\Psi_S$  structure should exhibit even larger p-proton coupling constant. The positive-charge spin-density separation concept previously outlined can be considered (222). This depends upon the fact the electron donation for C-H (or Si-H) sigma-bonds is encouraged by the positive charge. Thus there is a distortion of the wave function so as to place high positive charge density on the carbon atom adjacent to the substituent and concomitantly high spin-density on the remote p-carbon as in insert 6.6. Only a minor bias against such an extreme is required to explain the increase in  $A(^1\text{H})$  for the p-hydrogen.

(6.6)



This also shows why the coupling is greater for the alkyl than for the silyl derivatives.

## (2). Radical cations of heterocyclic derivatives.

### Radical cations of pyrrole, furan and thiophene

The data are given in table 6.2 and some typical spectra are shown in fig 6.3 and 6.4.

Figure 6.3. First-derivative X-band e.s.r. spectrum of furan radical cation.

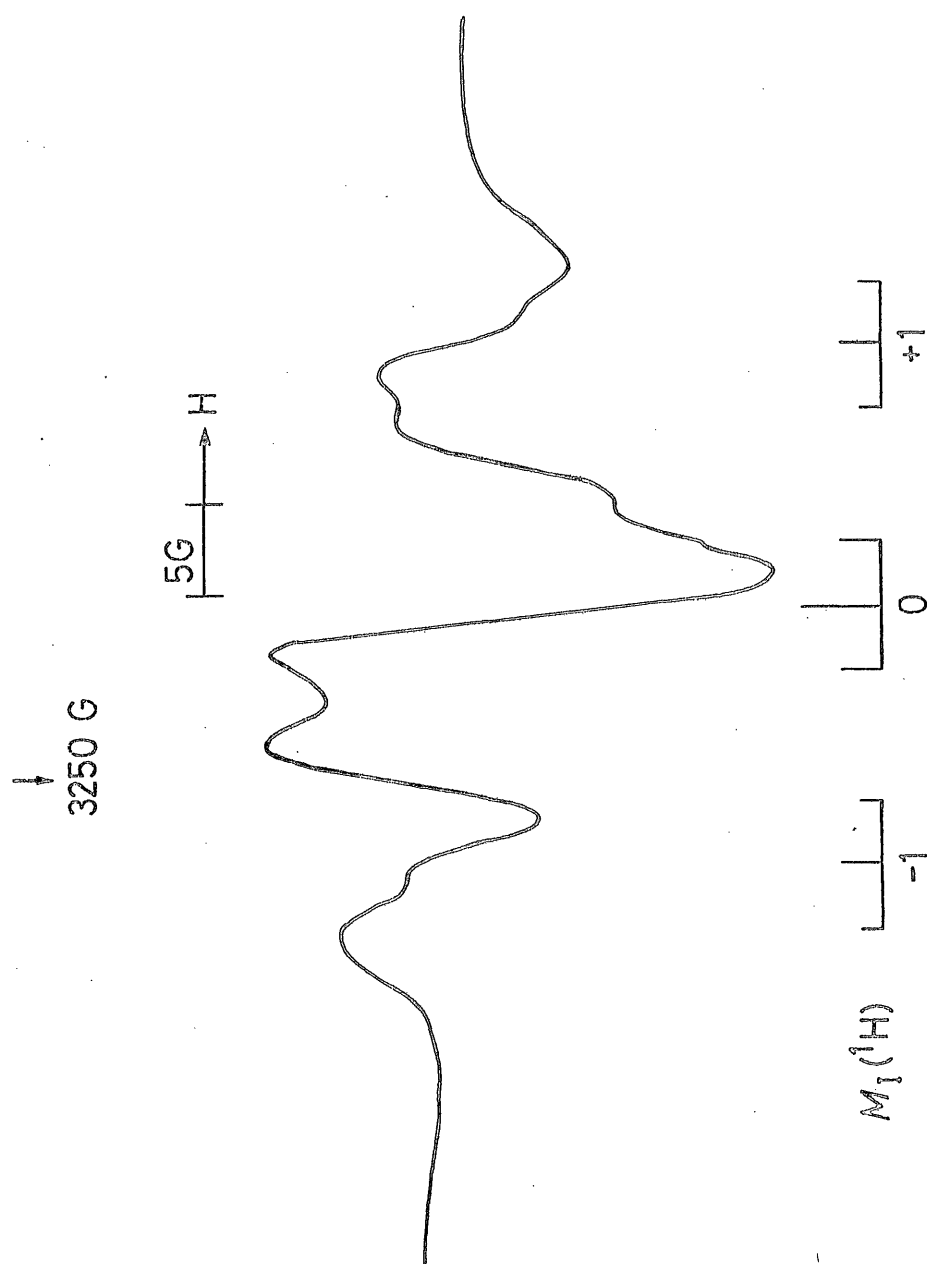


Figure 6.4. First-derivative X-band e.s.r.spectrum of 2,5-dimethylthiophene radical cation.

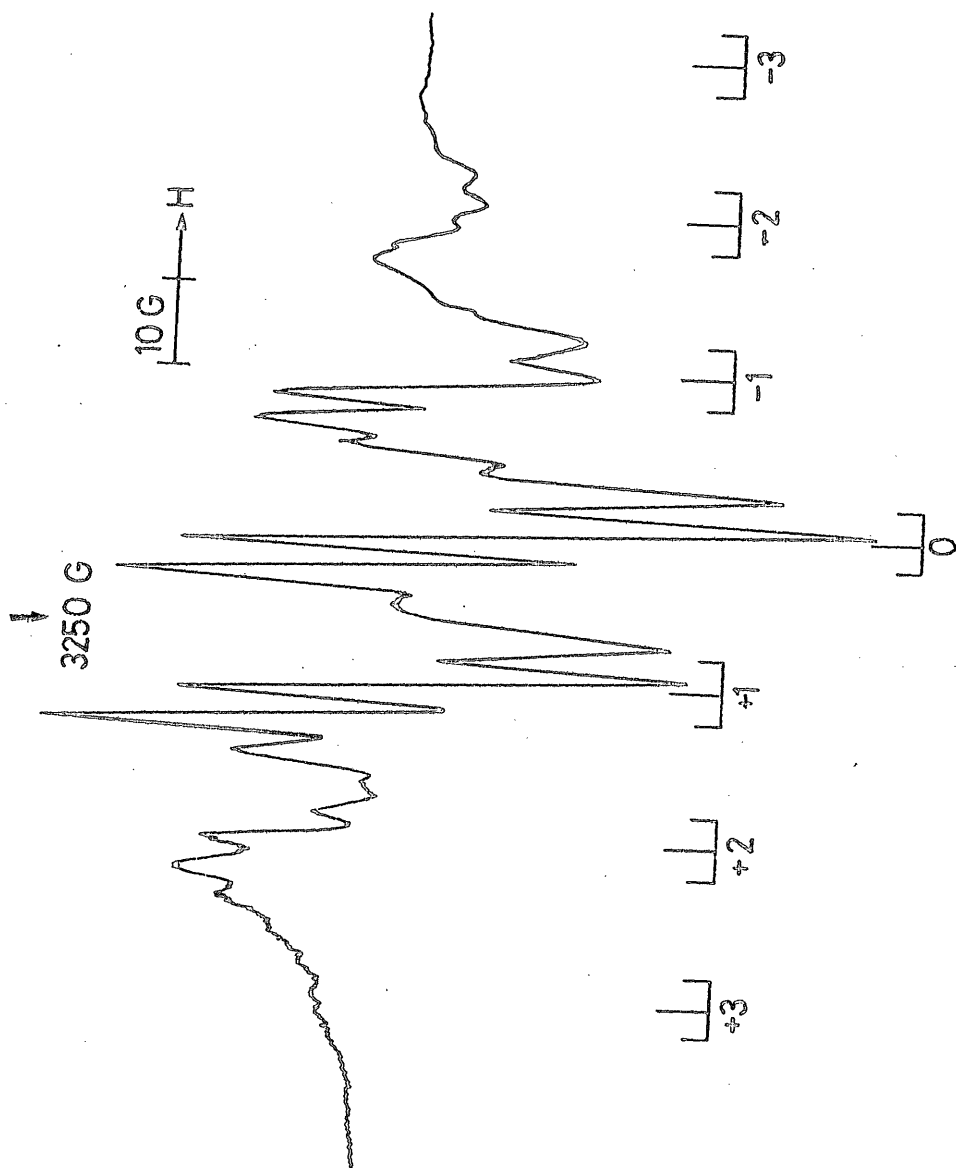


Table 6.2 E.s.r. parameters for some heterocyclic radical cations



Radical		Hyperfine coupling constants (G) <sup>a</sup>			
X	R	H <sub>2,5</sub>	H <sub>3,4</sub>	H(CH <sub>3</sub> )	Other nuclei
S	H	13	2.5		
S	CH <sub>3</sub>		3.5	18.1	
O	H	14	3.5		
NH	H	16	3.0		ca. 3 ( <sup>14</sup> N)
NH	CH <sub>3</sub>		3.5	17.5	ca. 3 ( <sup>14</sup> N)
NCH <sub>3</sub>	H	15.5	3.6		ca. 3.5 ( <sup>14</sup> N)
CH <sub>2</sub>	H <sup>b</sup>	11.6	3.5		<2 (CH <sub>2</sub> )
CH	H <sup>c</sup>	13	3.45		1.0 (CH)
CH	CH <sub>3</sub> <sup>c,d</sup>		3.7	13.5	1.1 (CH)

(a) 0.1 mTelsa.

(b) ref 228

(c) ref 225

(d) These are limiting values estimated in ref 225

### Pyrrole

The hyperfine coupling for the 2- and 5-protons is remarkably high. For the 3- and 4-pair it is normal, so one cannot invoke a shift of spin-density to explain the increase. However the positive charge effect was noticed, for example, on going from  $C_6H_6^-$  (3.4 G) to  $C_6H_6^+$  (4.4 G). The increase from the values deduced for  $\pi_3$  for cyclopentadienyl radicals (225) (ca. 1.6 G) then appears to be reasonable. The 2,5 dimethyl derivative also has an enhanced proton coupling. Thus the value for the dimethylcyclopentadienyl species ( $\pi_3$ ) is ca. 17.5 G. This is again a positive charge effect. As established some time ago, hyperconjugative electron release is strongly enhanced by a partial positive charge on carbon (226, 227). The increase observed here is comparable with those found for similar systems (227, 228).

As expected, data for the N-methyl derivative are very close to those for the parent cations. It is noteworthy that, for the latter, but not for the former, the characteristic blue colour associated with these ions changed to orange on annealing to ca. 180 K. There was no well defined change in the e.s.r. spectra during this modification. It is possible that this corresponds to the loss of the N-H proton, since this would probably not greatly affect the SOMO.

The small, almost isotropic hyperfine coupling to  $^{14}N$  (ca. 3 G) is characteristic of  $\sigma$ -orbital spin polarisation, and hence is probably negative. Spin polarisation of the N-C  $\sigma$ -electrons places spin directly into the  $2s$  orbital on

nitrogen, whereas pi-polarisation involves  $2p_x$  and  $2p_y$  orbitals so that the isotropic coupling dominates.

#### Furan

The value of the coupling to the 2,5-protons is appreciably less than that for pyrrole cations, whilst that for the 3,4 protons is slightly increased. These changes are presumably a direct electronegativity effect or it may be due to small changes in bond lengths and angles in the ring.

#### Thiophene

There is a further decrease in hyperfine coupling ( $2.5 \text{ G } ^1\text{H}$ ) on going from furan cations to thiophene cations, but in this case  $A(3,4 \text{ } ^1\text{H})$  also falls slightly. It was anticipated that, for this cation, there might be a small population of  $\pi_2$ , but at least in fast exchange, this would cause  $A(2.5 \text{ } ^1\text{H})$  to fall, but  $A(3,4 \text{ } ^1\text{H})$  should increase, so this explanation is improbable.

For the 2,5 dimethyl derivative, hfs ( $\text{CH}_3$ ) is even larger ( $18.5 \text{ G}$ ) than that for the pyrrole derivative ( $17.5 \text{ G}$ ). In this case, hyperfine coupling ( $3,4 \text{ } ^1\text{H}$ ) has increased to the average value of ca.  $3.5 \text{ G}$ .

The results clearly establish that all these cations share a common structure. Indeed, comparison with the results for 1,3 dimethylcyclopentadienyl radicals (225) and cyclopentadiene cations suggests that all these have a comparable SOMO. These are clearly established as the  $1a_2$  orbital.

It can be concluded that the nature of the atom or group at the 1-position for all these radicals has very little effect

on the form of SOMO. There is however, a marked positive charge effect on the proton coupling constants, and particularly on the extent of delocalisation exhibited by the methyl groups at the 2- and 5-positions.

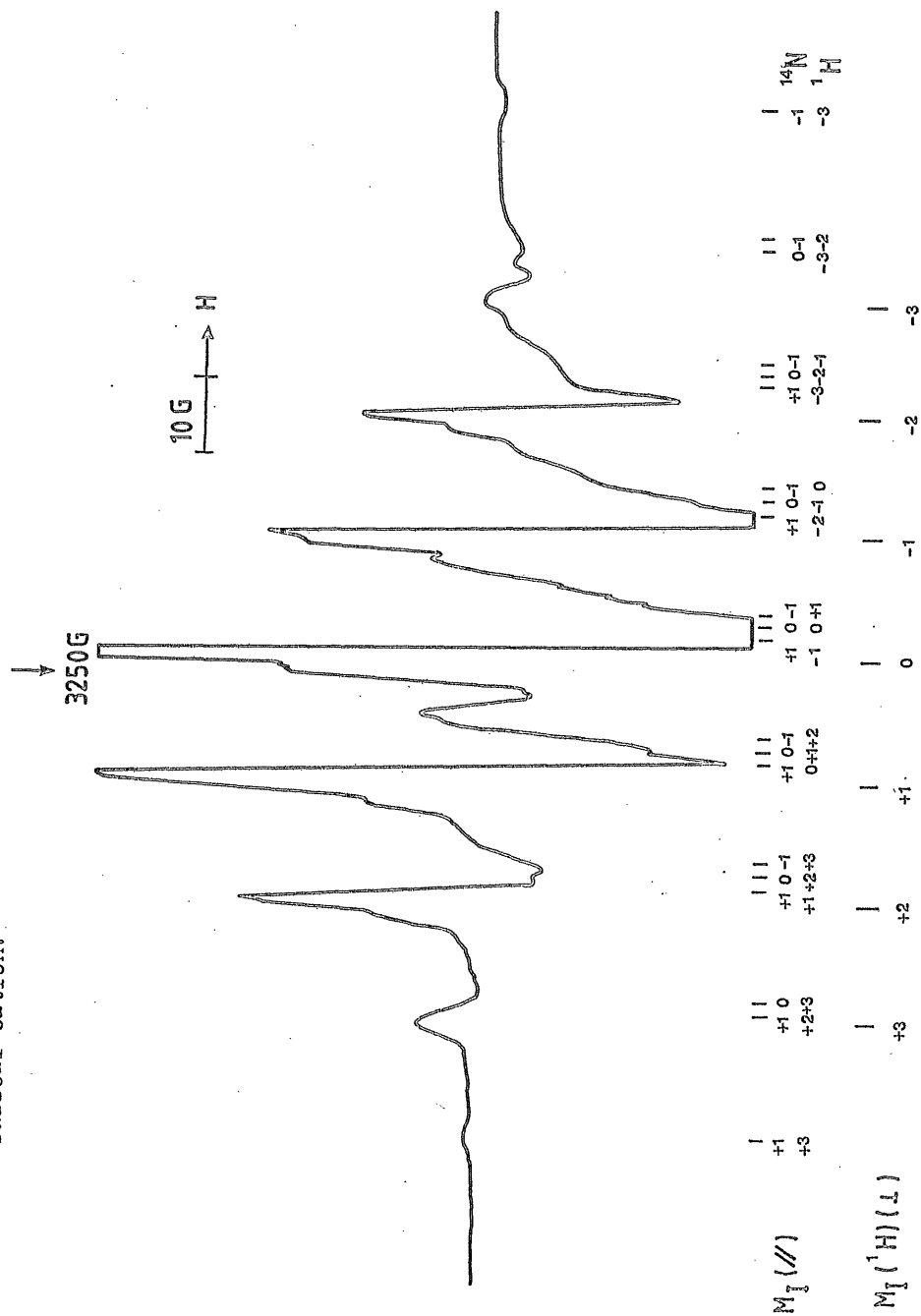
### (3). Radical cations of aliphatic derivatives

#### (i). Radical cations of some amides, thioamides and dimethyl sulphoxide

The spectra for dimethyl formamide and dimethyl acetamide were almost identical (fig 6.5). Unfortunately, the spectra derived from the mono methyl derivatives were poorly defined and hence they are not considered herein, whilst the parent amides, formamides and acetamide are insoluble because of their extensive intermolecular hydrogen bonding. The spectra for dimethyl derivatives comprise well-defined septets from two equivalent methyl groups associated with the  $M_I = 0$  components of the  $^{14}\text{N}$  triplets. Parallel ( $M_I = \pm 1$ ) components can be seen as weak shoulders throughout the spectrum, as indicated in the stick diagram. Hence the data given in table 6.3 have been derived. For the sulphur derivative, dimethyl thioformamide, the proton splitting was drastically reduced, and there were enhanced shifts in the  $g$  tensor components (Table 6.3).

The dimethyl amides are important non aqueous solvents which have many properties in common with dimethylsulphoxide. Therefore the DMSO cation was prepared and its e.s.r. spectrum is shown in fig 6.6. It is noteworthy that there is considerable  $g$ -anisotropy, and that the methyl proton hyperfine

	$M_I(//)$	$M_I^{\perp}(H)(\perp)$
$^1H$	1	1
$^{14}N$	+1	+1
$^{13}C$	+3	+3
$^{15}N$	1	1
$^{13}C$	+1	+1
$^{15}N$	+3	+3
$^{13}C$	1	1
$^{15}N$	+1	+1
$^{13}C$	+3	+3
$^{15}N$	1	1
$^{13}C$	+1	+1
$^{15}N$	+3	+3
$^{13}C$	1	1
$^{15}N$	+1	+1
$^{13}C$	+3	+3
$^{15}N$	1	1
$^{13}C$	+1	+1
$^{15}N$	+3	+3
$^{13}C$	1	1
$^{15}N$	+1	+1
$^{13}C$	+3	+3
$^{15}N$	1	1
$^{13}C$	+1	+1
$^{15}N$	+3	+3
$^{13}C$	1	1
$^{15}N$	+1	+1
$^{13}C$	+3	+3
$^{15}N$	1	1
$^{13}C$	+1	+1
$^{15}N$	+3	+3
$^{13}C$	1	1
$^{15}N$	+1	+1
$^{13}C$	+3	+3
$^{15}N$	1	1
$^{13}C$	+1	+1
$^{15}N$	+3	+3
$^{13}C$	1	1
$^{15}N$	+1	+1
$^{13}C$	+3	+3
$^{15}N$	1	1
$^{13}C$	+1	+1
$^{15}N$	+3	+3
$^{13}C$	1	1
$^{15}N$	+1	+1
$^{13}C$	+3	+3
$^{15}N$	1	1
$^{13}C$	+1	+1
$^{15}N$	+3	+3
$^{13}C$	1	1
$^{15}N$	+1	+1
$^{13}C$	+3	+3
$^{15}N$	1	1
$^{13}C$	+1	+1
$^{15}N$	+3	+3
$^{13}C$	1	1
$^{15}N$	+1	+1
$^{13}C$	+3	+3
$^{15}N$	1	1
$^{13}C$	+1	+1
$^{15}N$	+3	+3
$^{13}C$	1	1
$^{15}N$	+1	+1
$^{13}C$	+3	+3
$^{15}N$	1	1
$^{13}C$	+1	+1
$^{15}N$	+3	+3
$^{13}C$	1	1
$^{15}N$	+1	+1
$^{13}C$	+3	+3
$^{15}N$	1	1
$^{13}C$	+1	+1
$^{15}N$	+3	+3
$^{13}C$	1	1
$^{15}N$	+1	+1
$^{13}C$	+3	+3
$^{15}N$	1	1
$^{13}C$	+1	+1
$^{15}N$	+3	+3
$^{13}C$	1	1
$^{15}N$	+1	+1
$^{13}C$	+3	+3
$^{15}N$	1	1
$^{13}C$	+1	+1
$^{15}N$	+3	+3
$^{13}C$	1	1
$^{15}N$	+1	+1
$^{13}C$	+3	+3
$^{15}N$	1	1
$^{13}C$	+1	+1
$^{15}N$	+3	+3
$^{13}C$	1	1
$^{15}N$	+1	+1
$^{13}C$	+3	+3
$^{15}N$	1	1
$^{13}C$	+1	+1
$^{15}N$	+3	+3
$^{13}C$	1	1
$^{15}N$	+1	+1
$^{13}C$	+3	+3
$^{15}N$	1	1
$^{13}C$	+1	+1
$^{15}N$	+3	+3
$^{13}C$	1	1
$^{15}N$	+1	+1
$^{13}C$	+3	+3
$^{15}N$	1	1
$^{13}C$	+1	+1
$^{15}N$	+3	+3
$^{13}C$	1	1
$^{15}N$	+1	+1
$^{13}C$	+3	+3
$^{15}N$	1	1





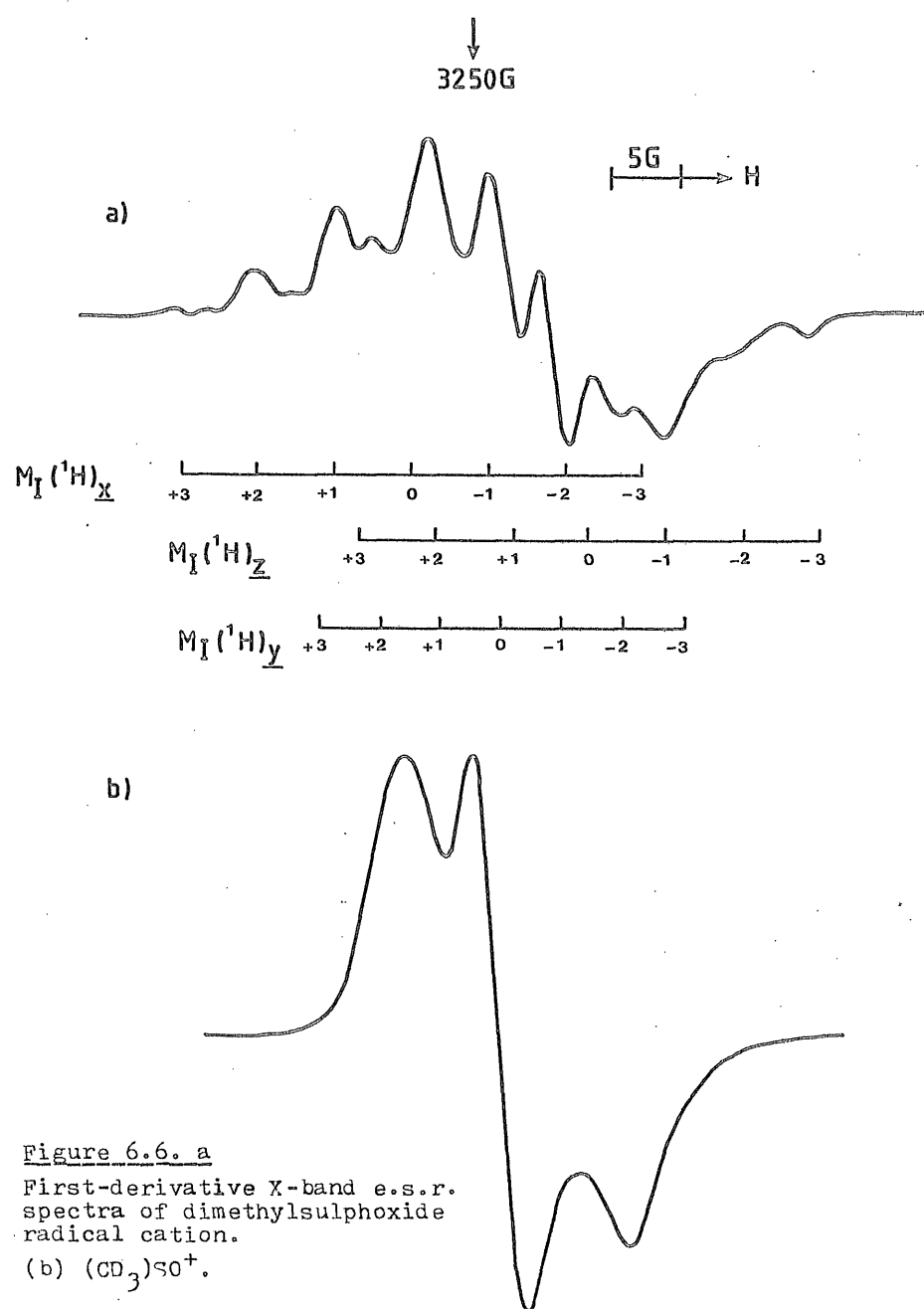


Table 6.3 E.s.r. parameters for some amides and related radical cations

Radical cation	Hyperfine coupling constant/G <sup>a</sup>				g-Value	
	A <sub>  </sub> ( <sup>14</sup> N)	A <sub>⊥</sub> ( <sup>14</sup> N)	A <sub>  </sub> ( <sup>1</sup> H)	A <sub>⊥</sub> ( <sup>1</sup> H)	g <sub>  </sub>	g <sub>⊥</sub>
Dimethylformamide	38 ± 1	0 ± 4	32 ± 1	33 ± 1	2.002	2.007
Dimethylacetamide	38 ± 1	0 ± 4	32 ± 1	33 ± 1	2.002	2.007
Dimethylthioformamide b)	0 ± 4	0 ± 4	8 ± 1	8 ± 1	2.002	2.014
Dimethylformamide						
(d <sub>6</sub> )	38 ± 1	0 ± 2	4.5( <sup>2</sup> H)	5.0( <sup>2</sup> H)	2.002	2.007
DMSO			5.5	5.5/4.5	2.0020	2.0079
						2.0122
DMSO(d <sub>6</sub> )					2.0020	2.0079
						2.0122

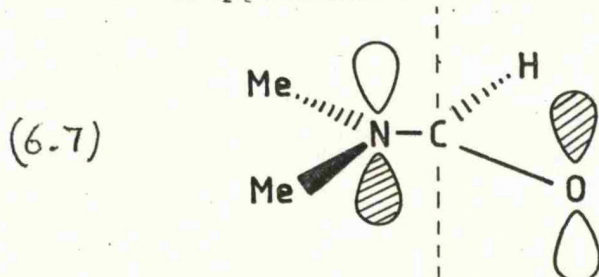
(a) = 0.1 mTelsa.

(b) = Parallel features are not well defined.

coupling is small compared with that for the amide cations (table 6.3). The  $g$ -tensor components were obtained unambiguously from the spectrum for DMSO( $d_6$ ) cations (fig 6.6b), whilst the anisotropic  $^{14}\text{N}$  parameters and  $g$ -values for the dimethyl formamide cations were confirmed using deuterated dimethyl formamide. A search for satellites from DMSO( $^{33}\text{S}$ ) cations was inconclusive because of competing contributions from the freon radicals.

#### Aspects of structure

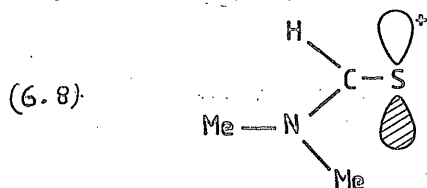
Amide cations: The results clearly show that there is a high spin density on the  $\text{Me}_3\text{N}^+$  unit, a low density on the  $-\text{CH}-$  unit, with some spin density on oxygen, clearly the orbital is the  $\pi(2)$  orbital depicted in insert 6.7, with a node close to the  $-\text{CH}-$  unit. Approximate estimation of the spin-density on



nitrogen can be made in three separate ways; (1) by comparing hyperfine coupling ( $^1\text{H}$ ) for the methyl groups with the coupling to the two methyl groups in  $(\text{Me}_2\text{NH})^+$  cations (37.2 G) (229). This comparison leads to a spin density of  $\sim 86\%$  on nitrogen. (2) By comparing the anisotropic coupling to  $^{14}\text{N}$  (2B) with the estimated value for a unit population of  $2p$  orbital ( $\sim 33$  G). This gives  $\sim 79\%$  with an error of some 5% in a view of uncertainty in the perpendicular hyperfine coupling. (3) By comparing the isotropic coupling with that for  $(\text{Me}_2\text{NH})^+$  cations (19 G) (230). This gives  $\sim 68\%$ , with an uncertainty of

~ 8% overall, Thus it is  $\sim 78 \pm 10\%$ , leaving some  $22 \pm 10\%$  on oxygen, which accounts reasonably well for the  $g$  anisotropy, since this stems largely from spin on oxygen.

Thioamide cations; It was interesting to see if the non-bonding, in plane,  $3p$  orbital on sulphur might have been favoured in this case (insert 6.8). This is the SOMO for the acetaldehyde cations (219) whose e.s.r. spectra is



dominated by a very large hyperfine coupling to the CH proton ( $\sim 137$  G). Had this been the SOMO for  $(\text{Me}_2\text{NCHS})^+$  cations, a large coupling should also have been observed (there is a fall from  $\sim 40$  G for  $\text{Me}_2\text{O}$  (231) cations to  $\sim 20$  G for  $\text{Me}_2\text{S}$  cations). One can predict a coupling of  $\sim 70$  G for this structure. The orbital involved is still  $\pi$  (insert 6.8), but there has been a marked shift in spin density from nitrogen to sulphur.

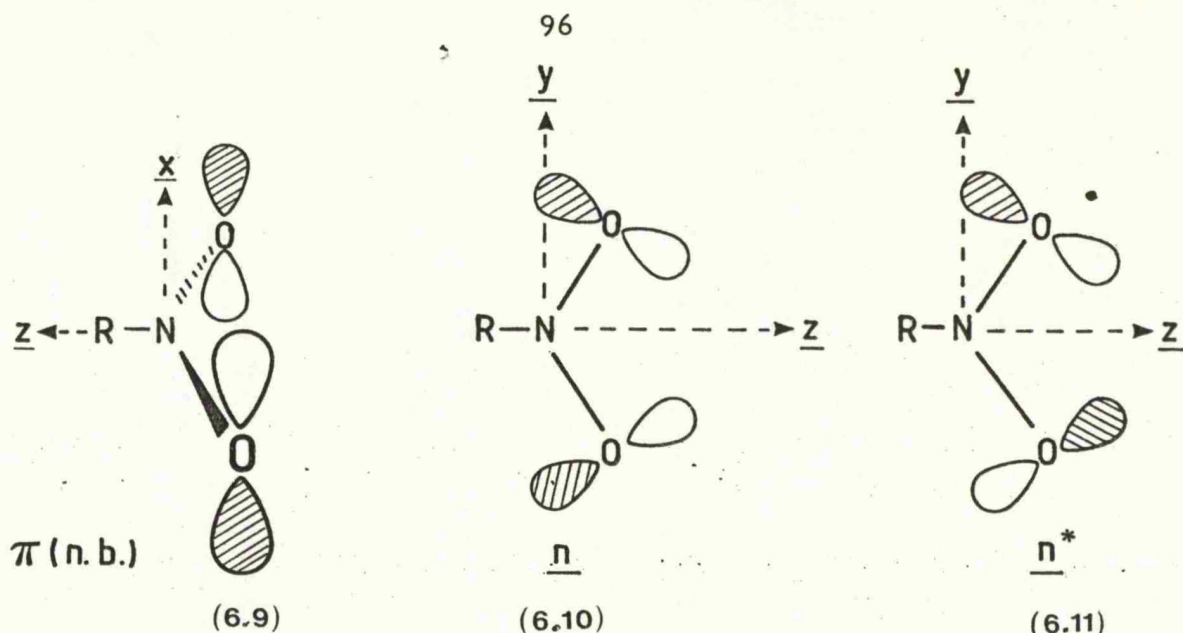
The magnitude of the methyl proton coupling suggests a spin density of  $\sim 22\%$ , if  $(\text{Me}_2\text{NH})^+$  is used for comparison. However loss of spin density is concomitant with the loss of positive charge density, so it may be that  $\text{Me}_2\text{N}^\bullet$  radicals would be better for comparison. These have  $A(\text{Me}) = 14.7$  G, giving a spin density of  $\sim 54\%$  on nitrogen. The increase in  $g$  reflects this shift in spin density, although the increase in spin-orbit coupling constant is also an important factor. This trend in spin density may seem surprising since oxygen has the

higher electron affinity. However, the orbital is antibonding and oxygen acquires a larger share in the electron pair of pi (insert 6.7), than does sulphur.

DMSO: The very small proton coupling constant for DMSO cation is expected for at least three reasons. One is that the radical is non-planar, and hyperconjugative overlap with the C-H sigma-orbitals is consequently reduced. Another, already stressed above, is that overlap with sulphur orbitals is less effective than that with similar nitrogen or oxygen orbitals. The third is that, judging from the relatively large g shifts, there is a considerable spin density on oxygen. An unfortunate consequence is that one cannot use  $A(^1\text{H}, \text{CH}_3)$  to obtain an estimate of the spin density distribution between sulphur and oxygen.

(ii) Radical cations of some nitro alkanes

Although nitroalkane and nitroarane radical anions have been extensively studied by e.s.r. spectroscopy, there are no reports concerning the e.s.r. spectra of corresponding radical cations. According to theory, and to the results of photoelectron spectroscopy (232, 233), the SOMO for the nitroalkanes is expected to be confined to the two oxygen atoms. There are three possible orbitals (pi(nb), n and n\* (inserts 6.9-6.11) which are close in energy. The expected situation is thus

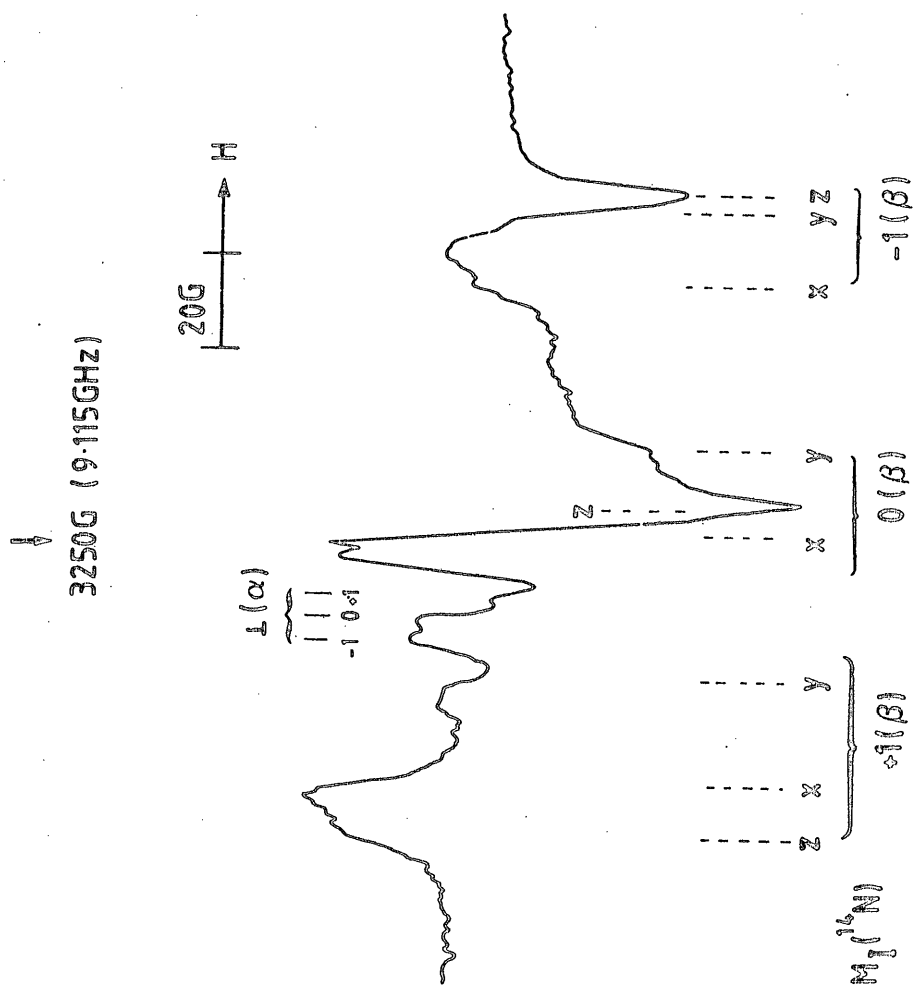


similar to that found for nitrates, where the electron addition gave  $\text{NO}_3^{2-}$ , the electron being in a combination of in-plane oxygen orbitals (234, 235).

#### Structure of the primary cations of Nitroalkanes

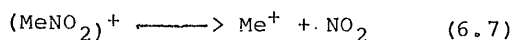
Typical e.s.r. spectra assigned to  $\text{RNO}_2^+$  ions are shown in figure 6.7, and the parameters derived therefrom are given in table 6.4. As expected for structures 6.9-6.11, the  $^{14}\text{N}$  hyperfine coupling is small, since it is due, primarily, to spin-polarisation of the O-N sigma-electrons (235). For all these structures, two  $g$ -components are expected to be greater than 2.0023 since the half-filled SOMO is coupled to one or other of the filled orbitals by field in the radical plane. For 6.11, the orbital is thought to be favoured for the SOMO of the cation (232, 233), or for 6.10,  $g_{\min}$  should be along  $\underline{x}$  and slightly greater than 2.0023, and considerably less than  $g_x$  or  $g_y$ . For insert 6.9,  $g_{\min}$  should be along  $\underline{x}$  but should be equal to 2.0023. Unfortunately, this species was always a minor component at 77 K and it is difficult to detect the low-field features, so no clear distinction between these structures can be drawn on the basis of the e.s.r. data.

Figure 6.7. First-derivative X-band e.s.r. spectrum of rearranged radical cation of nitromethane.

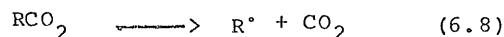


### Structure of NO<sub>2</sub>-type species

Although the <sup>14</sup>N hyperfine coupling components and *g*-tensor components derived approximately from the powder spectra are remarkably close to those for NO<sub>2</sub> radicals (table 6.4), the formation of NO<sub>2</sub> radicals is highly unlikely in these experiments. For example, for (MeNO<sub>2</sub>)<sup>+</sup> ions to give NO<sub>2</sub> radicals would require the formation of CH<sub>3</sub><sup>+</sup> ions, which are energetically most improbable:



The isoelectronic radicals RCO<sub>2</sub><sup>•</sup> decompose readily, usually at well below 77 K:



A major part of the driving force being the high stability of linear CO<sub>2</sub> molecules. A similar reaction for (RNO<sub>2</sub>)<sup>+</sup> cations would give R<sup>•</sup> and NO<sub>2</sub><sup>+</sup>, but alkyl radicals, R<sup>•</sup>, were not detected. This suggests that instead of giving separate fragments, incipient C-N bond fission is followed by a rearrangement to give (ONOR)<sup>+</sup> cations. Although these cations have not previously been detected, their A(<sup>14</sup>N) and *g*-tensor components are expected to be close to those for NO<sub>2</sub>, except that A<sub>iso</sub>(<sup>14</sup>N) should be somewhat enhanced for (ONOR)<sup>+</sup> radicals for the same reason that highly charged cations enhance the <sup>13</sup>C coupling for <sup>•</sup>CO<sub>2</sub><sup>-</sup> ions (236), as indeed does alkyl substitution



Table 6.4 E.s.r.Parameters for radical cations of Nitroalkanes

Radical cation	$^{14}\text{N}$ Hyperfine coupling constants <sup>a</sup>				g-Values		
	$A_x$	$A_y$	$A_z$	$A_{iso}$	$g_x$	$g_y$	$g_z$
$\text{NO}_2^b$	46.13	44.8	66.76	52.56	2.0062	1.9910	2.0020
$\text{MeONO}^{+c}$	52.5	44.9	66.2	54.5	2.005	1.994	2.002
$\text{EtONO}^{+c}$	52.0	44.7	66.8	54.5	2.0050	1.9935	2.0020
$\text{MeNO}_2^+$	3.0	3.0	$\bar{d}$	-	2.016	2.016	ca.2.002

(a) = 0.1 mTelsa.

(b) =  $\text{NO}_2$  in gas phase.

(c) = Not precisely equal to principal values since the symmetry does not require that the  $\bar{g}$ - and A-tensors share principal axis.

(d) Features hidden under  $M_I = 0$  component for  $\text{MeONO}^+$

on oxygen(237). In fact, data now assigned to  $(\text{ONOR})^+$  cations do show slightly enhanced isotropic coupling constants. Unfortunately there is no sign of proton hyperfine coupling, so delocalisation onto the alkyl groups must be small, if this assignment is correct. In particular, note that the spectrum for irradiated solutions of  $(\text{Me}_3)\text{C}-\text{NO}_2$  differ from the remainder, but this difference can be understood in terms of the rotation or libration of the  $-\text{ONO}$  unit.

For the ethyl derivative, despite all the attempts to remove impurities, another radical was detected in yields comparable with the  $(\text{ONOR})^+$  radicals. Although the spectra were well defined, it is difficult to identify this species.

#### Aryl derivatives

The e.s.r. spectrum assigned to  $(\text{PhNO}_2)^+$  at 77 K was poorly defined, but was undoubtedly due to major electron-loss from the benzene ring. That for the para-methyl derivative was better defined, showing a well resolved 1:3:3:1 quartet due to coupling to the methyl protons (Fig 6.8). Thus the SOMO must be very similar to the toluene cation, since the methyl proton coupling (20 G) is close to that for the toluene cations (222). However, features characteristic of  $\text{RNO}_2^+$  cations, having a SOMO confined to oxygen, were also detected, and these grew in intensity on warming and  $\text{NO}_2$ -like features appeared (Figure 6.8b). Similar results were obtained with various substituted nitrobenzenes.

#### (4) Inorganic radical cations

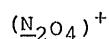
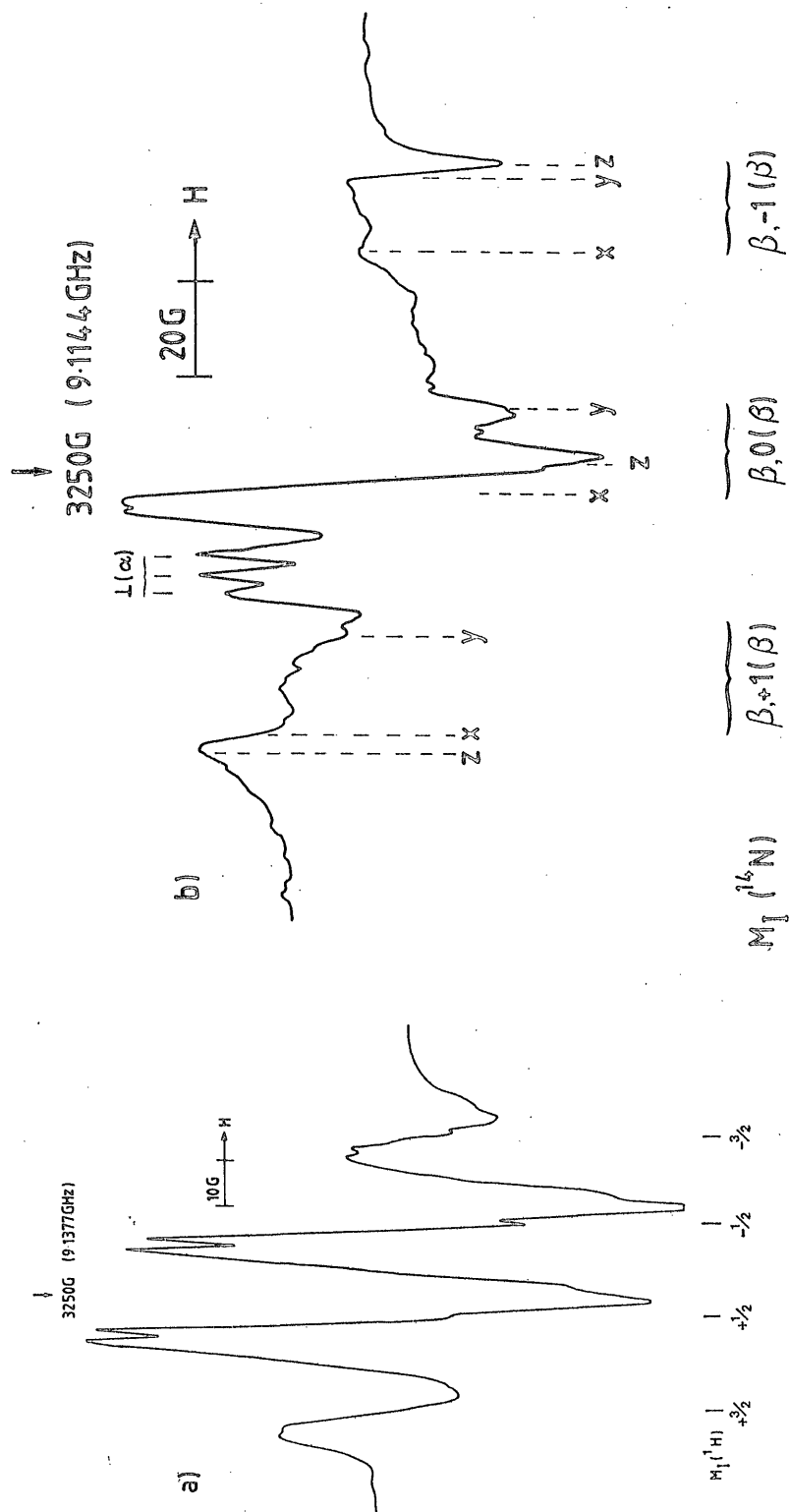
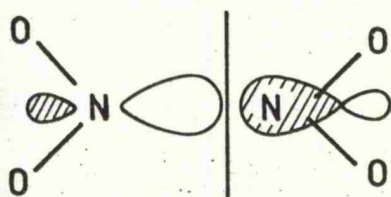


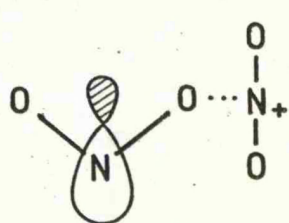
Figure 6.8. First-derivative X-band e.s.r. spectra of (a) p-nitrotoluene  
(b) rearranged radical cation of nitrobenzene.



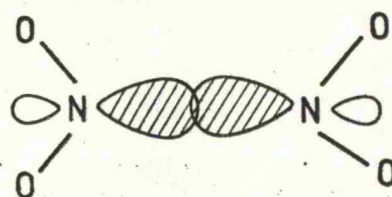
There has been a considerable controversy regarding the proper interpretation of the PES for dinitrogen tetroxide (238-241), all workers agree that the first ionization potential (11.4 eV) corresponds to electron loss from the  $6a_g$  orbital (242, 243), which is the sigma-orbital crudely represented in insert 6.12. However Yoshioka and Jordan



(6.13)



(6.14)

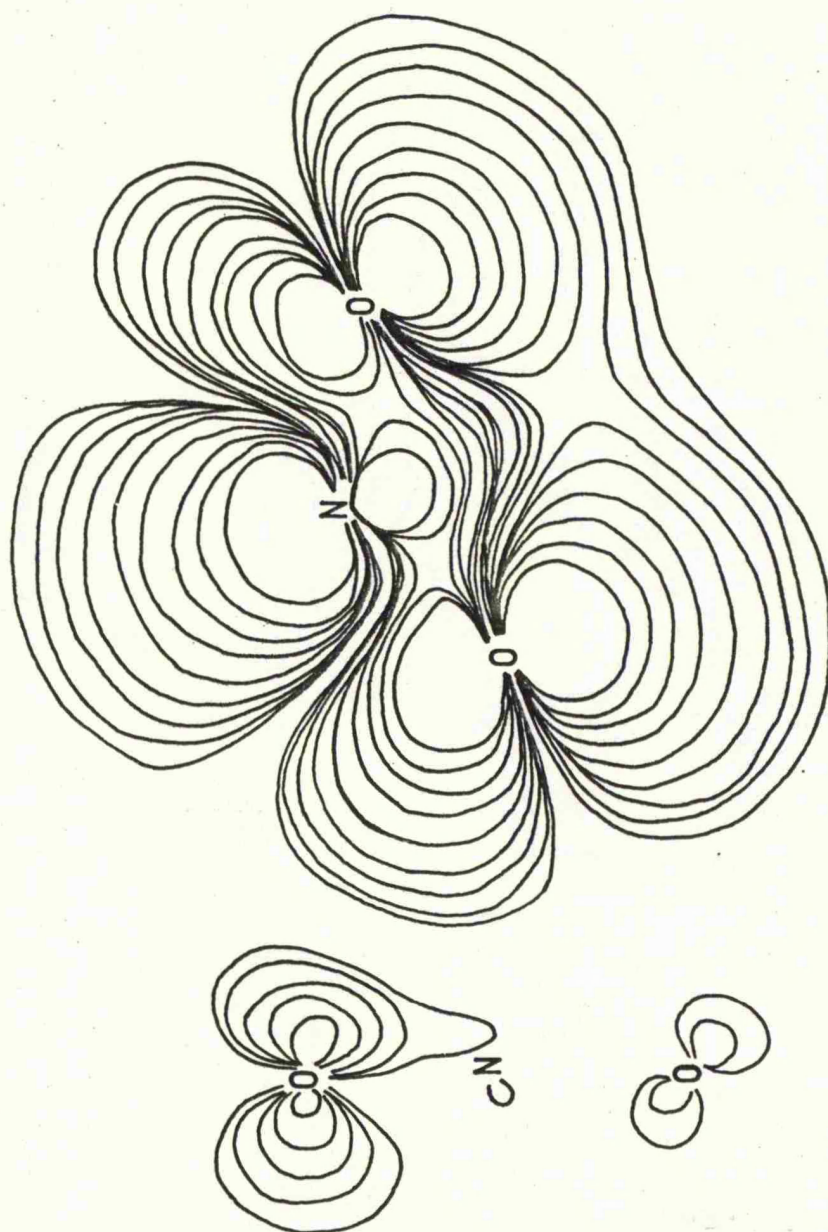


(6.12)

have recently shown by ab initio calculations that this is not the SOMO for relaxed  $[N_2O_4]^+$  radicals. Their calculations suggest that there is a major structural rearrangement to give the low symmetry species (insert 6.14), which resembles an  $NO_2$  radical associated with a linear  $NO_2^+$  cation (244). The charge density contour diagram for the HOMO, calculated by Yoshioka and Jordan, is given in fig 6.9. Their calculations suggest that the initially formed  $D_{2h}$  structure (insert 6.12) is 1.56 eV above that of the cation radical complex (insert 6.14),

the dissociation energy for the  $D_{2h}$  structure being only 0.54 eV to give  $NO_2$  and  $NO_2^+$ . The bond angles and bond lengths for the  $NO_2$  and  $NO_2^+$  portions of the stable structure (insert 6.14) closely resemble those of the separate species, and it seems that the weak bonding between them is dominated by charge-quadrupole and charge-induced dipole interactions (244).

Figure 6.2. The charge density contour diagram for the SOMO of the  $\text{N}_2\text{O}_4^+$  cation (reproduced from ref 244).



In view of these calculations it seemed reasonable to verify these calculations experimentally. Hence  $\text{N}_2\text{O}_4^+$  was studied by e.s.r. spectroscopy.

The form of the e.s.r. spectrum obtained from the tetroxide is remarkably similar to that for the  $\text{NO}_2$  radicals (fig 6.10). The derived e.s.r. parameters given in table 6.5 show that relative to the gas phase  $\text{NO}_2$  radical, the  $g$ -tensor components are closely similar but there is a clear increase from ca. 6 G in  $A_{\text{iso}}$  corresponding to an increase in estimated  $2s$  character (129) from ca. 9.56% to ca. 10.7%. However, there is a fall in the anisotropic coupling (2B) which corresponds to a reduction from ca. 45.4%  $2p_z$  character to ca. 31.2%. Thus there is a fall in total spin-density of ca. 13%. Unfortunately it cannot be judged if this corresponds to an increase in density on the two oxygen atoms of the  $\text{NO}_2$  group or to a transference of spin-density on to the  $\text{NO}_2^+$  unit. Probably both changes are involved. The reduction in estimated  $p/s$  ratio suggests a small decrease in the  $\hat{\text{ONO}}$  angle relative to the  $\text{NO}_2$  radicals. The calculations do not indicate such a reduction.

One curious aspect of the e.s.r. spectra (fig 6.10) is that most of the features appear as doublets with splitting in the range of 2-5 G. It has been previously suggested that a small extra doublet splitting observed and assigned to  $\text{C}_2\text{F}_4^+$  cations may be due to an intermolecular interaction with a fluorine atom in a neighbouring  $\text{CFCl}_3$  molecule (245). To check on this possibility  $[\text{N}_2\text{O}_4]^+$  cation in tetrachloromethane was prepared, but unfortunately the features were so broad that

Figure 6.10 a. First-derivative X-band e.s.r. spectrum of  $\text{N}_2\text{O}_4^+$  radical cation.

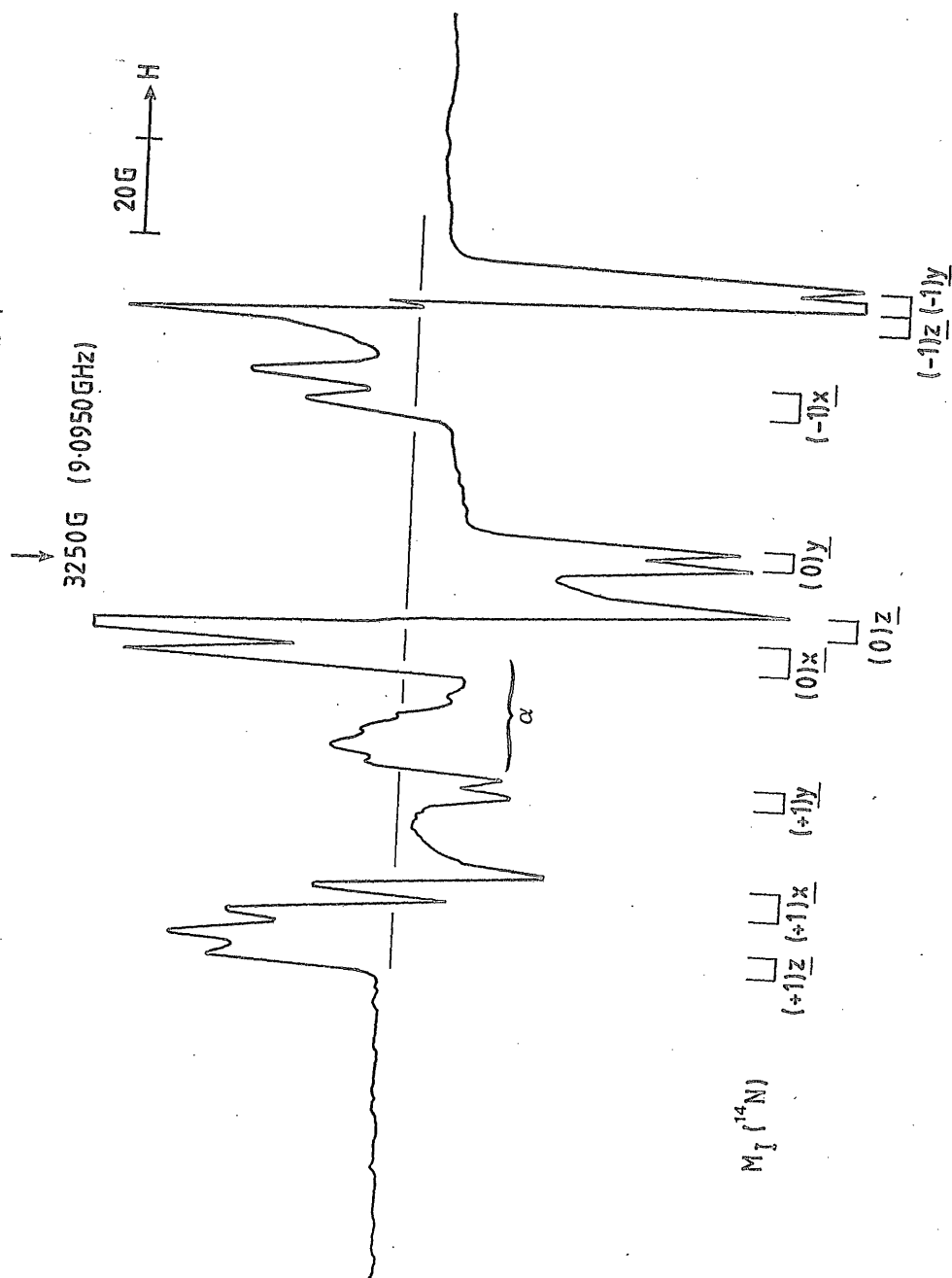


Figure 6.10.b First-derivative X-band e.s.r. spectrum of  $\text{N}_2\text{O}_4^+$  radical cation. (rearranged)

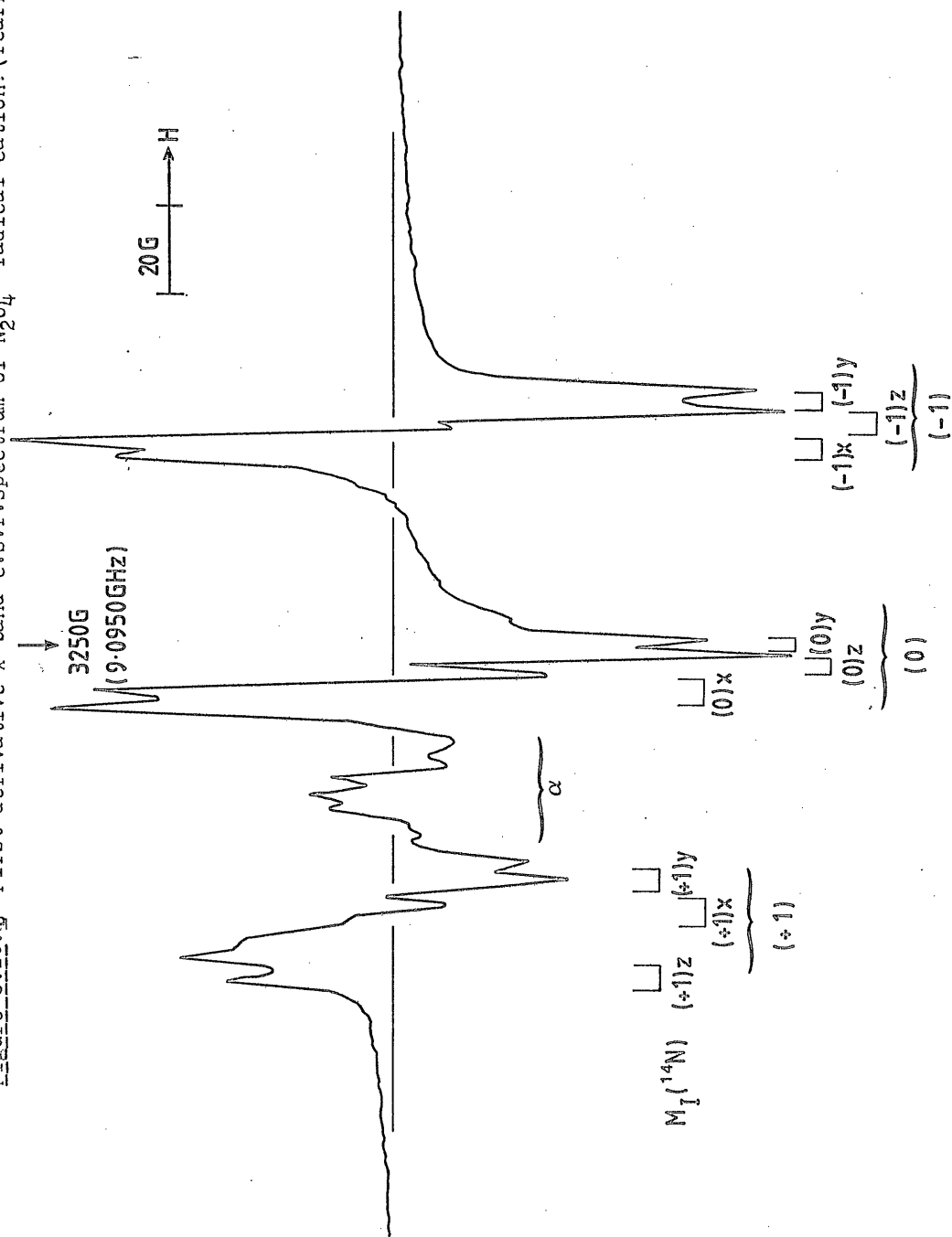




Table 6.5 E.s.r.parameters for Nitrogen tetroxide radical cation

Radical cation	Matrix	$^{14}\text{N}$ hyperfine coupling/G <sup>a</sup>				g-Values		
	77 K	A <sub>x</sub>	A <sub>y</sub>	A <sub>z</sub>	A <sub>iso</sub>	g <sub>x</sub>	g <sub>y</sub>	g <sub>z</sub>
$\text{N}_2\text{O}_4^+$	$\text{FCCl}_3$	54	53	69	58.7	2.0066	2.0017	1.9914
$\text{N}_2\text{O}_4^{+c}$	$\text{FCCl}_3$	54	54	63	57.0	2.0060	2.0017	1.9980
$\text{NO}_2^d$	Gas phase	46.13	44.88	66.76	52.59	2.0062	2.0020	1.9910
$\text{NO}_2^e$	$\text{N}_2\text{O}_4$	47.8	45.9	64.7	52.8	2.0050	2.0021	1.9920

(a) 0.1 mTelsa,

(b) Since  $\text{N}_2\text{O}_4^+$  has only C<sub>s</sub> symmetry the  $\underline{g}$  and A tensor components donot necessarily share common axis. However, the similarity of the derived values to those for  $\text{NO}_2$  radicals suggests that they must be close if not equal.

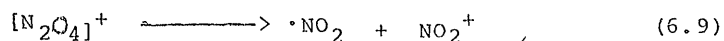
(c) After annealing.

(d) R.M. Lees, R. F. Curl & J. G. Baker. J. Chem. Phys. 45, 2037 (1966)

(e) D. R. Brown & M. C. R. Symons. J. Chem. Soc. Dalton. Trans 1389 (1977)

the small doublet splitting was not resolved. However the line-width did suggest that this splitting was still present. There is an alternative possibility that the splitting is due to coupling to  $^{14}\text{N}$  nucleus of the  $\text{NO}_2$  unit. This splitting would normally be a 1:1:1 triplet, but three factors could lead to doublets in the present case. One is that there is a strong linear electric field for  $\text{NO}_2^+$  which will exert a strong effect on the quadrupole  $^{14}\text{N}$  nucleus. Another possibility is that the directions for the turning points observed correspond to those for the  $\underline{g}$  and  $\underline{A}$  tensors for the  $\text{NO}_2$  unit which are not expected to be the near principal values for the  $^{14}\text{N}$  coupling for the  $\text{NO}_2^+$  unit. Hence the splitting observed will be for directions well removed from the principal directions. The third factor is that when the hyperfine coupling energy is small, the quadrupole effect may dominate and in off-axis directions a doublet is often observed rather than a triplet. This is the reason why doublets appear in the present case.

The decrease in spin-density and increase in  $A_{\text{iso}}(^{14}\text{N})$  for the  $\text{NO}_2$  unit strongly suggests that this centre is not  $\text{NO}_2$  formed according to reaction 6.9. In extensive studies of environmental effects on  $\text{NO}_2$  in various matrices, it was observed that strongly interacting matrices do give rise <sup>to</sup> a <sub>Λ</sub>



small increase in  $A_{iso}$ , the maximum value being 60.6 G for  $NO_2$  in  $La_2Mg_3(NO_3)_{12} \cdot 24 H_2O$  (246). However there is no major loss in total spin-density of non-librating radicals. It is possible, but unlikely, that the large fall in 2B for the  $N_2O_4^+$  cation is due to libratory motion. This is unlikely since the range of  $g$ -values is actually greater than that for  $NO_2$  radicals, furthermore, heating did not cause any immediate further reduction in the 2B term. There was however an irreversible change in the spectrum after annealing to ca, 162 K and re-cooling to 77 K., as shown in fig 6.10b. Clearly the overall anisotropies in both  $g$  and  $A$  values have been reduced and there seems to have been a small decrease in  $A_{iso}$ . Remarkably the small doublet splittings remain almost unchanged, suggesting that  $NO_2^+$  is still present. This suggests that some rearrangement of structure has occurred but that the  $NO_2$  and  $NO_2^+$  units have not been separated.

One facet of these spectra that one cannot be explained is the presence of features marked alpha in fig 6.10. These features are similar to those obtained for  $NO_3$  radicals and  $RNO_2^+$  cations, with a large  $\Delta g$  and a small  $^{14}N$  splitting, suggesting that the unpaired electron is confined to oxygen. Whilst it is just possible that there is yet another structure for the  $N_2O_4^+$  cation with a hole in some combination of oxygen orbitals, it is more likely that these features belong to an impurity cation. This is supported by the fact that the relative intensity of alpha varied markedly from one preparation to another. This is probably dinitrogen pentoxide.

#### REFERENCES

1. J.M.Pratt, Chemistry of Vitamin B<sub>12</sub>. Academic Press N.Y and London, 1972
2. Ed; D.Dolphin, B<sub>12</sub> Vol 1, Wiley-Interscience, N.Y. 1982.
3. Ed; D.Dolphin, B<sub>12</sub> Vol 2, Wiley-Interscience, N.Y. 1982.
4. Eds; Z.Boloslaw & F.Wilhelm, Vitamin B<sub>12</sub> Proceedings, European Symposium (1979) De Gruyter, Berlin FRG.
5. Ed; D.Dolphin, Adv Chem Ser (Biomemetic Chemistry) Vol 191, 1980.
6. Ed; D.B.McCormick & L.D.Wright. Methods Enzymol, 18c, 1 (1971)
7. W.S.Beck, B<sub>12</sub> Vol 1, (Ed; D.Dolphin) Wiley-Interscience, N.Y. 1982, pp 1.
8. D.M.Mathews, Vitamin B<sub>12</sub> Proceedings, European Symposium (Eds; Z.Boloslaw & F.Wilhelm) de Gruyter, Berlin FRG pp 681
9. M.J.C.Linnel, Brit.Med.J. 2, 533 (1979)
10. T.Toraya, M.Vesaka & S.Fukui, Biochem.Biophys. Res, Commun. 52, 350 (1973)
11. T.Toraya, M.Vesaka & S.Fukui, Biochemistry, 13, 3895 (1974)
12. T.Toraya, M.Kondo, Y.Isemura & S.Fukui. Biochemistry 11, 2599 (1972)
13. J.Retey, A.Umani-Ronchi & Arigoni. Experientia 22, 72 (1966)
14. B.Zagalak, P.A.Frey, Karabotsos & R.H.Abeles, J.Biol.Chem. 241, 3028 (1966)
15. J.Retey, A.Umani-Ronchi & D.Arigoni. Experientia, 22, 502

(1966)

16. O.C.Wallis, R.C.Bray, S.Gutteridge & M.R.Holloway.  
Eur.J.Biochem 125, 299 (1982)
17. D.J.Cram, J. Am. Chem. Soc. 95, 4210 (1973)
18. J.Halpern, Adv. Chem. Ser. (Biomimetic Chemistry) vol  
191, 165 (1980)
19. P.G.Lenhert. Proc. Roy. Soc. A 303, 45 (1968)
20. Ph.Mallard & C.Gionnotti. J. Organometallic Chem.  
182, 225 (1979)
21. Y.Tamao, Y.Morikawa, S.Shimizu & S.Fukui.  
Biochim. Biophys. Acta 151, 260 (1968)
22. H.Stokli-Evans, E.Edmond & D.C.Hodgkin. J. Chem. Soc. Perkin  
Trans II, 605 (1972)
23. T.Kato. S.Shimizu & S.Fukui. J. Vitaminol (Kyoto)  
10, 89 (1964)
24. R.H.Abeles. The Enzymes. (Ed; P.D. Boyer) Academic Press,  
N.Y. 1971.
25. R.J.P.Williams. Inorg. Chim. Acta. Rev, 5, 137 (1971)
26. R.G.Wilkins, The Study of Kinetics & Mechanisms of  
Reactions Of Transition Metal Complexes, Allyn Baker  
Inc, Boston
27. T.Toraya, K.Ushio, S.Fukui & H.P.C.Hogenkamp. J. Biol. Chem  
252, 963 (1977)
28. T.Toraya & S.Fukui. Adv. Chem. Ser. (Biomimetic Chem) vol  
191, 139 (1980)
29. G.W.Parshall. Acc. Chem. Res. 8, 113 (1975)
30. D.E.Webster. Activation Of Alkanes By Transition Metal

Complexes (Eds; F.G.A. Stone & R. West) Vol 15, Academic Press N.Y. 1978. pp 197

31. G.N. Schrauzer & R.J. Holland. J. Am. Chem. Soc. 93, 1503 (1971)
32. G.N. Schrauzer. Angew. Chem. (International Ed) 16, 233 (1977)
33. W.A. Pryor. Free Radicals, McGraw-Hill N.Y. 1966.
34. F.R. Jensen & R.S. Kiskis. J. Am. Chem. Soc. 97, 5825 (1975)
35. G.N. Schrauzer, R.N. Katz, J.H. Grate & T.M. Vickey. Angew. Chem. (International ed) 15, 170 (1976)
36. S.S. Kerwer, T.A. Smith & R.H. Abeles. J. Biol. Chem. 245, 1169 (1970)
37. J.M. Pratt & B.R.D. Whitear. J. Chem. Soc. A 252 (1971).
38. R.T. Taylor, L. Smucker, M.L. Hanna & J.L. Gill. Arch. Biochem. Biophys. 156, 521 (1973)
39. J.F. Endicott & G.J. Ferraudi. J. Am. Chem. Soc. 99, 243 (1977)
40. T.H. Finley, J. Valinsky, K. Sato & R.H. Abeles. J. Biol. Chem. 247, 4197 (1972).
41. K.L. Schepler, W.R. Dunham, R.H. Sands, J.A. Fee & R.H. Abeles. Biochim. Biophys. Acta. 397, 510 (1975)
42. J.E. Valinsky, R.H. Abeles & A.S. Mildvan. J. Biol. Chem. 249, 2751 (1974).
43. J.E. Valinsky, R.H. Abeles & J.A. Fee, J. Am. Chem. Soc. 96, 4709 (1974).
44. S.A. Cockle, H.A.O. Hill, R.J.P. Williams, S.P. Davies & M.A. Foster J. Am. Chem. Soc. 94, 275 (1972)
45. B.M. Babor, T.H. Moss, W.H. Orme-Johnson & H. Bienert. J. Biol. Chem. 249, 4537 (1974).
46. W.H. Orme-Johnson, W.H. Bienert & R.L. Blakley.

- J. Biol. Chem. 249, 2338 (1974)
47. J.F. Boas, P.R. Hicks, J.R. Pilbrow & T.D. Smith.  
J. Chem. Soc. Faraday Trans II, 74, 417 (1978)
48. J.W. Wolf. Free Radicals (ed; J.K. Kochi) vol 1, Wiley,  
London, 1973.
49. B.T. Golding & L. Radom, J. Chem. Soc. Chem. Comm. 939 (1973).  
J. Am. Chem. Soc. 98, 6331 (1976)
50. E-I Ochai, J. Inorg. Nucl. Chem. 37, 351 (1975).
51. L. Salem, O. Einstein, N.T. Ann, H.B. Burgi, A. Devaquel, G. Segal  
& A. Veillard. Novu. J. Chim, 1, 335 (1977).
52. P.B. Schevlin & H.J. Hansen. J. Org. Chem. 42, 3011 (1977)
53. C. Walling & A. Cioffani J. Am. Chem. Soc. 94, 6064 (1972)
54. L.L. Ingraham. Ann. N.Y. Acad. Sci, 112, 713 (1964).
55. R.H. Abeles & W.S. Beck. J. Biol. Chem. 242, 3589 (1967)
56. R.L. Blakley, R.K. Ghambeer, T.J. Batterham & C. Brownson.  
Biochem. Biophys, Res, Commun. 24, 418 (1966).
57. M.M. Gattesman & W.S. Beck. Biochem, Biophys, Res. Commun.  
24, 353 (1966).
58. T.J. Batterham, R.K. Ghambeer, R.L. Blakley & C. Brownson,  
Biochemistry, 6, 1203 (1967).
59. W.S. Beck, R.H. Abeles, & R.G. Robinson.  
Biochem. Biophys, Res, Commun. 25, 421 (1966). &  
J.A. Hamilton, R. Yamada, R.L. Blakley, H.P.C. Hogenkamp  
F. Looney & M.E. Winfield. Biochemistry, 10, 347 (1971).
60. H.P.C. Hogenkamp, R.K. Ghambeer, C. Brownson &  
R.L. Blakley. Biochem. J. 103, 5C (1967)
61. H.P.C. Hogenkamp, R.K. Ghambeer, C. Brownson, R.L. Blakley &

- E.Vitols.J.Biol.Chem.243,799(1968).
62. F.K.Gleason & H.P.C.Hogenkamp.J.Biol.Chem.245,4894  
(1970).
63. G.N.Sando & H.P.C.Hogenkamp.Biochemistry 12,3316(1973).
64. P.K.Tsai & H.P.C.Hogenkamp.J.Biol.Chem.255(1980).
65. E.Vitols,H.P.C.Hogenkamp,C.Brownson,R.L.Blakley &  
J.Connella.Biochem.J.104,58C(1967).
66. J.A.Hamilton,R.L.Blakley,F.D.Looney & M.E.Winfield.  
Biochim.Biophys.Acta,177,374(1979)
67. R.L.Blakley,W.H.Orme-Johnson & J.M.Bozolech,Biochemistry  
18,2335(1979)
68. R.Yamada,Y.Tamao & R.L.Blakley.J.Biol.Chem.249,3959  
(1971).
69. W.H.Orme-Johnson,H.Bienert & R.L.Blakley.J.Biol.Chem.  
249,2338(1974).
70. J.A.Hamilton,Y.Tamao,R.E.Coffman & R.L.Blakley.  
Biochemistry 11,4696(1969).
71. J.A.Hamilton & R.L.Blakley.Biochim.Biophys,Acta.  
184,224(1969).
72. R.E.Coffman,Y.Ishikawa,R.L.Blakley,H.Bienert &  
Orme-Johnson.Biochim.Biophys.Acta.444,307(1976).
73. H.P.C.Hogenkamp & G.N.Sando Structure & Bonding  
20,24(1974).
74. R.L.Blakley,B<sub>12</sub> vol 2,(Ed;D.Dolphin) Wiley-Interscience,  
N.Y.1982,pp 381.
75. K.Fuji & F.M.Huennkens.Biochemical Aspects Of  
Nutritional Proceedings Congress,Fed Asian,Oceania.



(1979) pp 173.

76. W.Friedrich & J.P.Nordmeyer.Z.Naturforsch.246,588(1969).
77. L.G.Ljungdahl & H.G.Wood.B<sub>12</sub> vol 2,(Ed;D.Dolphin) pp 165.
78. L.G.Ljungdahl,E,Irion & H.G.Wood.Fed.Proc.25,1642(1966).
79. R.E.De Semonie,M.W.Penley,L.Charbonneau,S.G.Smith,J.M.Wood,H.A.O.Hill,J.M.Pratt,S,Redsdale & R.J.P.Williams. Nature 304,851(1973).
80. Y.T.Fanchiang,W.P.Ridley & J.M.Wood.J.Am.Chem.Soc. 101,1442(1979)
81. L.J.Dizikes,W.P.Ridley & J.M.Wood.J.Am.Chem.Soc. 100,1010(1978)
82. J.H.Espenson & T.D.Seelers.J.Am.Chem.Soc.96,94(1974)
83. T.Frick,M.D.Francia & J.M.Wood Biochim.Biophys.Acta.428, 808(1976).
84. J.M.Wood.B<sub>12</sub> (Ed;D.Dolphin) vol 2,Wiley-Interscience. N.Y.pp 151.
85. G.Agnes,S.Bendle,H.A.O.Hill & R.J.P.Williams,J.Chem.Soc. Chem.Comm.850(1971).
86. J.C.Linnell,A.V.Hoffbrandh,H.A.A.Ausseine,I.J.Wise & D.M.Mathews.Cancer Res,37,2975(1977)
87. Y.T.Fanchiang,W.P.Ridley & J.M.Wood.Adv.Inorg.Chem. 1,147(1979).
88. J.A.Ewen,Texas.J.Sci.31,343(1979).
89. G.N.Schrauzer & J.A.Seck.J.Am.Chem.Soc.93,1503(1971).
90. G.N.Schrauzer.Angew.Chem(International ed)15,417(1976).
91. P.Dowd & M.Shapiro.J.Am.Chem.Soc.98,3725(1976).

92. A.I.Scott & K.Kang.J.Am.Chem.Soc.99,1997(1977)
93. D.Lexa & J.M.Saveant.J.Am.Chem.Soc.100,3220(1978).
94. D.Lexa,J.M.Saveant & J.Zickler.J.Am.Chem.Soc.  
99,2786(1977)
95. D.N.Ramakrishna Rao & M.C.R.Symons J.Chem.Soc.Faraday  
Trans,79,269(1983).
96. D.N.Ramakrishna Rao & M.C.R.Symons.J.Chem.Soc.Perkin  
Trans II 187(1983)
97. D.N.Ramakrishna Rao & M.C.R.Symons.J.Organometallic.  
Chem,244,C43(1983)
98. H.Seki.T.Shida & N.Imamura.Biochim.Biophys.Acta.  
372,100(1974)
99. S.Bachman,Z.Gaysna & A.Furmaniak-Suwalska.  
Studia,Biophysica,71,709(1978).
- 100.F.Endicott & T.L.Netzel.J.Am.Chem.Soc.101,4000(1979)
- 101,K.A.Rubinson,E.Habeshi & H.B.Mark Inorg.Chem.  
21,3571(1982).
- 102.H.P.C.Hogenkamp.Biochemistry 5,417(1966).
- 103,Ph,Maillard,J.C.Massot & C.Gionnotti.J.Organometallic.  
Chem.159,219(1978)
- 104.C.Gionnotti & J.R.Bolton.J.Organometallic.Chem.  
80,379(1974)
- 105.V.D.Ghanekar,R.J.Lin,R.E.Coffman & R.L.Blakley.  
Biochem.Biophys.Res.Commun.101,215(1981)
- 106.K.N.Joblin,A.W.Johnson,M.F.Lappert & B.K.Nicholson.  
J.Chem.Soc.Chem.Comm.441(1975).
- 107.D.J.Lowe,K.N.Joblin & D.J.Cardin.Biochim.Biophys,Acta.

539,398 (1978) .

108.M.Kyew,G.O.Phillips & A.J.Swallow.J.Chem.Soc.

Faraday.Trans I 2277 (1975) .

109.H.P.C.Hogenkamp B<sub>12</sub> (Ed;D.Dolphin) vol 1,

Wiley-Interscience,N.Y.1982,pp 293.

110.J.Halpern.B<sub>12</sub> (Ed;D.Dolphin) vol 1,Wiley-Interscience,

N.Y.1982.pp 501.

111,R.M.Davydov & S.N.Magonov,Russ,J,Phys,Chem.55,148 (1981) .

112,R.H.Yamada,S.Shimizu & S.Fukui.Biochim.Biophys.Acta

124,197 (1966)

113.D.Dolphin,A.W.Johnson & R.Rodrigo.J.Chem.Soc.3186 (1964)

114.A.J.Hartshorn,A.W.Johnson S.M.Kennedy,M.F.Lappert & J.J.

Mcquitty J.Chem.Soc.Chem.Comm.643 (1978)

115.I.P.Rudakova,T.E.Ershava,A.B.Bellikov & A.M.Yurkevich.

J.Chem.Soc.Chem.Comm.592 (1978) .

116.P.Y.Law & J.M.Wood.Biochim.Biophys.Acta,321,382 (1973)

117.W.H.Pailes & H.P.C.Hogenkamp.Biochemistry 7,4160 (1968)

118.D.Dolphin.A.W.Johnson & R.Rodrigo.Ann.N.Y.Acad.Sci,

112,590 (1964) .

119.E.Kaczka,D.E.Wolf & K.Folkers.J.Am.Chem.Soc.

71,1514 (1974)

120.D.Dolphin.Methods.Enzymol,18C,34 (1971)

121.E.L.Smith,L.Mervyn,P.W.Muggelton,Johnson,A.W.& N,Shaw.

Ann,N.Y.Acad.Sci.112,565 (1964)

122.J.R.Pilbrow & M.E.Winfield.Mol.Phys.25,1073 (1973)

123.R.J.Booth & W.C.Lin.J.Chem.Phys.61,1226 (1974)

124.M.C.R.Symons,M.M.Aly & D.X.West.J.Chem.Soc.Dalton,Trans

1744 (1979)

125. M.C.R. Symons, M.M. Aly & J.L. Wyatt. J. Chem. Soc. Chem. Comm. 76 (1981)
126. M.C.R. Symons & G.W. Eastland J. Chem. Res(S) 254 (1977); (M) 2901 (1977)
127. P.W. Atkins, M.C.R. Symons & P.A. Travalion. Proc. Chem. Soc, 222 (1963)
128. S.B. Barnes & M.C.R. Symons. J. Chem. Soc. A 66 (1966).
129. M.C.R. Symons. Chemical & Biochemical Aspects Of Electron Spin Resonance Spectroscopy. Van Nostrand Reinhold, Wokingham 1978.
130. G.N. Schrauzer & J. Kohnle. Chem. Ber, 97, 3056 (1964)
131. G.N. Schrauzer. Acc. Chem. Res. 1, 97 (1968)
132. J.M. Pratt & P.J. Craig. Adv. Organometallic. Chem. 11, 331 (1973)
133. D.G. Brown. Progr, Inorg, Chem. 18, 177 (1973)
134. C.M. Elliott, E. Herschenhant, R.G. Finke & B.L. Smith. J. Am. Chem. Soc. 103, 5558 (1981)
135. L. Salem, O. Einstein, N.T. Ann, H.B. Burgi, A. Delaquet, G. Segal & A. Veillard. Novu. J. Chem. 1, 335 (1979).
136. S. Tyrlik, M.M. Kucharska & I. Woolkowicz. J. Mol. Catalysis, 6, 393 (1979)
137. M.P. Atkins, B.T. Golding, A. Bury, M.D. Johnson & P.J. Sellers. J. Am. Chem. Soc. 102, 3630 (1980)
138. M.P. Atkins, B.T. Golding & P.J. Sellers. J. Chem. Soc. Chem. Comm. 954 (1978).
139. G.N. Schrauzer & R.J. Windgassen. J. Am. Chem. Soc.

- 88,3738 (1966)
140. G. Lenhert, J. Chem. Soc. Chem. Comm. 980 (1976)
141. G. N. Schrauzer, J. W. Silbert & R. J. Windgassen. J. Am. Chem. Soc.  
90,6681 (1968)
142. G. N. Schrauzer, L. P. Lee & J. W. Sibert. J. Am. Chem. Soc.  
92,2997 (1970)
143. E. G. Janzen & J. I. Singliu J. Magn. Reson, 9,513 (1973) .
144. E. G. Janzen, C. A. Evans & J. I. Singliu, J. Magn. Reson.  
9,510 (1973)
145. G. N. Schrauzer & R. J. Windgassen. J. Am. Chem. Soc.  
89,3607 (1967)
146. F. R. Jensen, V. Madan & D. H. Buchanan, J. Am. Chem. Soc.  
93,5283 (1971)
147. M. Tada & H. Ogawa. Tetrahedron. Lett, 2639 (1973)
148. R. Dreos, G. Tanzher, N. Marsich & G. Cosha.  
J. Organometallic. Chem. 108,235 (1976) .
149. J. P. Kitchin & D. A. Widdowson, J. Chem. Soc. Perkin  
I, 1384 (1979) .
150. M. Hoshino, S. Konishi Y. Terai & M. Imamura. Inorg. Chem.  
21, 89 (1982) .
151. G. N. Schrauzer. Inorg. Synth. 11,62 (1972) .
152. M. Green, J. Smith & P. A. Tusker. Discuss. Faraday. Soc  
47,172 (1969)
153. M. C. R. Symons, M. M. Aly & D. X. West. J. Chem. Soc.  
Dalton. Trans. 1744 (1979) .
154. M. C. R. Symons, M. M. Aly & J. L. Wyatt. J. Chem. Soc.  
Chem. Comm. 176 (1981)

155. G. Labuze & J. B. Raynor. J. Chem. Soc. Dalton. Trans. 2388 (1980)
156. S. Hayashida, T. Kawamwa & T. Yonezawa. Chem. Lett. 517 (1980)
157. A. Bencini, C. Benelli, D. Gatteschi & C. Zanchini. Chim. Inorg. 12, 221 (1979).
158. F. S. Kennedy, H. A. O. Hill, T. A. Kadem & B. L. Vallee. Biochem. Biophys. Res. Commun. 48, 1533 (1972).
159. E. Grell & R. C. Bray. Biochim. Biophys. Acta, 236, 503 (1971).
160. S. A. Cockle, S. Lindskog & E. Grell. Biochem. J. 143, 703 (1974).
161. A. Desideri, A. Tomlinson & J. B. Raynor. J. Inorganic. Biochem. 12, 221 (1980), A. Desideri, L. Morpurgo, J. B. Raynor & G. Rotilio. Biophys. Chem. 8, 267 (1978)
162. A. Galdes, H. A. O. Hill, G. S. Baldwin, S. G. Waley & E. P. Abraham. Biochem. J. 187, 789 (1980).
163. M. G. Patch, K. P. Simolo & C. J. Carrano. Inorg. Chem. 21, 2972 (1982).
164. T. Yonetani, H. Yamamoto & G. V. Woodrow. J. Biol. Chem. 249, 682 (1974).
165. T. Inubushi & T. Yonetani. Meth. Enzymol. 76, 88 (1981).
166. F. A. Walker. J. Am. Chem. Soc. 92, 4235 (1970)
167. D. N. Ramakrishna Rao, M. C. R. Symons & A. Harriman. J. Chem. Soc. Faraday. Trans I 78, 3393 (1982)
168. L. U. Boas, C. A. Evans, R. D. Gillard, P. R. Mitchell & D. A. Phipps. J. Chem. Soc. Dalton 582 (1978).
169. M. B. Celap & Lj. R. Solujic. Rev. Chim. Minerale, 16, 60 (1979)
170. B. B. Wayland & D. Mahajer. J. Am. Chem. Soc. 93, 5295 (1971).
171. B. B. Wayland & D. Mahajer. J. Chem. Soc. Chem. Comm 776 (1972).
172. B. B. Wayland, J. V. Minkiewicz & M. E. Ad-Elmazed.

- J. Am. Chem. Soc. 96, 2795 (1974) .
173. S. Konishi, M. Hashino & M. Imamura. J. Phys. Chem. 84, 3437 (1980)
174. H. C. Styner & J. A. Ibers. J. Am. Chem. Soc. 94, 5125 (1972)
175. Ed; D. Dolphin, The Porphyrins, vol 3, Academic Press. N.Y. 1979.
176. J. M. Assour & W. K. Kahn. J. Am. Chem. Soc. 87, 207 (1965)
177. A. B. P. Lever, Adv. Inorg. Chem. Radiochem, 7, 28 (1965) .
178. R. Taube. Pure & Appl. Chem. 38, 427 (1974)
179. R. J. P. Williams. Pure & Appl Chem. 54, 1889 (1982) .
180. J. Z. Hearn & D. Burk. J. Natl. Cancer. Inst. 9, 337 (1949)
181. C. E. Brown & W. E. Antholine. Biochem. Biophys. Res. Commun. 88, 529 (1979)
182. E. L. Smith. Mineral Metabolism, An Advanced Treatise. vol 11 B (Eds; C. L. Comar & F. Bronner) Academic Press N.Y. 1962. pp 349.
183. J. Harding & T. L. Margolis. Brain. Res. 110, 351 (1976) .
184. J. W. Fischer & B. J. Birdwell. Acta. Haematol. 26, 224 (1974)
185. J. W. Fischer & J. W. Langston. Ann. N. Y. Acad. Sci. 149, 75 (1976) .
186. N. D. Chasteen. Coord. Chem. Rev, 22, 1 (1977) .
187. M. Sussman. Iron In Biochemistry and Medicine (Eds; A. Jacobs & M. Wood) Academic Press. N.Y. 1974. pp 649.
188. V. L. Pecararo, W. R. Harris, C. J. Carrano & K. N. Raymond Biochemistry 20, 7033 (1981)
189. A. Harriman & G. Porter. J. Chem. Soc. Faraday. Trans. 2 75, 1543 (1979)

190. I. A. Duncan, A. Harriman & G. Porter. J. Chem. Soc. Faraday Trans II, 76, .1415 (1980)
191. A. Harriman & G. Porter J. Chem. Soc. Faraday Trans. 2, 75, 1532 (1979)
192. M. C. R. Symons. Pure & Appl Chem. 53, 223 (1980)
193. G. C. Dismukes & Y. Siderer. Proc. Natl. Acad. Sci. (USA) 78, 274 (1981)
194. J. E. Packer, In The Chemistry Of Thiol Group (Ed; S. Patai) Wiley, N.Y. 1973, pp 482.
195. G. E. Adams, M. S. Mcnaughton & D. B. Michael. The Chemistry Of Ionization (Ed; G. Scholes and G. R. A. Johnson) Taylor and Francis London. 1967, pp 281.
196. M. Bonifacic, H. Mockel, D. Bahnemann & K. D. Asmus. J. Chem. Soc. Perkin Trans II, 676 (1976).
197. W. Gordy, W. B. Ard & H. Shield. Proc. Natl. Acad. Sci. (USA) 41, 983 (1955)
198. R. L. Peterson, D. J. Nelson & M. C. R. Symons. J. Chem. Soc. Perkin II, 2005 (1977); 225 (1978).
199. H. C. Box, H. G. Freund, K. T. Lilga & E. E. Budzinski. J. Phys. Chem. 74, 40 (1970)
200. M. C. R. Symons. J. Chem. Soc. Perkin Trans. 2, 1618 (1974).
201. J. H. Hadley & W. Gordy. Proc. Natl. Acad. Sci. (USA) 71, 3106 (1974).
202. J. E. Bennett & G. Brunton. J. Chem. Soc. Chem. Comm. 62 (1979).
203. F. K. Truby, J. Chem. Phys. 40, 2768 (1964).
204. J. H. Hadley & W. Gordy. Proc. Natl. Acad. Sci. (USA) 71, 4409 (1974)



205. J.T.Wang & F.Williams. J.Chem.Soc.Chem.Comm, 1184 (1981) .
206. B.C.Gilbert, D.K.C.Hodgeman & R.O.C.Norman. J.Chem.Soc.  
Perkin Trans II, 1748 (1973) .
207. M.C.R.Symons & R.L.Petersen. Biochim, Biophys, Acta,  
535, 241 (1978) .
208. M.C.R.Symons & R.L.Petersen. J.Chem.Res(S) 382; (M)  
4572 (1978)
209. M.C.R.Symons & R.L.Petersen. Biochim, Biophys, Acta,  
535, 247 (1978) .
210. B.B.Singh & M.G.Ormerod. Biochim, Biophys, Acta  
109, 204 (1965); 120, 413 (1966)
211. K.Stratton. Radiation. Res. 35, 182 (1968)
212. M.D.Sevilla, J.B.D.Arcy & D.Suryanarayana.  
J.Phys.Chem. 13, 119 (1979)
213. H.Schuessler. Int.J.Radiation.Biol.Rel.Stud.Phy.Chem.Med.  
40, 483 (1981) .
214. D.N.R.Rao, M.C.R.Symons & J.Stephenson. J.Chem.Soc.  
Perkin.Trans 2, 727 (1983)
215. T.Shida & W.H.Hamil J.Chem.Phys. 44, 2369 (1966)
216. M.C.R.Symons & I.G.Smith. J.Chem.Res(S) 382 (1979)
217. T.Shida, Y.Egawa, H.Kubodera & T.Kato. J.Chem.Phys.  
73, 5963 (1980)
218. T.Ichikawa, N.Ohta & H.Kujioka. J.Phys.Chem. 83, 284 (1979)
219. M.C.R.Symons & P.J.Boon. Chem.Phys.Lett. 89, 516 (1982)
220. D.N.R.Rao & M.C.R.Symons. Tetrahedron.Lett. 24, 1293 (1983)
221. G.Eastland, D.N.R.Rao, J.Rideout, M.C.R.Symons & A.Hasegawa  
J.Chem.Res(S) 1983 (In Press)

222. M.C.R. Symons & L. Harris. J. Chem. Res(S) 268 (1982),  
(M) 2746 (1982)
223. B. Wren & M.C.R. Symons. J. Chem. Soc. Perkin Trans, 2, 1983  
(In Press)
224. B. Wren. R. Rao & M.C.R. Symons. J. Chem. Soc. Perkin II  
(Submitted for Publication)
225. A.G. Davies, E. Lusztyk & J. Lusztyk. J. Chem. Soc. Perkin. Trans  
II, 729 (1982)
226. J.A. Brivati, R. Hulme & M.C.R. Symons. Proc. Chem. Soc.  
385 (1961)
227. R. Hulme & M.C.R. Symons. J. Chem. Soc. 1120 (1965)
228. T. Shida, Y. Egawa, H. Kato & H. Kubodera, J. Chem. Phys.  
73, 5963 (1980)
229. M.C.R. Symons. J. Chem. Soc. Perkin. Trans. 2, 797 (1973)
230. W.C. Danen & R.C. Rickhard, J. Am. Chem. Soc. 94, 3254 (1972)
231. J.T. Wang & F. Williams. Chem. Phys. Lett. 82, 177 (1981)
232. H. Kato, Y. Yonezawa, K. Morokuma & K. Fukui. Bull. Chem. Soc.  
Japan, 37, 1710 (1964)
233. C.N.R. Rao. Indian. J. Chem. 14a, 147 (1976)
234. P.W. Atkins, N. Keen & M.C.R. Symons. J. Chem. Soc. 2873 (1962)
235. P.W. Atkins & M.C.R. Symons. The Structure Of Inorganic  
Radicals, Elsevier, Amsterdam 1967.
236. H. Sharp & M.C.R. Symons, J. Chem. Soc(A), 3075 (1970)
237. D. Griller & B.P. Roberts, J. Chem. Soc. Chem. Comm. 1035 (1971)
238. D.L. Ames & D.W. Turner. Proc. Roy. Soc. (London) Ser A  
348, 175 (1976)

239. D.C. Frost, C.A. McDowell & N.P.C. Westwood.  
J. Electron. Spectrosc Relat. Phenomenon. 10, 293 (1977)
240. T.H. Gan, J.B. Peal & G.D. Willet. J. Chem. Soc.  
Faraday. Trans. 2, 73, 1450 (1977)
241. N. Nomoto, Y. Achiba & K. Kimura. Chem. Phys. Lett. 63, 277 (1979)
242. R.D. Harecourt. Chem. Phys. Lett. 61, 25 (1979)
243. W. Von. Nissen, W. Domcke, L.S. Cederbaum & J. Schimmer.  
J. Chem. Soc. Trans. 2, 74, 1550 (1978)
244. Y. Toshioka & K.D. Jordan. J. Am. Chem. Soc. 102, 2621 (1980)
245. A. Hasegawa & M.C.R. Symons. J. Chem. Soc. Trans II  
79, 93 (1983)
246. B. Bleaney. Nature 179, 140 (1957)